

Aus dem Department für Augenheilkunde Tübingen
Universitäts-Augenklinik
Sektion für experimentelle vitreoretinale Chirurgie

**The effects of a single intravitreal injection of the
VEGF-A-inhibitors aflibercept and ranibizumab on
glomeruli of monkeys**

Inaugural-Dissertation
zur Erlangung des Doktorgrades
der Zahnheilkunde

der Medizinischen Fakultät
der Eberhard Karls Universität
zu Tübingen

vorgelegt von

Christner, Sarah

2017

Dekan: Professor Dr. I.B. Autenrieth
1. Berichterstatter: Professor Dr. U. Schraermeyer
2. Berichterstatter: Professor Dr. K. Januschowski

Tag der Disputation: 12.10.2017

Meinen Eltern
Rainer und Andrea Christner

Table of contents

Table of contents	I
List of figures	III
List of tables	IV
List of abbreviations	V
I) Introduction and scientific issue	1
1. VEGF characteristics and receptors	1
2. VEGF and the kidney	5
3. VEGF and the eye.....	13
4. Anti-angiogenesis in tumors and other angioproliferative diseases	22
5. Therapy of wet AMD	23
6. Therapy of other ocular diseases with anti-VEGF agents.....	25
7. Side effects of anti-VEGF therapy	25
8. Aim of the study	29
II) Material and Methods	0
1. Animals	0
2. Enucleation and preparation of eye tissue samples	1
3. Analyses of eye tissue samples	2
4. Preparation of kidney and blood samples	4
5. VEGF-A plasma levels	4
6. Immunohistochemistry of kidney samples	5
7. Light and transmission electron microscopy of kidney samples	6
8. Quantification of the glomerular endothelial fenestrations	18
9. Statistical analyses of fenestrae per μm	29
III) Results	34
1. Immunohistochemistry- Ranibizumab/aflibercept fluorescence staining, quantification and normalization....	34
2. Immunohistochemistry- Quantification and normalization of VEGF staining	35
3. Measurement of VEGF-A ¹⁶⁵ plasma levels	36
4. General examinations by light and transmission electron microscopy	37

	5. Quantification of the glomerular endothelial cells fenestrations.....	47
	6. Conclusion of Results	58
IV)	Discussion	61
	1. Analyses of eye tissue samples.....	61
	2. Analyses of kidney samples	70
	3. Conclusion of the work	87
V)	Summary	89
	1. English summary	89
	2. Deutsche Zusammenfassung	91
VI)	References	94
VII)	Personnel contribution	106
VIII)	Publications	107
	1. „Effects of a Single Intravitreal Injection of Aflibercept and Ranibizumab on Glomeruli of Monkeys“	107
	2. „The Effects of VEGF-A-inhibitors aflibercept and ranibizumab on the ciliary body and iris of monkeys“	107
	3. Poster presented at the annual ARVO meeting	108
IX)	Appendix	109
X)	Acknowledgement	112
XI)	Curriculum vitae	113

List of figures

Figure 1: Schematic presentation of the glomerular capillary and (in detail) glomerular capillary wall	6
Figure 2: A representative example of fenestrated glomerular endothelium.....	6
Figure 3: Healthy retina-RPE-choroid complex in light microscopy (semi-thin section stained with toluidine blue).....	15
Figure 4: Overview of the transitions zone between iris (right side) and ciliary body, pars plicata (left side)	18
Figure 5: Neovascular AMD	21
Figure 7: Transmission Electron microscope	7
Figure 8: Ultramicrotom.....	8
Figure 9: Electron microscope and camera in use	8
Figure 10: Formvar-coating and preparation of grids for TEM (1 st step)	9
Figure 11: Formvar-coating and preparation of grids for TEM (2 nd step)	9
Figure 12: Ultramicrotome.....	10
Figure 13: Toluidine Blue staining of kidney specimens for light microscopy (1 st step)	11
Figure 14: Toluidine Blue staining of kidney specimens for light microscopy (2 nd step)	11
Figure 15: Toluidine Blue staining of kidney specimens for light microscopy (3 rd step)	12
Figure 16: Lead citrate post-staining for transmission electron microscopy (1 st step)	13
Figure 17: Lead citrate poststaining for transmission electron microscopy (2 nd step)	13
Figure 18: Preparation of glutaraldehyde fixed specimens for light and electron microscopy	14
Figure 19: Schematic composition of a transmission electron microscope (TEM)	17
Figure 20: Example of a MIA.....	21
Figure 21: Demonstration of the SURS method on a MIA	22
Figure 23: TEM Example to distinguish between peripheral and mesangial portions.....	25
Figure 24: Demonstration of the estimation of the ratio fenestrae per μm	26
Figure 25: Examples for surrounding structures of the glomerulus.....	27
Figure 27: Quantification of VEGF-A ₁₆₅ plasma concentrations in EDTA blood samples	37
Figure 28: Overview over semithin sections.....	39
Figure 29: MIA of ranibizumab day 7	40
Figure 30: MIA of untreated control.....	41
Figure 31: 2 MIA's of two glomeruli of aflibercept day 7, incomplete.....	42
Figure 32: MIA of a glomerulus of ranibizumab day 1	43
Figure 33: MIA of aflibercept vehicle	44
Figure 34: Detail of glomerular electron microscopy	45
Figure 35: Examples of TEM used for the quantification of fenestrations	46

Figure 36: Histograms of the distribution of the number of fenestrations per μm in the different independent groups.....	49
Figure 37: Box plot representation of the quantification of the number of fenestrations per μm depending on the treatment and its duration, Version 1	50
Figure 38: Box plot representation of the quantification of the number of fenestrations per μm depending on the treatment and its duration, Version 2	52
Figure 39: One-way ANOVA analysis	54
Figure 40: Sorted list of differences between the means of the groups, Tukey-Kramer-HSD test	54

List of tables

Table 3: Significant differences between means of groups in staining of drugs and VEGF.....	36
Table 4: Statistical values of the distribution analysis of the number of fenestrations per μm , all values and groups separately	47
5.2. Pooling of control samples	51

List of abbreviations

AMD	age-related macular degeneration
APE	anterior pigment epithelium
ARVO	Association for Research in Vision and Ophthalmology
BL	blood space
CC	choriocapillaris
Ch	choroid
CL	capillary lumen
CNV	choroidal neovascularization
ECM	extracellular matrix
FDA	US Food and Drug Administration
GBM	glomerular basement membrane
GCL	ganglion cell layer
HSD	honestly significant difference
IPL	inner plexiform layer
KDR	kinase-insert-domain-containing receptor
LSN	least significant number
LSV	least significant value
M	melanocyte
MIA	multiple image array
mRNA	messenger ribonucleic acid
NCE	non-pigmented ciliary epithelium
NFL	nerve fiber layer
OCT	optical coherence tomography
ONL	outer nuclear layer
OPL	outer plexiform layer
PCE	pigmented ciliary epithelium
PIGF	placental growth factor
PDGFs	platelet-derived growth factors
POD	podocyte
PPE	posterior pigment epithelium
PR IS	photoreceptor inner segments
PR OS	photoreceptor outer segments
PV-1	plasmalemmal vesicle-associated protein-1
RPE	retinal pigment epithelium cells
SURS	systematic uniform random sampling protocol
TGFb	transforming growth factor b
TMA	thrombotic microangiopathy
UR	urinary space
V	choroidal vessel
VEGF	vascular endothelial growth factor
VEGFR	vascular endothelial growth factor receptor
VPF	vascular permeability factor

l) Introduction and scientific issue

1. VEGF characteristics and receptors

VEGF (Vascular Endothelial Growth Factor) is an important signal molecule for vasculogenesis and angiogenesis [1, 2] having influence on the formation of blood vessels in the embryo [3, 4] as well as having an impact on the vascular system in the adult body. VEGF describes a family of proteins with different functions. Seven different isoforms of VEGF are known: VEGF A-F and PlGF (Placental Growth Factor) [5]. Originally, it was described as Vascular Permeability Factor (VPF) which was discovered in the surrounding of tumor cells leading to vascular leakage [6]. In 1989, two groups independently purified a mitogen that is characteristic for endothelial cells, which they called VEGF and vasculotropin, respectively [7, 8].

VEGFs are predominantly produced by endothelial, hematopoietic, and stromal cells in response to hypoxia and upon stimulation by growth factors such as transforming growth factor b (TGFb), interleukins, or platelet-derived growth factors (PDGFs) [9].

1.1. VEGF functions

The proliferative action of VEGF is predominantly restricted to vascular endothelial cells as they almost exclusively express VEGF receptors [10]. Besides, mitogenetic effects of VEGF in lymphocytes, retinal pigment epithelial cells and Schwann cells have been described (reviewed by [10]). In conclusion, binding of VEGF to non-endothelial cells seems to have effects different from proliferation- such as the induction of monocyte migration [11].

The vital role of VEGF in vasculogenesis was demonstrated with the help of two knockout mice studies in 1996 [3, 4]: the loss of a single VEGF allele had a disastrous impact on the de novo formation of blood vessels. In the studies, this led to embryonic death between days 11 and 12.

Apart from the above described functions of proliferation and migration and its role in vasculogenesis, VEGF has a couple of other functions contributing to its

outstanding role as the angiogenetic factor: the induction of plasminogen activators [12] and interstitial collagenase expression [13] in endothelial cells, the stimulation of microvascular leakage and thus increasing the permeability of capillary vessels to macromolecules [6] (which led to its originally used name VPF) and hexose transport [14]. Besides, VEGF acts as a survival factor for newly formed retinal vessels [15]. These additional functions contribute to angiogenesis by delivering energy, facilitating migration and maintaining the process.

There are several splice variants of VEGF with specific functions in blood and lymph vessel formation and homeostasis [10].

1.2. VEGF gene and protein structure, VEGF isoforms

Vincenti *et al.* assigned the Vascular Endothelial Growth Factor Gene to Human Chromosome 6p21.3 in 1996 [16]. The VEGF coding region spans ~14 kb and it contains eight exons [17, 18]. Six different proteins are produced by alternative splicing of the primary transcript (pre-mRNA) generated from a single-copy gene.

VEGF is secreted as a (covalently linked homo-) dimer [10]. Through the work of several groups, six isoforms of VEGF have been found and they differ in length ranging from 121 to 206 amino acid residues (VEGF₁₂₁₋₂₀₆) [18-22]. Thus, the known splice variants to date of human VEGF are: VEGF₁₂₁, VEGF₁₄₅, VEGF₁₆₅, VEGF₁₈₃, VEGF₁₈₉ and VEGF₂₀₆. They differ by the presence or absence of sequences encoded by exons 6 and 7 [18]. The isoforms are secreted by several cell types and in different frequencies. Most cells appear preferentially to express VEGF₁₂₁, VEGF₁₆₅ and VEGF₁₈₉ [10] with VEGF₁₆₅ as the most biologically active variant. The other splice variants seem to be found less frequently.

Further differences between the isoforms can be found in their heparin binding affinity and in how much they are more or less cell and ECM associated or freely released from producing cells. All forms, except homodimeric VEGF₁₂₁, which is weakly acid, can bind heparin *in vitro* and bind heparin derivatives of the extracellular matrix *in vivo* [16]. This is due to the presence or absence of

sequences of amino acids encoded by exon 6 that determine the acid or basic character of the proteins [7, 8, 23]. For example, VEGF₁₆₅ has moderate affinity for heparin and 50-70% remain cell and ECM associated [20]. VEGF₁₂₁ is freely released whereas VEGF₁₈₉ and VEGF₂₀₆ stay completely sequestered in the ECM and partly at the cell surface and bind heparin strongly [20].

1.3. VEGF expression

VEGF mRNA is expressed in a variety of normal adult tissues (predominantly endothelial, hematopoietic, and stromal cells) and during embryogenesis but also in many tumors (see below). VEGF mRNA expression is strongly and rapidly up regulated by oxygen deprivation *in vitro* in several cell types as well as by ischemia *in vivo* [16, 24-26]. This was particularly observed in necrotic areas of tumors [27]. The secretion of VEGF is triggered by hypoxia in cells [27]. When there is a shortage of oxygen, cells produce hypoxia-induced factors, which lead to the distribution of VEGF and finally to angiogenesis in order to compensate for the oxygen deficit.

Moreover, many cytokines and growth factors up regulate VEGF mRNA or induce VEGF release (among these are different tumor growth and tumor necrosis factors TNF-ALPHA, TGF-ALPHA, epidermal growth factor EGF, interleukins etc.) [10].

1.4. VEGF secretion, VEGF-related proteins

Besides PlGF, there are a couple of VEGF-related growth factors, namely VEGF -B, -C, -D and -E and platelet- derived growth factor (PDGF). Thus, the „originally“ discovered VEGF and the one considered to be the major regulator of angiogenesis and vascular permeability [28] is often also referred as VEGF -A. In humans, the VEGF-related proteins are also ligands for the different VEGF receptors. VEGF- C and -D are mainly involved in lymphangiogenesis and VEGF-E was found to be a viral variant of VEGF₁₆₅ [10]. PlGF is believed to play important roles in various physiological and pathological processes and VEGF-B resembles PlGF in many aspects. VEGF-B has a wide tissue distribution but it is particularly abundant in the heart and skeletal muscle (reviewed by [10]).

1.5. VEGF Receptors

Structurally and functionally the receptors are membrane-bound [29] type V tyrosine kinases, whose extracellular domains consist of seven immunoglobulin-like (Ig-like) domains followed by a membrane-spanning region and a conserved intracellular tyrosine kinase domain interrupted by a kinase insert sequence [9, 10, 30]. Three different receptors have been identified (VEGF receptor-1, -2, and -3) [9]. In addition, heparan sulphate proteoglycans and neuropilins also interact with ligands. The neuropilins are isoform-specific receptors for certain VEGF family members [10]. Among others, those previously named partly act as co-receptors and are of importance for VEGF₁₆₅. Neuropilin-1, for example, is likely to enhance the binding of VEGF₁₆₅ to VEGFR-2 [31].

The first receptor discovered was flt-1, also known as VEGFR-1, a ~180-kDa glycoprotein that has the highest affinity for VEGF [30, 32]. Its functions are described as endothelial maintenance and vasculogenesis and it also has different roles in other cell types (reviewed by [10]). Subsequently, KDR (kinase-insert-domain-containing receptor, also known as flk-1 or VEGFR-2 [33] and flt-4 or VEGFR-3 was discovered. VEGFR-2 is a 200-230 kDa high-affinity receptor for VEGF [33], whereas VEGFR-3 (flt-4) does not bind VEGF. Expression of VEGFR-3 is restricted mainly to the lymphatic endothelium of adult tissues [34-36] and is possibly involved in the control of lymphangiogenesis [10]. There seems to be evidence that most endothelial cell responses to VEGF are mediated by VEGFR-2 [10].

These receptors have different affinities for VEGF and VEGF-related proteins as well as for different isoforms: VEGF only binds to receptor types 1 and 2, PlGF and VEGF-B only bind to receptor type 1 and VEGF-C and VEGF-D only bind to receptors type 2 and 3. VEGF-E and VEGF-F bind to receptor type 2 (reviewed by [10]).

2. VEGF and the kidney

2.1. Anatomy and function of the glomerulus

The following text contains information combined from the following sources: [37-39]

The kidney plays an important role in the regulation of blood pressure, acid-base balance and in the production of hormones. However, its main function is the ultrafiltration of plasma and the production of urine with the glomerulus as the main site of action. The human kidney consists of lobi renales with an inner medulla and an outer cortex. Besides other important renal components, the glomeruli are located in the cortex.

Glomerulus (and Bowman's capsule), proximal, intermediate and the distal tubules and collecting duct form so-called nephrons (the functional unit) in which urine is produced.

Kidney glomeruli and ultrafiltration

Each glomerulus contains one arterial capillary arranged in loops, beginning as the vas afferens and ending as the vas efferens. The urinary and the blood space of the glomerulus are separated by the glomerular capillary wall (figure 1). The glomerular capillary wall is also considered as the visceral portion of Bowman's capsule (see below) and it consists of three distinct but closely interacting layers: the fenestrated endothelium with its glycocalyx, the podocytes with their interdigitated foot processes and slit diaphragms, and the intervening glomerular basement membrane (GBM) [40] (figure 2).

In between the capillaries lies the mesangium with the mesangium cells. They stabilize the capillary tuft, contribute to the high glomerular filtration pressure by contraction and act as phagocytes.

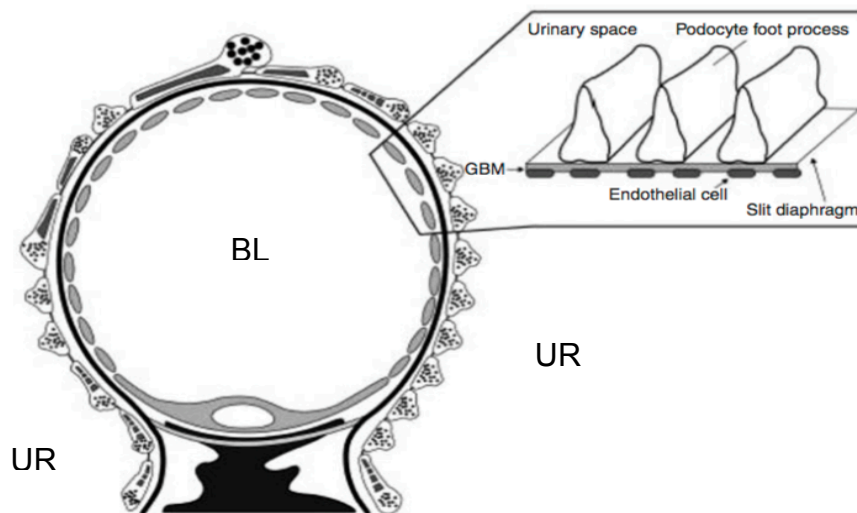


Figure 1: Schematic presentation of the glomerular capillary and (in detail) glomerular capillary wall

In the glomerular capillary, urinary space (UR, outside) and blood space (BL, inside) are separated by the capillary wall. The glomerular capillary wall (detail image) consists of three distinct but closely interacting layers: the fenestrated endothelium with its glycocalyx (glycocalyx not shown), the podocytes with their interdigitated foot processes and slit diaphragms, and the intervening glomerular basement membrane (GBM).

Figure taken from [41] by courtesy of the authors, modified.

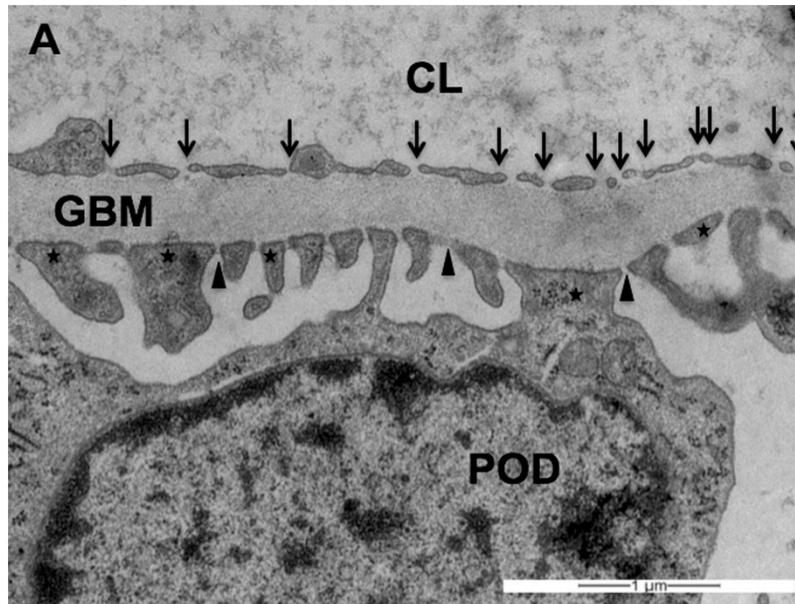


Figure 2: A representative example of fenestrated glomerular endothelium

“Blood lumen on the upper part, urinary space on the lower part of the image...

GBM= glomerular endothelial basement membrane, CL= capillary lumen, POD= podocyte. Arrows mark fenestrae, asterisks mark podocyte foot processes, arrowheads mark podocyte slit diaphragma.” [42]

Transmission electron microscopy (magnification x 20.000), own picture, sample: Aflibercept day1, published in [42].

The glomerulus works as a protein sieve, the glomerular capillary wall is thus also called the **glomerular filtration barrier** which requires the contribution of all three layers of the glomerular capillary wall: endothelium, GBM, and podocytes [40, 43] as well as the glycocalyx [44]. Filtration is driven by Starling forces acting across the glomerular capillary wall, and depends on its large surface area and extremely high water permeability [44].

Glomerular endothelial cells are extremely flat and perforated by trans-cellular pores- the **fenestrae**. The existence of fenestrae is VEGF-dependent and is responsible for the glomerular endothelium's high water permeability [44]. Podocytes are highly differentiated epithelial cells on the visceral side of the glomerular capillary tuft [45]. Their long primary and secondary foot processes enwrap the glomerular capillaries and interdigitate, leaving filtration slits with a constant width of 30 – 40 nm in between [45]. The existence of a slit diaphragm, a highly structured layer of interacting transmembrane proteins [45] – including nephrin- which covers the space between podocyte processes and fenestrae of endothelial cells is still an issue of discussion as it was not observed in all studies. It was not seen for example by Satchell *et al.* [46] but this view is challenged by others [47-49]. It is supposed to be crucial in establishing the size and charge selectivity of the filtration barrier and is an important platform for intracellular signaling pathways [45, 50].

Bowman's capsule

This structure is a delicate capsule consisting of a parietal and visceral layer of epithelium. A simple squamous epithelium forms the parietal layer, which is separated from the visceral layer by the so-called Bowman's space (urinary space) into which the filtrate enters. This epithelium is turned into the epithelium of the tubules. Podocytes on a thickened glomerular basement membrane form the visceral layer lying on the glomerular capillaries [39, 51].

As any epithelium, the parietal layer also contains a basement membrane. In this case it is prominent, thick and consists of three layers: the thin lamina lucida, the thicker lamina densa and the outer lamina reticularis (lamina fibroreticularis) containing an interweaving network of reticular fibers [51].

Proximal and distal tubules and collecting ducts

All the different sections of the tubules have a single-layered epithelium but differ in a couple of morphologic and functional features and their localization within the kidney [51]. In the course of passing the functional system of the nephron, the primary urine filtered in the glomeruli is modified in the system of tubules and collecting ducts and leaves the kidney through the renal pelvis into the ureter [39].

At the urinary pole of the glomerulus the tubule system starts with the proximal tubules (initially pars recta, followed by pars convolute). Its single-layered cuboidal epithelium with its characteristic brush border and round cell nuclei forms the continuation of the parietal layer of Bowman's capsule. Its densely packed microvilli and vesicles in the apical cell part and mitochondria in the infoldings of the basal plasma membrane [51] are expression of the high absorption and secretion in this part of the kidney.

The following smaller calibered intermediate tubules have a large lumen and flattened single-layered epithelium. The nuclei are lenticular and the nucleus-carrying cell part projects into the lumen. These cells do not carry microvilli or have basal infoldings [51].

The distal tubules (pars convolute and pars recta) have a couple of similarities with the proximal tubules: round cell nuclei and basal infoldings and a single-layered cuboidal epithelium. In contrast to the proximal tubules the epithelium is flatter and does not contain a brush border. Moreover, it has a smaller diameter and a slightly larger lumen [51].

The connecting tubules lead to the collecting duct system. Both cell types show a single-layered cuboidal epithelium with distinct cell borders. Two different cell types can be distinguished: intercalated cells (with a high amount of organelles and short microvilli) and principal cells. As the ducts get larger and are converted to Ductus papillares, the cells become higher prismatic and the amount of principal cells increase [51].

Localization of the different structures in the kidney parenchyma

The kidney parenchyma is organized in pyramidal lobi renales which again

consist of cortex and medulla (table 1). The tubules system runs from the cortex to the medulla, makes a hairpin turn back to the cortex and is there continued to the collecting duct system. The descending pars recta of proximal tubules and pars descendens of intermediate tubules and the pars ascendens of intermediate tubules and pars recta of distal tubules are also called the loop of Henle [39](adapted from [51]).

Table 1: Histological organization of the kidney parenchyma

Adapted from [51]

Cortex - Labyrinth	- Glomeruli - pars convoluta of proximal and distal tubules
Cortex - cortical columns at the contact area of two lobi	- pars recta of proximal and distal tubules - collecting ducts
Medulla - outer segment with stripes	- same structures as cortical columns
Medulla - inner segment	- intermediate tubules - pars recta of distale tubules - collecting ducts - ductus papillares

Due to the nature of my study, I was mainly interested in the glomeruli. Thus, I selected parts of the kidney cortex and besides glomeruli, mainly proximal and distal tubules can be seen on my pictures (Table 2).

Table 2: Recognition of important histological kidney structures

Adapted from [51] and own observations

Glomerular endothelial cells	Extremely flat and perforated by fenestrae, prominent nuclei, form the inner surface of glomerular capillaries.
Podocytes	Epithelial cells with cell body and large and small branched foot processes in association with the glomerular

	basement membrane of capillaries, numerous coated vesicles and coated pits along the basolateral domain, prominent endoplasmic reticulum and Golgi apparatus.
Glomerular mesangial cells	Prominent nuclei, irregular shape, many cell processes with microfilaments, surrounded by amorphous mesangial matrix.
Cells of parietal part of Bowman's capsule	Exhibit a cilium and show numerous vesicles and intermediate filaments [51], with a thick basement membrane and prominent lamina reticularis.
Proximal tubules	Single-layered cuboidal epithelium with thick brush border, many mitochondria, indistinct lateral borders and basal infoldings.
Intermediate tubules	Single-layered flattened epithelium, large lumen, nuclei projecting into lumen.
Distal tubules	Single-layered flatter cuboidal epithelium, no/less brush border, smaller diameter, larger lumen, cells paler, bulge into the lumen, indistinct lateral borders.
Collecting duct system	Single-layered cuboidal to higher prismatic epithelium with distinct cell borders, intercalated cells and principal cells.

3.2. VEGF under physiological conditions

The two key vascular growth factor families implicated in glomerular biology and function are the vascular endothelial growth factors (VEGFs) and the angiopoietins [52]. VEGF was found in the kidney during embryogenesis [53] and in the adult kidney [54]. Further indications were found that the interaction between VEGF and its receptors is vital for the development of the kidney as well as for the maintenance of the filtration barrier [55]. VEGF production is induced by hypoxia [56] (see below), but as the kidney is not always hypoxic and as VEGF is constantly produced in the healthy state, other processes have to be involved. Integrins were suggested as non-hypoxic mediators of constitutive VEGF podocyte expression [41, 56]. Also, it has been found that

VEGF is up-regulated by renin and angiotensin II [57, 58]. In turn, VEGF has a stimulating influence on the production of angiotensin II and expression of angiotensin-converting enzyme [59, 60]. These findings seem to indicate a correlation between VEGF and blood pressure.

There is agreement that in the kidney, podocytes are (except for the distal tubule and collecting duct) the main site of local VEGF production [41, 61, 62]. Besides, different groups have found VEGF production in the glomerulus *in vitro* in glomerular epithelial cells [62], endothelial cells [63] and mesangial cells [64]. VEGF receptor (VEGFR) tyrosine kinases are expressed by both podocytes and glomerular endothelial cells [45].

The glomerular epithelium is fenestrated. This is supposed to enable the kidney to perform its high rate of glomerular ultrafiltration. It has been suggested that VEGF produced by glomerular epithelial cells may be vital for the maintenance of the fenestrated phenotype of glomerular epithelial cells [62, 65, 66]-especially with VEGFR-2 [45]. Simon *et al.* were able to localize VEGF mRNA in glomerular epithelia and collecting duct cells and the medulla [65]. These and findings by other groups led to the speculation that the constitutive expression of VEGF in the adult kidney may be required for the function of VEGF receptor positive- fenestrated endothelia in glomeruli and post-glomerular vessels [65].

In conclusion, VEGF is mainly produced by podocytes and mainly affects glomerular epithelial cells. For the development of the kidney and the integrity and function of the glomerular filtration barrier, VEGF is essential [41, 67]. Its surplus or reduction may have a pathological impact.

2.3. VEGF under pathological conditions

VEGF can also play a role in the pathogenesis of renal diseases. VEGF podocyte production must be tightly regulated as not only a lack, but also a surplus of VEGF may damage the glomerular filtration barrier [41]. In preclinical murine models, heterozygous deletion of VEGF in podocytes led to a loss of endothelial cell fenestration, a loss of podocytes, mesangiolysis, and proteinuria, suggesting that VEGF has a critical protective role in the

pathogenesis of microangiopathic process [68], reviewed by [61].

As mentioned above, lack of oxygen is the main inducer of VEGF. The induction of VEGF by hypoxia was demonstrated in mice *in vivo* [54]. The effect was highest in brain, but also occurred in the kidney (tubular cells), testis, lung, heart, and liver. Interestingly, these authors found that the organ-specific distribution of VEGF and its receptors changes under the influence of hypoxia.

VEGF over-expression was found to induce proteinuria, renal failure and neonatal death [69]. As it is a highly potent inducer of microvascular permeability, dysfunctions in the VEGF system might lead to leakage in the glomerular filtration barrier. Its upregulation during mesangioproliferative disease was described [70]. Additionally, VEGFR receptors were also found on human mesangial cells *in vitro* and mesangial cell proliferation *ex vivo* was induced by VEGF₁₆₅ [71]. In the same study, expression of VEGF receptors was found on the mesangium in mesangioproliferative disease. These facts might be of interest in understanding the pathogenesis of renal diseases, as mesangial cell proliferation is a common response of the glomerulus to diverse injuries [71]. Further increased VEGF expression was found in chronic renal allograft rejection [72], indicating that VEGF plays a role in the pathogenesis of rejection and in renal cysts of patients with adult polycystic kidney disease [73]. Also of importance, excessive VEGF-A expression in podocytes was reported in diabetic nephropathy [74]. Moreover, it was reported that VEGF serum levels are increased in renal cell carcinoma [75] and that VEGF levels corresponded with the size and grade of the tumor [76], indicating that VEGF levels may correlate with patients' outcome [66].

Of interest, also a decrease of VEGF can indicate a pathological situation. One study showed a decreased VEGF expression in patients with various renal diseases [77]. VEGF expression was decreased or absent in sclerotic glomeruli, amyloidosis and glomerulonephritis.

On the other hand, there are studies showing VEGF's beneficial effects in glomerular diseases. VEGF is supposed to support the healing by stimulation of

capillary repair. For example in glomerulonephritis, glomerular endothelial cells have an active role in the glomerular response to injury by VEGF-mediated endothelial proliferation [78]. A study of Kim *et al.* in rats shows that VEGF serves to limit thrombotic microangiopathy which is characterized by renal microvascular injury [79] and Ostendorf *et al.* documented that VEGF may play a distinct role in small vessel repair after a given injury to the kidney [80].

In summary, strict regulation of VEGF seems to be extremely sensitive to the development and function of the kidney and especially a vital factor of the healthy glomerular filtration barrier.

3. VEGF and the eye

3.1. Anatomy and function of the retina (reviewed by [81] and [82])

The retina is approximately 0.5 mm thick and lines the back of the eye. The macula or macula lutea is a small region of the retina with a diameter of about 5,5 mm where the cone photoreceptors, responsible for acute and color vision, are predominant. Its center is named fovea centralis. Posterior to the photoreceptors lies the retinal pigment epithelium [83].

About 15° nasally lies the optic nerve and from its center radiate the major blood vessels of the retina. The optic nerve contains the ganglion cell axons running to the brain and, additionally, incoming blood vessels that open into the retina to vascularize the retinal layers and neurons [82]. In contrast to the rest of the retina, the macula/fovea is physiologically avascular.

The functional anatomic complex of the macula region contains photoreceptors, the retinal pigment epithelium cells (RPE), the Bruch's membrane and the choroid (figure 3). The retina has an inverse structure so that light must pass the whole way through the retina before activating the rods and cones. The ganglion cells lie innermost in the retina closest to the lens and front of the eye, and the photosensors lie outermost in the retina against the pigment epithelium and choroid [82].

The two types of photoreceptors, namely rods and cones, absorb photons of light. They consist of inner and outer segments and form monolayers. Their outer segments are in tight contact with retinal pigment epithelium cells containing visual pigments and being vital for the function and survival of photoreceptors, contributing to the blood-retina barrier and evacuating of metabolites (especially capturing, phagocytosis and contributing to the rebuilding of outer segments of photoreceptors) and delivering of nutrients [81]. Five layers of collagen and elastin form the Bruch's membrane. It has the important task to separate the retina from the choroidal microvessels, thus separating neural from vascular structures. As both the RPE cells and the photoreceptors are physiologically avascular, the choroid/ choroidal system is responsible of the nutrition (with oxygen and microelements) of the formerly named via its choriocapillaris. Apart from the choriocapillaris, the central retinal artery is the second source of blood supply for the retina.

3.2. VEGF and the retina

Four AMD research, the interaction of VEGF with retinal pigment epithelial cells is of special interest. The data demonstrate that human retinal pigment epithelial cells can synthesize the secreted vascular endothelial growth factor *in vitro* and *in situ* [84]. The production and secretion of this factor by human retinal pigment epithelial cells may be important in the pathogenesis of ocular neovascularization as it acts as survival factor for newly formed retinal vessels [15]. Retinal pigment epithelial cells do not only produce VEGF, they are also target to the protein. VEGF was shown to induce proliferation [84, 85] and migration in these cells and they were shown to express both VEGFR-1 and VEGFR-2 [85].

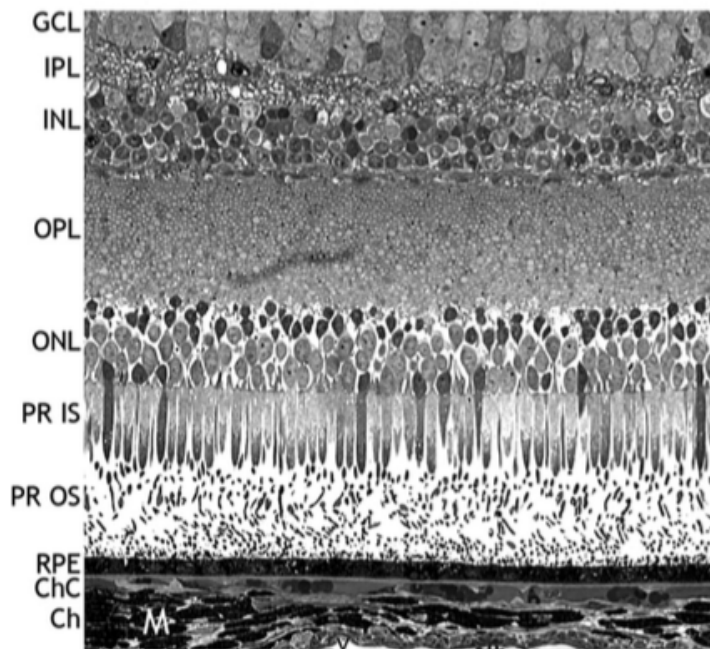


Figure 3: Healthy retina-RPE-choroid complex in light microscopy (semi-thin section stained with toluidine blue)

“NFL nerve fiber layer; GCL ganglion cell layer; IPL inner plexiform layer; OPL outer plexiform layer; ONL outer nuclear layer; PR IS photo- receptor inner segments; PR OS photoreceptor outer segments; RPE retinal pigment epithelium; ChC Choriocapillaris; Ch Choroid; V choroidal vessel; M melanocyte. “[86] NFL not shown.

Picture and description taken from [86] by courtesy of the authors.

3.3. Anatomy and function of the iris and the ciliary body

The iris

The iris is –besides choroid and ciliary body- part of the middle layer of the eye which is also called uvea. It contains blood vessels, pigment cells and muscles and the number and disposition of pigment cells (melanocytes) determines the color of the eye.

The pupil is the central aperture of the iris. The anterior surface of the iris is an incomplete layer of fibroblasts without a lining epithelium [87]. The stroma contains blood vessels and nerves and the sphincter and dilator pupillae muscles that are responsible to regulate the aperture of the pupil depending on lighting conditions. Only a double layer of pigmented epithelial cells that are reflected at the pupillary margin covers the posterior side [87] . The basal lamina of the inner layer (PPE= posterior pigment epithelium) faces the

lens. The basal lamina of the outer layer (anterior pigment epithelium) is adjacent to the stroma of the iris [87]. The posterior pigment epithelium of the iris is continuous with the non-pigmented ciliary epithelium (figure 4).

The ciliary body

At the base of the iris the ciliary body extends from the limbus (corneoscleral junction) and the root of the iris to the ora serrata (the anterior limit of the retina and the choroid). The ciliary body is grossly subdivided into two portions, the pars plicata near the lens, also called the ciliary processes) and the pars plana [88]. Zonule fibers originate from the surface of the ciliary body between the ciliary processes to the lens.

The ciliary body consists of smooth muscle fibers (ciliary muscles) and ciliary processes [89]. There are large diameter fenestrated (in the stroma of the ciliary processes) and smaller caliber non-fenestrated capillaries (which serve the ciliary muscle) in the center of these processes, which are covered by a double-layered epithelium [88, 89].

This double-layered epithelium lines the complete inner surface of the ciliary body. One layer that is pigmented (containing melanin pigment, facing the ciliary stroma) and one layer is non-pigmented (facing the lens). This non-pigmented layer is the continuation of the posterior pigment epithelium of the iris and the neurosensory retina at the ora serrata posteriorly continues it. The pigmented ciliary epithelium continues anteriorly as the anterior myoepithelium of the iris (which includes the iris sphincter muscle) and posteriorly as the pigmented epithelium of the retina. As a result of their embryogenic development, basement membrane of the non-pigmented ciliary epithelium faces the posterior chamber and that of the pigmented ciliary epithelium joins both epithelial layers to the ciliary body stroma with the apical surfaces of both layers facing one another [88].

The ciliary body is responsible for the attachment of the lens and its functions are lens accommodation and aqueous humor production and secretion [89]. Moreover, it assists in aqueous humor drainage [88].

Aqueous humor is vital for the nutrition of the avascular tissues of the eye. Moreover, it determines intraocular pressure. A selective barrier (called the blood-aqueous barrier) must be positioned between the bloodstream and the aqueous humor as a high amount of proteins would reduce optical efficiency and as antigens are not supposed to reach the anterior and posterior chambers of the eye [88]. Here, the fenestrated capillaries serve as a selective permeability barrier and also provide a reservoir from which aqueous humor is secreted by the ciliary epithelium through a complex system of intercellular and transcellular junctions [88, 89].

After being secreted into the posterior chamber, the aqueous humor passively flows past the lens, through the pupil into the anterior chamber where it is drained through the trabecular meshwork in the iridocorneal angle into the canal of Schlemm (a circumferentially oriented vessel) and then into the venous system [88]. By extension of certain smooth muscle fibers and their tendons into the adjacent trabecular meshwork, the ciliary body can assist in the drainage of aqueous humor from the eye [88]. Any disturbance of this in- and outflow has direct impact on intraocular pressure.

Ageing changes that can be expected in the ciliary body and the iris are increased pigmentation of the trabecular meshwork, an increase in the resistance to the outflow of aqueous humor with an increased risk of glaucoma [90] and thickening of the basement membrane of the pigmented ciliary epithelium [88]. The iris tends to become less reactive with age and loses pigment and also the shape and tone of ciliary body changes with age [90].

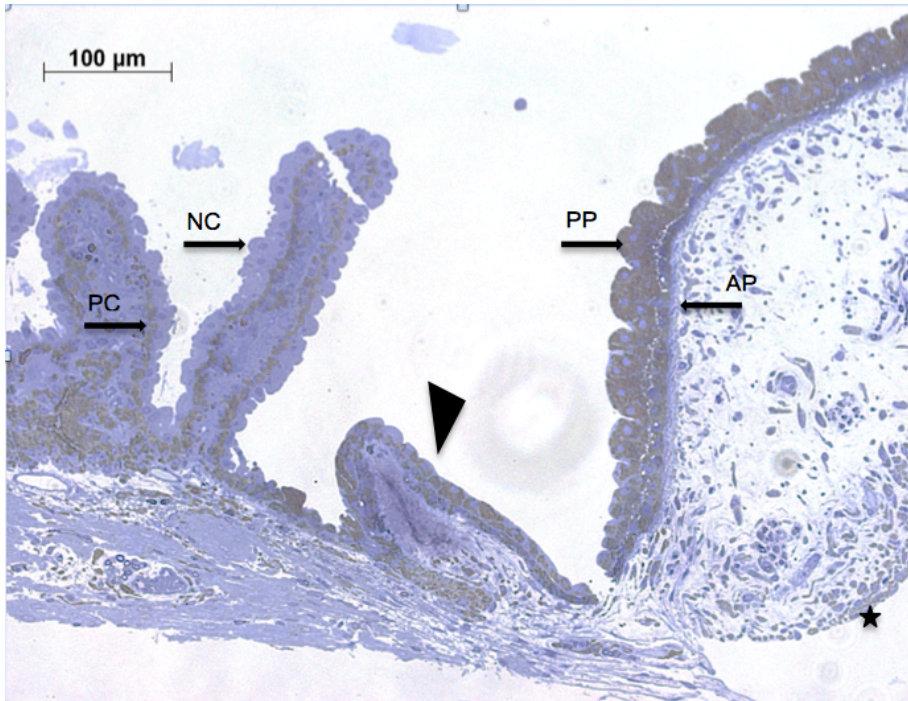


Figure 4: Overview of the transition zone between iris (right side) and ciliary body, pars plicata (left side)

Posterior side facing the lens on the upper part, anterior side facing the inside of the eye on the lower side of the picture.

Iris: Asterisk marks the endothelium-free anterior surface of the iris. The posterior side facing the lens is covered by a double-layered epithelium. PPE= posterior pigment epithelium. The outer layer (APE= anterior pigment epithelium) is adjacent to the stroma of the iris.

Arrowhead marks the transition zone at the iris root where the posterior pigment epithelium of the iris passes into the non-pigmented ciliary epithelium (NCE)

Ciliary body: The inner surface of the ciliary processes is covered by a double-layered epithelium. One layer is pigmented (PCE= pigmented ciliary epithelium, containing melanin pigment, facing the ciliary stroma) and one layer is non-pigmented (NCE= non pigmented ciliary epithelium, facing the lens).

Semi-thin section, light microscopy, magnification x5000, sample: monkey, Aflibercept day1, picture from our group taken by Maximilian Ludinsky.

3.4. VEGF and the ciliary body

Only few studies on the role of VEGF-A in the ciliary body have been performed. Ford *et al.* revealed the role of VEGF-A in the embryogenesis of the ciliary body as well as in the homeostasis and in the maintenance of the fenestrated phenotype of its capillaries in the adult [89]. It seems that VEGF-A is expressed by the pigmented epithelium, whereas VEGFR2 is localized primarily to the capillary endothelium and non-pigmented epithelium [89].

3.5. Age-related macular degeneration

Age-related macular degeneration (AMD) is the most common cause of severe loss of vision and blindness in people over 50 years in the industrialized world (followed by glaucoma and diabetic retinopathy) [83]. It affects several dozen million of people worldwide [81].

Clinical classification

In 2013, a clinical AMD classification was compiled by a committee of 30 experts [91]. AMD was defined as: “fundus lesions assessed within 2 disc diameters of the fovea in persons older than 55 years“. This definition is supposed to separate AMD disease from pigmentary abnormalities or small drusen (<63 μm), also termed drupelets *as they are part of physical aging process*. Additionally, an **early form** of AMD was defined for persons having medium drusen (≥ 63 -<125 μm), but without pigmentary abnormalities and persons with large drusen or with pigmentary abnormalities associated with at least medium drusen to have **intermediate AMD** [91].

The most common form is the slowly progressive atrophic or **dry AMD** with around 85% of all AMD cases followed by advanced or late stage AMD, also called **geographic atrophy AMD** with 35 % of cases. The third and with 10-15% of cases rarest but also rapidly progressing form is the exudative or **wet AMD** [91, 92], reviewed by [81].

Pathological features

AMD is a disease of the outer retina. It results in atrophy of photoreceptors and retinal pigment epithelium accompanied with or without choroidal neovascularization (wet or dry AMD) [93]. As the macula is responsible of sharp vision, its damage threatens the ability to see fine details and colors. Additionally to vision incomfort or loss which drafts the patient to visit an ophthalmologist, further pathological features can be detected in AMD: the presence of drusen in the macula region (amorphous deposits accumulating extracellularly under the retina in the area between RPE and the inner collagenous zone of Bruchs membrane [92]), pigmentary abnormalities (hypo-

and/ or hyperpigmentation) of the retinal pigment epithelium (RPE) or newly formed subfoveal blood vessels originating from the choroid [81]. These go in line with RPE/photoreceptor degeneration and Bruch's membrane disruption. RPE cells are the first to be affected. They undergo degeneration due to metabolic inefficacy, followed by the photoreceptors which are dependent on RPE cells [94].

As already mentioned, AMD and any other disease of the eye has to be distinguished from physiological aging processes. In the retina they include steady loss of photoreceptors, thickening of Bruch's membrane, thinning of the choroid and forming of hard drusen in the periphery [93]. Many of these features can be found even stronger in AMD as well as additional soft macular drusen and other disease-specific changes [93]. The retina persists in a state of chronic inflammation and increased expression of certain cytokines and inflammasomes are a sign of its constant unsuccessful struggle to maintain ocular homeostasis which probably leads to tissue degeneration [93].

Dry AMD

Dry or geographic AMD is characterized by discrete regional loss of the retinal pigment epithelium accompanied by death of the overlying photoreceptors [95]. Till now, there is no approved therapy for dry AMD.

Wet AMD

The wet form of the disease is characterized by an abnormal growth of new blood vessel originating from the choroid through Bruch's membrane toward the retina [95]. The newly formed blood vessels are abnormal because they are immaturely formed and leaky [95]. This process starting subretinal is called choroidal neovascularization of the retina and leads to pathologic fluid leakage and hemorrhage under and into the photoreceptor cell layer in the macula region [81] (figure 5).

The pathogenesis of this formation of new blood vessels is still not clear. It includes local hypoxia due to the existence of drusen between RPE monolayer and Bruch's membrane. The growing number and size of drusen, as well as the appearance of soft drusen, may lead to local detachment of RPE from Bruch's

membrane and the choriocapillaries [81]. Others see the cause in oxidative stress and chronic low grade inflammatory process response [96]. Whether the wet form is a complication of dry AMD is not clear.

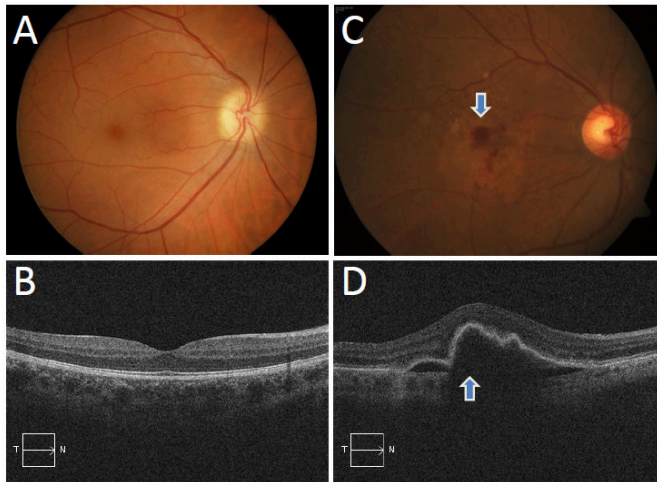


Figure 5: Neovascular AMD

“A healthy eye without AMD (Panels A, B) has a normal retina without signs of bleeding on color fundus photograph (A). On optical coherence tomography (OCT) image, the anatomical structure of a healthy retina is intact (B). In neovascular AMD, bleeding under the retina due to choroidal neovascularization (blue arrows) disrupts the retinal anatomy (D) and can lead to hemorrhage under the macula (C) that can cause dramatic sudden loss of sharp vision.” [95]
 Pictures and description taken from [95] by courtesy of the authors.

Risk factors

A couple of genetic risk factors have been identified (reviewed by [81]) implicating that there is a heritable component in the disease. However, as the name foretells, various age-dependent cellular and organic dysfunctions are the strongest risk factors contributing to the pathogenesis of AMD. These include extracellular drusen formation, Bruch’s membrane stiffening (including increasing thickness of Bruch’s membrane and lipid accumulation), intracellular debris (resulting from oxidative stress-induced cell/tissue damage, lipofuscin, advanced glycation end products), mitochondrial defects, cell loss and tissue degeneration [81].

On the other hand several environmental and behavioral factors have been identified: smoking [97], history of intensive light exposure (reviewed by [81]), fatty, vegetable-poor diet [98] and eventually hypertension [81].

4. Anti-angiogenesis in tumors and other angioproliferative diseases

Angiogenesis is essential in embryonic development and wound healing as well as in physiological situations such as the female reproductive cycle and the formation and growth of bone [10]. However not only in physiological processes but also in the pathogenesis of many disorders, vasculogenesis as an unwanted phenomenon was found to play a major role. Some examples are tumors, rheumatoid arthritis, psoriasis but also proliferative retinopathies, age-related macular degeneration and several kidney diseases.

Folkman *et al.* proposed in 1971 a hypothesis that tumor growth is angiogenesis-dependent [99]. Consequently, he propagated that the inhibition of angiogenesis was supposed to be a strategy for the treatment of solid tumors [100]. This strategy is based on the assumption that without the growth of new vessels, tumor growth will suspend and metastases will not arise (reviewed by [101]). Before it was thought that the growth of new blood vessels around tumors was an inflammatory response, a side product of tumor growth without any therapeutic consequences. The following experiments and new insights revolutionized cancer therapy.

By the late 1980s, suppression of tumor growth by anti-angiogenic therapy in mice was shown for breast and lung carcinomas and that metastases remain in a microscopic dormant and avascular state [102, 103]. After these achievements, anti-angiogenic agents quickly encroached on cancer therapy as supplement to conventional cytotoxic chemotherapy [104]. It was referred to antiangiogenic chemotherapy, low-dose chemotherapy, or metronomic chemotherapy.

Besides cancer therapy, also non-neoplastic angioproliferative diseases were proven to be successfully when treated with anti-angiogenic agents. After haemangiomas in children were successfully treated [105], it was again Folkman who set up a new thesis that would open new ways in dermatology and ophthalmology (reviewed by [101]). They hypothesized that also psoriasis [106], rheumatoid arthritis, and ocular neovascularization could also be

angiogenesis-dependent and suggested that angiogenesis inhibitors developed for cancer therapy could possibly be used to treat non-neoplastic angiogenesis-dependent diseases [101]. In 1992, it was again those scientists who attempted to extend their anti-proliferative therapy approach to ophthalmology and that find the molecular target for choroidal and retinal neovascularization in humans [107, 108]

5. Therapy of wet AMD

5.1. Phototherapy

An early treatment of AMD was **photocoagulation**, showing efficacy in extrafoveal CNV lesions, but showed a high rate of recurrences (reviewed by [95]). In 2000, **photodynamic therapy** was approved for the treatment of wet AMD. This two-step procedure consists of intravenously injected verteporfin that accumulates in CNV lesions and which is activated by a low energy visible red laser (689 nm). This therapy has the aim to occlude new vessels. Activation of verteporfin by light transfer of its energy to molecular oxygen, results in the formation of highly reactive singlet oxygen capable of producing direct damage of endothelial cells [81]. Due to limited effects on patients' vision and recurrences, photodynamic therapy is not used as primary or single AMD therapy [109].

5.2. Drugs

It was expected that not only tumor patients but also patients suffering from angioproliferative eye diseases might benefit from **anti-VEGF therapy**. Currently, three anti-VEGF agents are in intravitreal use in ophthalmology: bevacizumab (Avastin[®]), ranibizumab (Lucentis[®]) and aflibercept (Eylea[®]) [81]. The RNA aptamer **Pegaptanib sodium (Macugen[®])**, Eyetech Pharmaceuticals, New York, NY, USA) containing polyethylene glycol was the first substance that reached FDA approval for AMD in 2004. In contrast to other agents, it selectively binds only one member of VEGF-A family (VEGF₁₆₅) with high affinity. Despite good efficiency in slowing the progression of wet AMD and also due to the fact that only few patients gained vision under the treatment [95],

clinical use has vastly ceased.

In 1997, **bevacizumab (Avastin[®])**, Genentech Inc., San Francisco, CA, USA), a humanized full length anti-VEGF monoclonal antibody was developed [110] and was FDA approved in 2004 for intravenous use after a randomized phase III study on metastatic colorectal carcinoma [111]. Bevacizumab targets all isoforms of VEGF-A family, binds with two VEGF molecules. The mechanism of action is similar to ranibizumab, although the two drugs differ in size, pharmacokinetics, and cost [95]. It was tested for intravitreal use in wet AMD in 2005 and showed good efficiency. In 2006, bevacizumab led to an increased visual acuity in patients with neovascular age-related macular degeneration and is until today used on an “off-label” basis in ophthalmology [112].

Ranibizumab (Lucentis[®]), Genentech Inc., San Francisco, CA, USA) is a recombinant humanized monoclonal antibody fragment (a modified fragment of bevacizumab) that inhibits all isoforms of VEGF-A and binds only one VEGF molecule [81]. It binds to a location on the VEGF molecule that is required for VEGF to bind to its receptor on the surface of blood vessel cells [95]. After positive results in two phase-III, randomized, controlled, two-year, multicenter studies (MARINA [113] and ANCHOR [114]), Lucentis[®] was FDA- approved for wet AMD in 2006. One intravitreal injection contains 0.5 mg ranibizumab in 50 µL volume.

Aflibercept (Eylea[®]) / VEGF- Trap/ VEGF-Trap-Eye, Regeneron, Tarrytown, NY, USA) is a soluble fusion protein. It contains fragments of two types of VEGF receptors, VEGFR-1 (domain 2) and VEGFR-2 (domain 3), linked with the Fc fragment of human immunoglobulin G (IgG) [81]. It binds all members of VEGF-A family (with a greater affinity than that of bevacizumab or ranibizumab), VEGF-B and PlGF and acts as a soluble decay receptor [81]. It was registered for wet AMD in 2011/2012 after having proven to be as efficient as ranibizumab and bevacizumab in two large clinical trial studies (VIEW 1 and VIEW 2 [115]). One intravitreal dose of Eylea[®] contains 2 mg aflibercept (50 µL).

5.3. Results of wet AMD therapy

The primary aim in wet AMD therapy is the reduction of the visual loss. The success of the therapy is hardly predictable as it depends on a variety of factors including patient's age, lesion characteristics, lesion duration, baseline visual acuity and the presence of particular genotype risk alleles [116]. In the definition of patient's response, resolution of fluid (intraretinal fluid, subretinal fluid and retinal thickening), improvement of letters (with the important landmark of +5 letters), the amount of reduction from the baseline in the central retinal thickness [116] are tested.

Overall, antiangiogenic therapy in wet AMD can provide vision maintenance in over 90% and significant improvement in 25-40% of patients [44]. In order to reduce the re-treatment frequency and to maintain the treatment benefit, occlusive therapies like photodynamic therapy can be combined [44].

6. Therapy of other ocular diseases with anti-VEGF agents

Recent research has established the role of vascular endothelial growth factor (VEGF) as a key mediator of retinal angiogenesis and vascular permeability in ocular neovascular conditions other than wet AMD. These diseases and thus potential fields of application of anti-VEGF agents include diabetic macular oedema or retinal vein occlusion [117], glaucoma [118], iris rubosis [119] and others [120, 121].

7. Side effects of anti-VEGF therapy

7.1. Side effects of systemic therapy

Systemic anti-VEGF therapy is widely used in cancer treatment and improves the outcome of patients dramatically. Besides, tyrosine kinase inhibitors that inhibit VEGF receptors can also target the VEGF family of cytokines. However, as with every drug, side effects may occur. In systemic antiangiogenic therapy the most common are: fatigue and oral toxicity, later skin toxicity and less frequent hypothyroidism [122].

Side effects in the kidney

Adverse side effects concerning the kidney were observed during systemic antiangiogenic therapy. A frequent side effect is **kidney toxicity**. In particular, asymptomatic albuminuria/ **proteinuria** (but rarely nephrotic) is a common side effect [123]. It is dose-dependent and can result in severe glomerular damage by inducing down-expression or suppression of nephrin, an important protein for the maintenance of the glomerular slit diaphragm, sometimes leading to **nephritic syndrome** and/or renal/ **glomerular thrombotic microangiopathy (TMA)** [67, 123]. TMA is a common risk, found in bevacizumab [67, 124] and aflibercept [125] treated patients. Thus, a cohort study was performed and it was assumed that TMA and podocytopathies are a risk for all anti-VEGF agents [126]. Histological lesions were seen even when patients were asymptomatic and VEGF-down regulation in glomeruli was found. For all anti-VEGF agents used in cancer therapy, the incidence of mild and asymptomatic **proteinuria** ranges from 21% up to 63%, but heavy proteinuria has been reported in up to 6.5% of renal cell carcinoma patients [123]. Moreover, proliferative glomerulopathies, and focal segmental glomerulosclerosis have been reported [68].

The incidence and severity of hypertension in anti-angioproliferative therapy is related not only to the type of the drug used, dose of the drug and dosing schedule, but also to the age of the patients, pre-existing hypertension and coexisting cardiovascular disease [41]. Proteinuria and hypertension partly led to drug discontinuation or counteractions like antihypertensive agents [68]. In the worst case, nephrotic syndrome or acute renal failure can occur and blood pressure and proteinuria surveillance and renal biopsies were suggested to decide whether the continuation of the treatment is safe [126]. The mechanism as to how VEGF inhibition causes renal pathologies is unclear. There are indications that a certain VEGF level in the glomerulus is vital to maintain kidney function as anti-VEGF agents seem to be toxic for the glomerular filtration barrier [127]. Findings by other authors that anti-VEGF agents may have an effect on the expression of slit diaphragm proteins [126] confirmed this presumption. It was also shown that inhibition of podocyte VEGF receptors may

result in decreased podocyte survival [128]. Although not yet completely revealed, this pathologic mechanism should not be a surprise, as these findings (hypertension and thrombotic microangiopathy) are similar to the known pathology of preeclampsia, in which expression of the soluble form of the VEGF receptor (sFLT1) increases and circulating VEGF decreases [126, 129].

Transmission electron micrography

In glomeruli of patients with bevacizumab-induced TMA Izzedine *et al.* found, major alterations in TMA glomeruli, including duplication of glomerular basement membrane, loss of fenestrations, detachment of endothelial cells from original basement membrane (endotheliosis), interposition of cells, and marked effacement of visceral epithelial cell foot processes in some areas. Some podocytes exhibited cytoplasm vacuolization, as well as endoplasmic reticulum enlargement and mitochondrial swelling, suggesting an underlying apoptotic process [68, 130]. Vigneau *et al.* found electron microscopic abnormalities in patients with TMA lesions:

Microangiopathic lesions with swelling of the endothelium as well as mesangiolysis were occasionally seen [126]. Also, they saw subendothelial accumulation of electron lucent material in some of the capillaries and doubling of the capillary basement membrane [126].

7.2. Side effects of intravitreal therapy

Local side effects in the eye

Most research concerning local side effects of intravitreal anti-VEGF therapy in wet AMD have been performed for bevacizumab as it has always been and is still used in an off-label mode and as safety studies are thus necessary to increase clinical safety. Preclinical studies carried out on monkeys show that repeated anti-VEGF therapy strongly reduced the diameter of the choriocapillaries [131] and it was shown that bevacizumab reduced the diameter of retinal capillaries in patients with AMD [132]. This may result in atrophy of RPE-photoreceptor complex of the macula and was also found to correlate strongly with poor visual outcome [133]. Bevacizumab was shown to

accumulate and form deposits on the walls of retinal veins and between red and white blood cells, activate thrombocytes and induce retinal vein thrombosis and might result in alterations of retinal blood flow [131]. In a previous study, our group showed that choriocapillaris endothelial cell fenestrations were significantly reduced after a single intravitreal injection of bevacizumab [86]. Moreover, the lumen of the choriocapillaris was regionally occluded by densely packed thrombocytes and even photoreceptors were damaged to some extent. In another study, our group found formation of immune complexes and thrombotic microangiopathy in the choriocapillaris and choroidal vessels (stasis, swelling of the endothelium, loss of fenestrations and complete collapse of the capillaries) [134]. Other authors found retinal artery occlusion caused by bevacizumab [135] as well as a reduction of the central retinal artery velocity 7 days after injection [136]

Independently of the drug, the intravitreal injection itself carries a certain risk of local side effects. Several studies show that multiple injections can lead to retinal thinning and geographic atrophy (reviewed by [137]). Sigford *et al.* reviewed the endophthalmitis occurrence following the intravitreal injection of the anti-VEGF agents ranibizumab and bevacizumab (0.029% *versus* 0.058%) [116]. This can be considered as a risk of the surgery rather than an adverse effect of the drug itself. Ocular inflammation and increased intraocular pressure [138] as well as cataract formation, hemorrhage and retinal detachment [137] are reported as further local risks after intravitreal injection.

Possible systemic side effects

The possibility that intravitreally injected anti-VEGF agents might escape from the eye and reach systemic circulation is widely accepted. Penetration of these drugs through the retina was demonstrated, and also that the Fc receptor could facilitate transport of antibodies from the vitreous across the retinal vasculature's endothelium into the circulation [139-141].

The second question that has to be answered in this field is whether the small doses used in ophthalmology have an effect on systemic VEGF concentration and if this potential VEGF reduction might have systemic side effects.

Several groups have proven that intravitreally injected anti-VEGF agents reach systemic circulation and do reduce systemic VEGF concentrations (reviewed by [141]). Reduction in plasma VEGF levels one day, one week and one month after bevacizumab injection was found [142]. In other studies, effects of different anti-VEGF agents were compared. In a prospective series of AMD patients, the effects of intravitreal bevacizumab and ranibizumab on plasma VEGF were compared with the result that VEGF levels were much lower in bevacizumab than in ranibizumab treated patients [143]. IVAN [144] was the largest study to date to measure serum VEGF levels in AMD. The authors found a reduction of 69% for bevacizumab and 20% for ranibizumab at 1 year, and a reduction of 78% for bevacizumab and 28% for ranibizumab at 2 years [141]. Despite the variation in absolute VEGF levels between studies, the recurrent finding is that bevacizumab lowers systemic VEGF levels much more than ranibizumab [141]. For aflibercept, there is not yet much evidence in this field of research. The differences between ranibizumab and aflibercept can be explained by the differences in their molecular structure (with or without Fc fragment that is responsible for the recycling of a molecule and thus its half-life). Therefore, it can be assumed that due to its high VEGF-binding affinity and the fact that it contains an Fc fragment, aflibercept also significantly reduces VEGF plasma levels. Avery *et al.* measured the systemic exposure after the third monthly intravitreal injection to be 13-fold greater for aflibercept than ranibizumab and 70-fold greater for bevacizumab than ranibizumab [141]. In summary, the systemic effect of ranibizumab appears to be the lowest, consistent with pharmacological differences between the agents [141].

8. Aim of the study

The aim of my thesis was to evaluate possible side-effects of the two anti-VEGF agents aflibercept and ranibizumab when intravitreally injected in monkey eyes. In one study I contributed, the ciliary body and the iris were investigated as these two ocular components have only rarely been more closely evaluated. Due to their localization, they are reached by anti-VEGF agents that are intravitreally applied for the therapy of wet AMD. Moreover, they also contain

VEGF-dependent endothelium and there are also pathologic states in which these tissues benefit from antiangiogenetic therapy- in neovascular glaucoma, for example. In addition to the examination of local effects in the eye, possible systemic side-effects should also be considered. This work was the main topic of my thesis. Given the possibility of penetration of the drugs through the retina and reducing systemic VEGF concentration, other organ systems could be influenced. The kidneys are of special interest as- similar to the choriocapillaris and ciliary body - their glomerular endothelium is fenestrated and the number of fenestrae is strongly VEGF-dependent. Counting of fenestrae in glomeruli was performed using a systematic uniform random sampling protocol (similar to [145]) to obtain a random and objective counting character and analysis. For these studies, monkeys were chosen as antibody molecules and their interaction with Fc receptor mimic those present in humans and monkey eyes are also more closely related to the human pathophysiology than rat or mouse [146]. Transmission electron microscopy is not widespread in research and the clinic as it demands specialized personnel and is very technically sensitive. Consequently,, only a few people are able to interpret the findings. However, it offers unique possibilities in analyzing the histology and also pathology of diseases and was especially indispensable for the quantification of fenestrated endothelia in my study, as it is required to image these sub-100-nm structures. My scientific issue was mainly focused on kidney histology and pathology. To this aim, I performed light and electron microscopic studies (including SURS protocol and MIA= multiple image arrays) and quantification of glomerular endothelial fenestrations. Moreover, I compared the findings I obtained in the kidney with those obtained in the ciliary body and iris as well as with earlier results from the retina performed by the group of Prof. Schraermeyer and other researchers [86, 131, 134, 147-151]. Moreover, I performed extensive literature studies in order to be able to discuss the results I obtained. During my graduation, our group published two international peer-reviewed journal articles [42, 148, 150] in which I was twice co-first author. In addition, my findings were presented as a poster at the biggest annual meeting (ARVO) for Research in Vision and Ophthalmology in Orlando in USA in 2014 [152].

II) Material and Methods

1. Animals

„Ten cynomolgus monkeys (Macaca fascicularis, aged 3 to 8 years) were raised at the Covance Laboratories (Muenster, Germany) under standard conditions.”

[42, 148] „The monkeys in this study were an average of 5.5 years old for the aflibercept group, and an average of 6.5 years old for the ranibizumab group.“

[150] ”All animals were housed and handled in strict accordance with good animal practice under supervision of veterinarians in accordance with the German Animal Welfare Act and were monitored for evidence of disease and changes in attitude, appetite or behaviour suggestive of illness.” [42, 148, 150]”

“The naive Cynomolgus fascicularis monkeys are from a closed breeding colony (Noveprim Mauritius). Tests for TB, B-Virus, SIV, SRV, STLV, are carried out during export and import quarantine. Additionally tests for TB, B-Virus, SIV, SRV, STLV are carried out regularly for all animals on site regardless if they are in studies or not. Cynomolgus monkeys are housed in social groups before and during studies. The space requirements are according to the EU directive (DIRECTIVE 2010/63/EU OF THE EUROPEAN PARLIAMENT AND OF THE COUNCIL of 22 September 2010 on the protection of animals used for scientific purposes). The animals live under a 12-hour dark light cycle, have ad libitum access to water and food provided twice daily, lab diet plus fresh fruit. The foremost enrichment is social housing. Additionally mirrors, wooden trunks, balls are supplied as a standard. Further enrichment devices are available and made available on a rotating scheme. The animal welfare officer on site regularly checks the housing and handling conditions. Since animals are housed in groups during the study the individuals are not randomized to the dose group, but rather a stable group of animals created a long time before the study.” [42]

“For the notice of approval by the appropriate institutional animal care and use committee, please see Covance Studies 8260977 and 8274007.”[42, 148] For the ethical statement see our publication [42].

On days one and seven after intravitreal injection, *„the animals were sacrificed*

under general anesthesia, i.e., intramuscular injection of ketamine hydrochloride followed by an intravenous sodium pentobarbitone (Lethabarb, Virbac, Australia) overdose. Only the further investigations: electron microscopy and immunohistochemistry were performed in our lab in Tuebingen. These investigations did not necessitate approval by an institutional review board. Covance Laboratories GmbH test facility is fully accredited by the AAALAC. This study was approved by the local IACUC, headed by Dr. Jörg Luft, and performed in consideration of the following recommendation:

Commission Recommendation 2007/526/EC on guidelines for the accommodation and care of animals used for experimental and other scientific purposes (Appendix A of Convention ETS 123).“ [42]

2. Enucleation and preparation of eye tissue samples

Both eyes of four animals of each the aflibercept and the ranibizumab group were intravitreally injected with the corresponding anti-VEGF drug in the doses that are clinically used in humans: 2 mg of aflibercept and 0,5 mg of ranibizumab, respectively (also provided and recommended by the manufacturers in this formula [153, 154]). For this procedure, which was carried out in the morning, the animals were intramuscularly injected with medetomidine (Domitor) and slightly sedated with ketamine hydrochloride and diazepam. Prior to the injections, the eyes were examined for any signs of inflammation. [42, 148, 150] Then, *„pupils were dilated (Mydriasis with 1% tropicamide) and anaesthetised (proxymetacaine; Proparacain-pos 0.5%; Ursapharm). The conjunctival and corneal surface was disinfected (povidone iodine 10%). After sterile coating and insertion of a lid speculum, 0.5 mg ranibizumab or 2 mg aflibercept were injected into the vitreous cavity using a 27-gauge canula. When removing the canula, the injection site was compressed with forceps to prevent reflux and a topical antibiotic (gentamicin) was administered. Animals were monitored for signs of inflammation until sacrificed.“ [148, 150]*

During the whole duration of the animal experiment, ophthalmic examinations were performed (figure 6). For this, *„a mydriatic agent (tropicamide) and a local*

ophthalmic anaesthetic (proxymetacaine) were instilled in the eyes of the sedated animals before examination.“[148]. These examinations contained macroscopic and slit lamp examinations, direct/indirect ophthalmoscopy (during the predose phase on the day of dosing and on the day of necropsy), funduscopy and fluorescein angiography (FA) (once during the predose phase and on the day of necropsy), spectral-domain-optical coherence tomography (SD-OCT) (once during the predose phase directly after injection (only for aflibercept) and on the day of necropsy) and measurement of intraocular pressure (IOP) (once during the predose phase, before administration of the drugs, directly and 10 min after administration and on the day of necropsy).(A more detailed description has been published in [148]).

After enucleation, the eyes of the treated as well as of the untreated monkeys were slit at the limbus and fixed in glutaraldehyde and cacodylate buffer for electron microscopy or into formalin for immunohistochemistry [148, 150].

3. Analyses of eye tissue samples

Immunohistochemical analysis was performed to detect ranibizumab and aflibercept in retinal sections and in the ciliary body using a goat antiserum to human Fab of IgG (for ranibizumab) and a goat antihuman IgG-Fc antibody (for aflibercept). A secondary antibody (cy3-rabbit antigoat antibody) was needed as well as further primary and secondary antibodies to also detect immune reactivity of astrocytes and activated and non-activated Mueller cells, macrophages and microglia and a hypoxia marker. “*Stained sections were embedded and inspected with a fluorescence microscope (Axioplan2; Carl Zeiss, Oberkochen, Germany).*“[148] (For more details see [148] and [150]). Specimens were prepared for light and electron microscopy following standard procedures (described below). Four different regions per time point were examined: fovea and lateral of the fovea [150] and ciliary body and iris [150]. The areas occupied by the choriocapillaris and free haemoglobin were quantified. Moreover, quantification of choriocapillaris endothelial cell fenestrations and measurement of endothelial thickness were performed and statistically evaluated (for details see [150]). In another study [150] endothelial

fenestrations of the ciliary body were quantified. Then VEGF was immunohistochemically localized in the ciliary body. For this, “a monoclonal mouse anti-human vascular endothelial growth factor, Clone VG1, which labels the VEGF-165, VEGF-121, and VEGF-189 isoforms of vascular endothelial growth factor [...] was used as a first antibody and detected with (a) [...] detection system [...] and inspected with a light microscope (Axioskop; Carl Zeiss, Oberkochen, Germany).“ [150]. These VEGF stainings in the ciliary body were photographed and semi-quantitatively investigated using a light microscope with AxioVision software and the „colour cube based“ function in the Image-Pro Plus software. [150] For quantification of endothelial fenestrations of the vessels of the ciliary body, whole blood vessels were investigated and endothelial length was measured and fenestrations were counted, the ratio fenestrations/10 µm was calculated and statistically analyzed (details in [150]).

Ophthalmic examinations

Parameters and order of examination	General information
Preparation of animals	Sedation by i.m. injection of medetomidine (Domitor) and ketamine hydrochloride, Mydriasis with 1% tropicamide
Macroscopic examinations	Eye and connected tissue
Direct/indirect ophthalmoscopy	Ocular fundus with macula lutea, papilla, ocular vessels and retina
Slit lamp examinations	Anterior and medium segments with conjunctiva, cornea, anterior chamber, iris, lens and vitreous body; fluorescein instillation for epithelial staining
Fundus photographs Equipment used: digital stationary fundus camera from Topcon (trc-50ex)	Instillation of a local ophthalmic anesthetic (Proxymetacain) into both eyes prior to fundus photography; Mydriatikum eye drops for pupil dilatation
Fluorescence angiography , Equipment used: digital stationary fundus camera from Topcon	Once during predose phase, on the day of necropsy
OCT , Equipment used: Spectralis, Heidelberg Engineering	On the day of dosing (before injection), on the day of necropsy (only day1).
Ocular pressure Equipment used: Tono Vet	Predose, before administration, directly after administration, 10 min after administration, on the day of necropsy

Figure 6: Overview of ophthalmic examinations performed and time points.

Figure used with kind permission of Sylvie Julien-Schraermeyer and Ulrich Schraermeyer, first presented at the Novartis Meeting, November 2012.

4. Preparation of kidney and blood samples

Two animals per time point and drug were available as well as one untreated monkey sacrificed on day seven and one monkey injected with aflibercept's vehicle and sacrificed one day after injection that served as controls. The untreated monkey showed aplasia of the left kidney. *„On days one and seven after intravitreal injection, the animals were sacrificed under general anaesthesia, i.e., intramuscular injection of ketamine hydrochloride followed by an intravenous sodium pentobarbitone (Lethabarb, Virbac, Australia) overdose.“* [42, 148, 150] *„The kidneys were extracted five minutes post-mortem. The left kidney of each animal was fixed in paraformaldehyde uncut for immunohistochemistry; a specimen of the right kidneys was dissected into small cube-like pieces with a length of 2–3 mm and then fixed in glutaraldehyde (ice cooled) for electron microscopy (the only available kidney of the monkey described above was prepared for electron microscopy). The kidneys of the monkey without treatment, or with aflibercept's vehicle injection, were handled in the same manner.“*[42] *“Blood samples were taken before injection (predose) and on days one and seven after injection. Platelet-poor plasma was prepared by centrifugation. “*[42]. EDTA tubes prevented blood clotting.

5. VEGF-A plasma levels

„Blood samples of all monkeys were collected in tubes containing EDTA before intravitreal injection (predose) and on day one and seven after injection of anti-VEGF agents, and plasma was prepared by centrifugation, transferred to new tubes and stored at –70 C. Plasma samples were analyzed using commercially available ELISA kits for human VEGF-A (DVE00) (R&D Systems, Minneapolis, Minnesota). Briefly, the microtitration plates were coated with monoclonal antibodies specific for VEGF-A, standards and probes were added, incubated and washed. Then, an enzyme-linked polyclonal antibody specific for VEGF-A was added and its substrate solution followed after a second incubation and wash step. After stopping the colour development, the intensity of colour (Optical Density) was measured by photospectrometry with the lower detection limit of VEGF-A set at 30 pg/ml. Calculation of VEGF concentration was

performed according to the manufacturer's recommendations."[42]

This kit uses human VEGF-A specific antibodies and an enzyme-linked polyclonal antibody specific for human VEGF-A and a substrate solution employing the quantitative sandwich enzyme immunoassay technique. Color develops in proportion to the amount of VEGF bound in the initial step. The color development is stopped and the intensity of the color (Optical Density) is measured by photospectrometry and VEGF concentration is calculated. The lower detection limit of VEGF-A of this array is 30 pg/ml (for more details please see [42, 155]).

6. Immunohistochemistry of kidney samples

(These experiments were performed by Alexander Tschulakow and described in [42])

The aim of the immunohistochemical analyses and fluorescence stainings was to evaluate the distribution of VEGF, aflibercept and ranibizumab in kidney glomeruli of treated animals and the untreated animal serving as control.

The distribution of VEGF was evaluated using primary mouse anti-VEGF antibodies [42]. Also, immune reactivity against the two drugs was tested. For ranibizumab, a primary mouse antibody against the human IgG-Fab- fragment and for aflibercept a primary mouse antibody against the human IgG- Fc- fragment were used [42].

Additionally, using fluorescent antibodies (*"a mouse antibody against the human IgG-Fab-fragment of IgG... and a goat anti-mouse alexa488 labeled secondary antibody [...] were used for ranibizumab staining. Goat anti-human IgG-Fc antibody [...].and a donkey anti-goat alexa488 labeled secondary antibody [...] were used for aflibercept staining."* [42]), an immune reactivity analysis was performed for aflibercept and ranibizumab [42].

The different stainings (VEGF/ ranibizumab/ aflibercept) were quantified using a semi- quantitative computer-assisted method [42]. For each kidney, ten randomly chosen regions containing glomeruli were photographed at a magnification of 400x using a computer software which also assisted in counting nuclei and determining the stained area after the glomeruli were

defined as the area of interest (aoi). For this purpose, several color deconvolution plugs, filters and algorithms for nuclei count were used as widely used for immunohistochemistry analysis [156],[157, 158] and pictures of the control samples served as references. Then, statistical analysis of the calculated ratio of stained area/nuclei was performed and samples were compared (for a more detailed description and pictures please see [42]).

7. Light and transmission electron microscopy of kidney samples

(Sigrid Schultheiss and Tatjana Taubitz performed the procedures described.)

7.1. Fixation

Organic sample material can either be fixed in formaldehyde or glutaraldehyde depending on the planned examination method. For common histological staining methods in light microscopy as well as for immunohistochemistry, organic samples are fixed in (para-) formaldehyde and embedded in paraffin as was performed for the left kidney of each animal in this study. These routine examination methods cannot be applied to glutaraldehyde- fixed specimens for electron microscopy. In this study, the fixation method for light microscopy is also performed with the right kidney of each animal with the aim of being able to assess histological features of the samples as well as to perform immunohistochemical analyses. Moreover, specimens are thus conserved in good quality for further use for a time period of one to two years [159].

“(Glutaraldehyde-fixed) specimens were postfixed with 1% OsO₄ at room temperature in 0.1 M cacodylate buffer (pH 7.4), en bloc stained with uranyl acetate and lead citrate, and embedded in Epon after dehydration in a graded series of [...] (ethanols)” [42, 148, 150]. More details concerning fixation, dehydration and embedding protocol will be described later.

Glutaraldehyde causes cross-linking and fixation of proteins, osmiumtetroxid fixes and colors lipids black. Epon is necessary to make samples sliceable. The staining achieved with lead citrate is called “negative stain” as heavy atoms disperse electrons more strongly and thus enhance contrast [159].

7.2. Preparation for examination and technical equipment

“Semithin sections were stained with Toluidine Blue and examined by light microscopy (Zeiss Axioplan2 imaging, Zeiss, Jena, Germany). For electron microscopy, the sections were cut ultrathin and analyzed with a Zeiss 902 a electron microscope (Zeiss, Jena, Germany)” [42, 148, 150]. In the following I will describe these processes more explicitly.

In figures 7-12, technical equipment needed for the preparation and examination of sample material including the transmission electron micrograph can be seen (light microscope not shown).



Figure 7: Transmission Electron microscope

Transmission Electron microscope Zeiss EM 902a with Digital camera MegaView III
Its height is about 3 meters and it requires a dark room.
Picture used with kind permission of Prof. Schraermeyer.



Figure 8: Ultramicrotom

Ultramicrotom Ultracut Reichert-Jung and electric control device to adjust slide thickness (here $0,7\mu\text{m}$ for semi-thin slides).

Different diamonds are used to cut different thicknesses for light (semithin $0,7\mu\text{m}$) and electron (ultrathin $0,05\mu\text{m}$) microscopy under microscopic control. Slides swim on a water film and have to be fished for further processing.

Own picture.

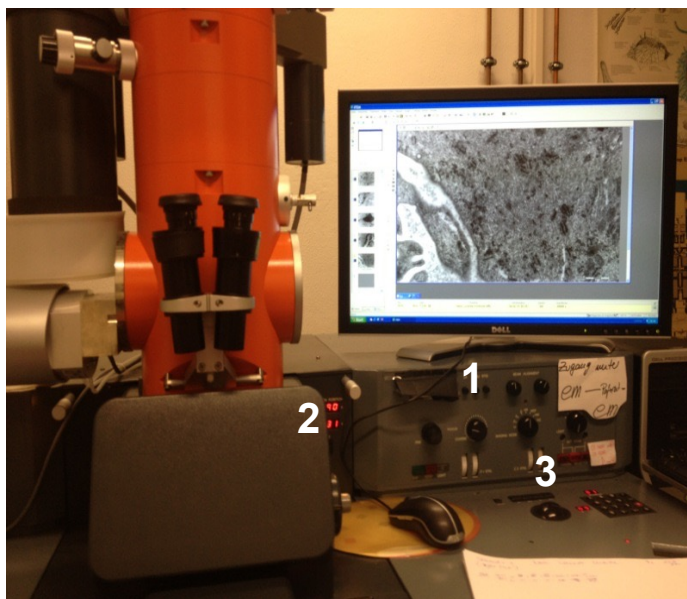


Figure 9: Electron microscope and camera in use

Live pictures are visible with the help of the camera and the monitor

1. Tools to adjust magnification and contrast
2. Grid coordinate display (X and Y)
3. X and Y grid position control keys
4. Side entry to lock in specimens into vacuum

Own picture.

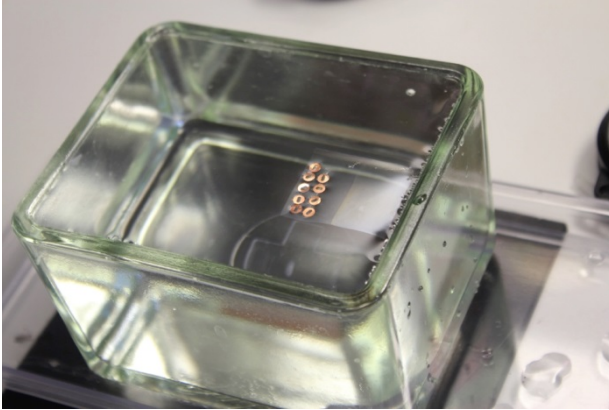


Figure 10: Formvar-coating and preparation of grids for TEM (1st step)

First, glass slides are coated with the support film formvar (a thermoplastic resin in dichloroethane) under a flue (not shown). Then the formvar layer is cut into smaller pieces with a razor blade and transferred to the surface of a water basin filled with aqua dest. Then empty aluminum grids are set in rows on these formvar layers.

Own picture.

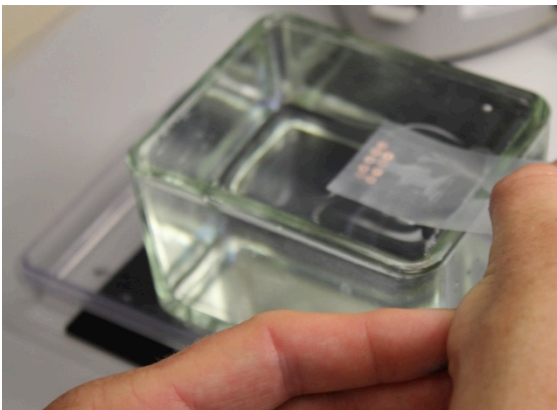


Figure 11: Formvar-coating and preparation of grids for TEM (2nd step)

The upper part of the grid is covered with parafilm (a plastic paraffin film), turned and transferred to a petri dish to dry. Then the grids are ready to be coated with the ultrathin cut slide.

Own picture.

We use formvar-coated one-hole grids (see figures 10+11) for electron microscopy to provide a larger area to examine under the microscope and take pictures although these grids are fragile and have to be treated with care. Other laboratories also use mesh, bar, slot or tabbed grids with the advantage of being more stable and of facilitating navigation within the sample. On the other hand, these grids impair the quality of the pictures obtained and probably make it more difficult to assess histological and pathological features.

Formvar is a thermoplastic resin and forms an electron-transparent film commonly used to support specimens for transmission electron microscopy. Moreover, it offers more radiation resilience but it also provides an unwanted background in the image [159].

A Reichert/ Leica UltraCut E ultramicrotome (see Figure 8) is used to cut semi-thin (for light microscopy) and ultra-thin (for TEM) sections of resin-embedded biological specimens. For cutting, glass and diamond knives are used. First, the plastic block is clamped in the ultramicrotome, and then trimmed so that the sample location is optimally cut (pyramid). For semi-thin sections and ultra-thin sections, the slide thickness can be exactly adjusted with an electric control device (see Figure 8) to $0,7\mu\text{m}$ or $0,05\mu\text{m}$, respectively. After cutting, the sections float on the water and can be caught with an eyelet to be further processed for light microscopy. For electron microscopic processing, a grid has to be placed angularly under the floating section so that the section is attached when the grid is slowly pulled out of the water.

It should be noted that these procedures have to be performed under microscopic control.

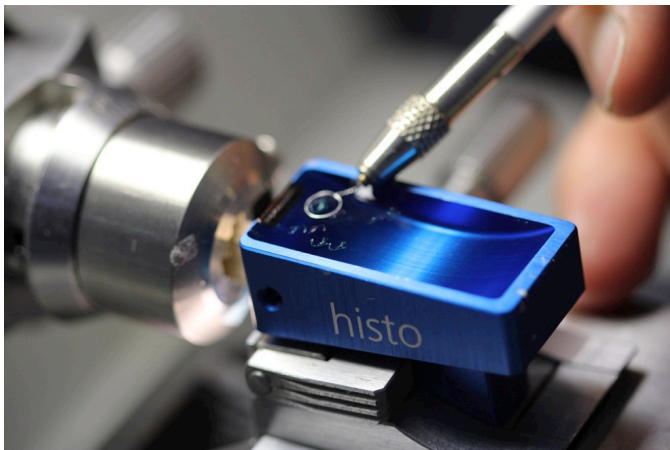


Figure 12: Ultramicrotome

After trimming of the block (pyramid), a semi-thin slide ($0,7\mu\text{m}$) has been cut with the ultramicrotome (Reichert/ Leica UltraCut E) using a diamond knife and is being captured from the water surface with an eyelet to be transferred to a glass slide to dry before staining with Toluidine Blue for light microscopy (see below).

Ultramicrotome (Reichert/ Leica UltraCut E); Own picture.

For transmission electron microscopy, slides are cut ultrathin (0,05 μm). For staining with lead citrate, the ultrathin slide has to be captured with a formvar-coated grid and dried (process not shown).

7.3. Staining

Toluidine Blue staining for light microscopy

Toluidine Blue (0,5% Toluidine Blue with 2,5% NaHCO_3 1:1) stains membranes and nuclei (Figures 13-15). Light microscopy allows better orientation within the sample and excludes pathologies.

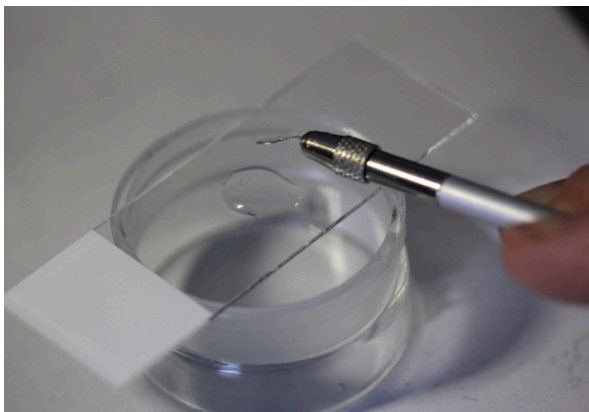


Figure 13: Toluidine Blue staining of kidney specimens for light microscopy (1st step)

The slide captured from the water basin of the ultramicrotome (see figure 12) is set on a drop of aqua dest on a glass slide.
Own picture.

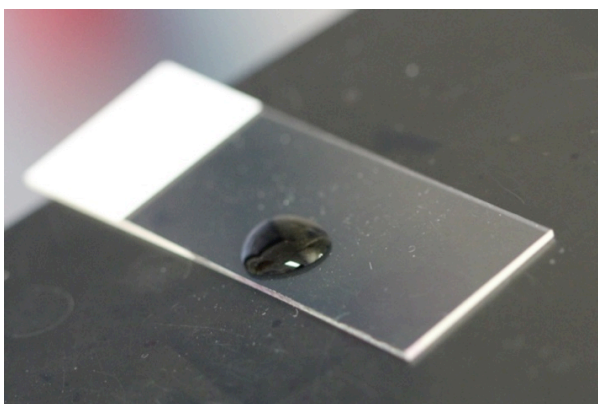


Figure 14: Toluidine Blue staining of kidney specimens for light microscopy (2nd step)

After the water has evaporated at 80°C, a drop of Toluidine Blue mixture (0,5% Toluidine Blue with 2,5% NaHCO₃ 1:1) is applied for 1 minute, then first rinsed with water, then with aqua dest. In the following it is covered with one drop of epon and kept at 60°C overnight.
Own picture.

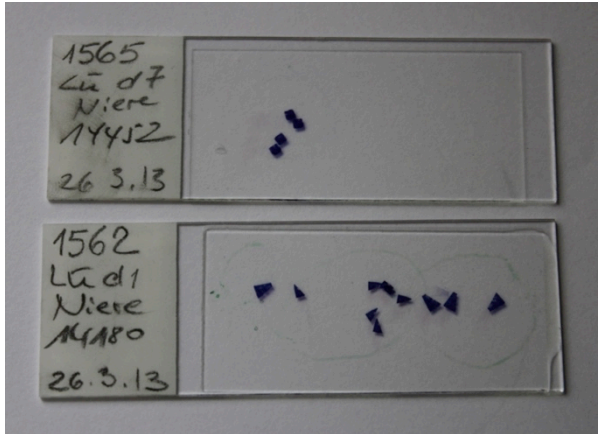


Figure 15: Toluidine Blue staining of kidney specimens for light microscopy (3rd step)

The semi-thin slides on glass slides ready for light microscopy. Here Lucentis (ranibizumab) days 7 and 1. Numbers from top to bottom: Block number, specimen: medicament, day and organ, slide number, date of preparation of slide.
Own picture.

Lead citrate staining for transmission electron microscopy

Post-staining of sections is optional in electron microscopy (Figures 16-17). The indication depends on the purpose of the analysis. If the aim is mainly to take qualitatively good pictures and perform ultrastructural analyses or counting of fenestrations as in my case, contrasting with heavy metal ions is useful to represent the structures (membranes, vesicles.). But as this technique doesn't allow antigen-antibody binding it cannot be applied in immunohistochemistry [159].

The grid loaded with the ultra-thin slide captured from the water basin of the ultramicrotome (see figure 12) is first dried for at least one hour. Then, it is placed on a drop of lead citrate ((0,1g/ 25ml+ NaOH) on a parafilm. After this, the sections have to dry again for 24 hours. The described procedures of fixation, cutting and staining are concluded in figure 18.

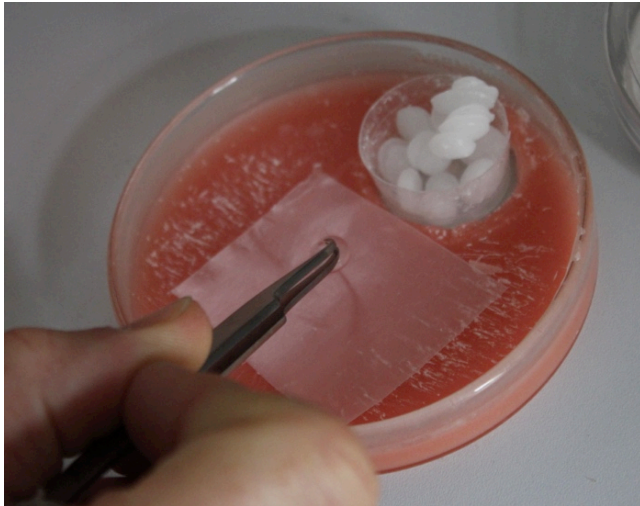


Figure 16: Lead citrate post-staining for transmission electron microscopy (1st step)

Own picture.



Figure 17: Lead citrate poststaining for transmission electron microscopy (2nd step)

Own picture.

Preparation of samples for light and electron microscopy

1) Fixation and Embedding

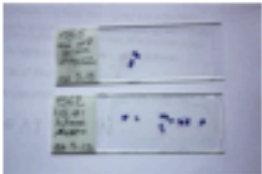
- **Fixation:** glutaraldehyde 5% in 0,1M cacodylate buffer agent (1 h ice / 4°C, overnight)
- 3 wash steps in 0,1M cacodylate (10 min each, room temperature)
- **postfixation** in 1% osmiumtetroxid in 0,1M cacodylate (room temperature, 2 h)
- 3 wash steps in 0,1M cacodylate (10 min, room temperature)
- **dehydration part 1:** 30 – 50 – 70% ethanol, (15 min each, room temperature)
- **en-bloc staining:** Uranylacetat 3% in 70% ethanol (over night, 4°C)
- **dehydration part 2:** 70 – 80 – 95% ethanol (70% for 24 hours, 4°C, rest :15 min each, room temperature)
 then 2x 100% ethanol (20 min each, room temperature)
- **embedding** in epon: 2 times in propylenoxide (20 min, room temperature)
 1 time in propylenoxide and epon 1:1 (2 h, room temperature)
 2 times in epon (first 2 h, then 1 h, room temperature)
- **polymerisation** in bins: first 12 h at 45°C, then 24 h at 60°C

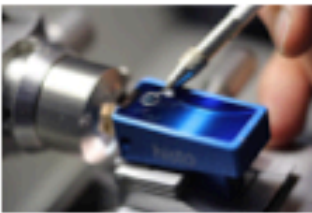
2) Cutting of slides

semi thin (0,7µm)

•
staining with
Toluidine Blue
(0,5% Toluidine
Blue with
2,5% NaHCO₃ 1:1)

**light
microscopy**






ultra thin (0,05 µm)

••
staining with
lead citrate
(0,1g/ 25ml+ NaOH)

**electron
microscopy**








Figure 18: Preparation of glutaraldehyde fixed specimens for light and electron microscopy

The figure shows the procedures as performed in the laboratory of the eye hospital Tübingen at the time of preparation of the kidney samples for this study.

*For details of Toluidine Blue staining see figures 13-15

**For details of filming of the one-hole grids with the help of formvar- films before staining with lead citrate see figures 16-17

Own pictures, composition and description similar to a work instruction in the section for experimental vitreoretinal surgery of the eye hospital Tübingen, adaption by kind permission of Prof. Schraermeyer

7.4. Transmission electron microscopy (TEM)

(The major source of information for the following is the script “Instructions for the internship Analytical Electron Microscopy for natural and life sciences“ [159] of Prof. Dr. O. Eibl (Institute of Applied Physics) and Prof. Dr. U. Schraermeyer (University Eye Hospital) edited January 27, 2014 containing information from the following sources: [160-171].)

Transmission electron microscopy is an exclusive and also cost-intensive research method. Technically sensitive, preparation of samples is complex and needs specialized experienced personal. There are only a few scientific institutions owning and working with an electron microscope, thus studies and scientific issues have to be planned thoroughly and users have to work accurately as sample numbers are limited and very fragile (with one grid having a diameter of about 3mm [172]). Moreover, the time for viewing one piece of specimen is limited before the focused area is destroyed by the electron beam. But to follow up complex ultrastructural considerations it offers unique possibilities due to its high resolution of 0,5-0,2nm [173] and the trend is even higher (0,1nm) in modern devices which is in the range of the size of atoms [159].

Figure 19 shows the setup of a transmission electron microscope.

“The finding that rotationally symmetric electric and magnetic fields act as lenses for charged particles“ [159] was the beginning of electron optics [159]. In electron microscopy, these lenses are used to guide high energetic electrons [159]. The basis of electron microscopy is the interaction of primary electrons with the atoms in the sample [159]. In the TEM free electrons are generated and accelerated to energies around 150keV [172]. Then, „an (ultrathin) specimen is irradiated with an electron beam of uniform current density“ [173]

where electrons are partly scattered. Specimens have to be cut ultrathin to avoid too much scattering and absorption of electrons [172].

The microscope operates under a vacuum in order to prevent electrons from being additionally deflected [172]. Thus, specimens fixed on grids (see above) have to be locked in (side entry in our microscope see Figure 9). The electrons provided by a heated wolfram cathode are accelerated by a high voltage source [172]. They are deflected by the condenser lens system so as to provide illumination uniformity with the electrons hitting the specimen nearly parallelly. Having passed the specimen, the electrons change their direction due to different interactions with the atoms contained (the most important ones are: elastic and inelastic scattering; also: generation of x-radiation) [172]. The contrast of the obtained image depends on the kind of the specimen (solid, amorph, crystalline, metals, organic....) as electron-specimen interactions differ between materials due to different nuclear composition [172].

Elastically scattered electrons are responsible for the majority of the resulting contrasts. Heavy atoms scatter electrons more strongly than light ones; a higher density of atoms in a volume scatters more than a smaller amount of atoms in the same volume [159]. Two types of imaging can be distinguished: Dark-field image and bright field image microscopy depending on whether the beam of unscattered (bright field) or scattered (dark field) electrons is used to produce the image [159]. In the most commonly used bright-field image, heavy atoms and densely packed atoms appear dark. Staining with heavy metals allows identification of cell components in biological material [159]. Our samples are stained with lead citrate.

The main lens of each electron microscope is the objective lens close to the specimen. The objective lens system generates an intermediate image which is magnified by the following lenses [159]. In the objective aperture in the back focal plane of the objective lens, a specific ray is manually selected for imaging which enhances the contrast of the image [159]. This is also called the contrast aperture and decides on the imaging mode depending on whether the transmitted beam is selected (bright-field image) or the diffracted beam is selected (dark-field image) [159].

The projective lens system, which forms the next level, casts the first intermediate image generated by the objective-lens-system on a detector and magnifies it. This detector can be a fluorescent screen for direct observation or a camera (as we perform with the MegaView III camera in addition to the possibility of looking directly at the image). *Note that all the TEM pictures shown in my work are bright-field camera images of lead citrate poststained samples.*

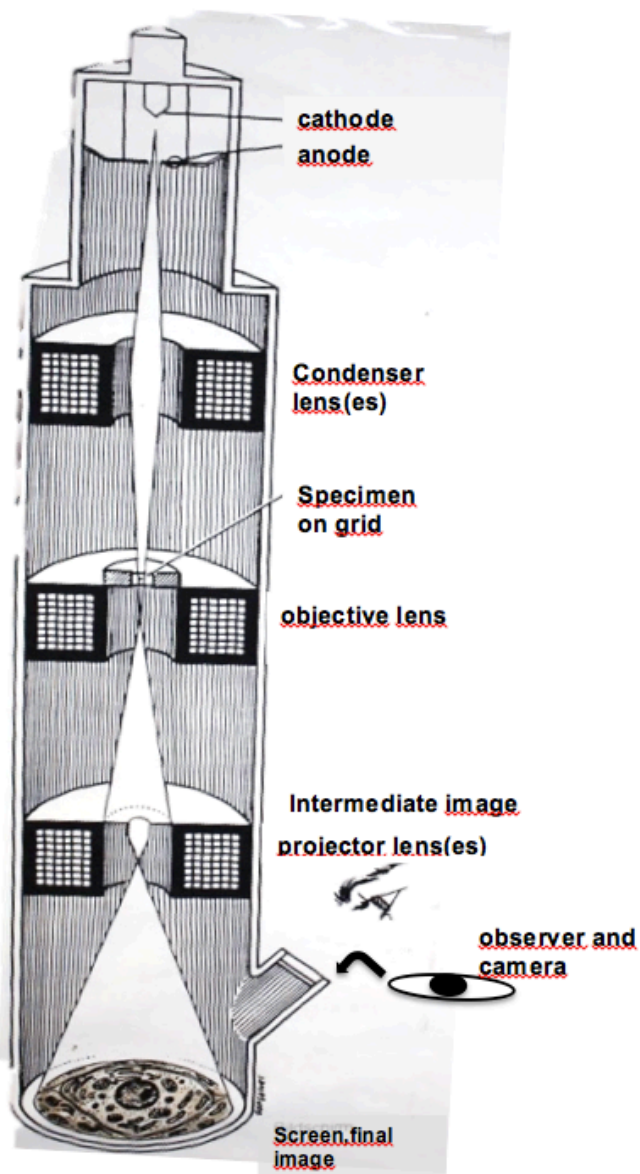


Figure 19: Schematic composition of a transmission electron microscope (TEM)

Picture probably taken from manufacturer's manual, image serving as illustrative material in the room used for electron microscopy, with kind permission of Prof. Schraermeyer, modified.

8. Quantification of the glomerular endothelial fenestrations

“Under the light microscope at a low magnification (x10) glomeruli were identified in semi-thin sections and checked (for) mechanical or fixation artifacts and pathological features at a higher magnification. Three glomeruli per kidney (six per time point for ranibizumab and aflibercept, three for controls) with middle to large diameter and intact bowman’s capsules were chosen and cut ultrathin for electron microscopy. After examination of the ..(samples) at a magnification of 3000 fold, montages of transmission electron micrographs were performed by using the multiple image arrangements (MIAs) in order to provide montages of the entire glomeruli (figure 20). The montages consist of overlapping images that were taken using an image analysis software (iTEM, Olympus Soft Imaging Solutions, Muenster, Germany). Similarly to a previously described method [145], high- magnification images were taken from the chosen glomeruli according to a systematic uniform random sampling protocol (SURS). Starting at the top-most portion of the glomerular tuft, x 20.000 images were taken moving the position of the thin section grid with the help of the X and Y grid position control keys. For this purpose, the grid was moved ten units horizontally taking a picture at each stop point until the opposite portion of the capsule was reached. Then the position of the grid was moved 10 units vertically and 5 units to the right or left, respectively. This procedure was continued until the entire glomerular profile was scanned through (published in [150], also see figure 21). After pictures were scanned through for artifacts by a blinded observer, high- magnification images were used for quantification of glomerular fenestration using a counting tool of the iTEM software. Only pictures on which glomerular endothelium was undoubtedly identifiable were analyzed. A line was drawn and measured along the lamina rara interna of the endothelial basement membrane adjacent to the fenestrated endothelium and fenestrations were counted by a single observer under standardized conditions. As capillary walls can be divided into peripheral and mesangial regions [145], only peripheral portions where glomerular basement membranes and capillary walls show parallelism were considered. We found that the quantification in the mesangial portions is not comparable to the peripheral parts as the

predominant amount of mesangial endothelium is not fenestrated whereas on the other hand there are parts with increased fenestration (as described as “alveolus fenestratus endothelialis” by Kondo et al. [174]). Thus, this endothelium is morphologically not comparable to the single layered endothelium in the peripheral portions so that applying the same quantification method would not be admissible (published in [150] , see also figure 23 A+B). Therefore, the mesangial portions were excluded from the quantification of the fenestrations” [42].

The random character of the analysis is of importance as well as the standardized protocol to obtain pictures of each glomerulus. This is an objective procedure and it regulates which parts of the capillaries are evaluated. Measuring the diameter/endothelial length of each capillary and counting the fenestrations to obtain the ratio fenestrae/ μm as performed for the choriocapillaries in other studies (for example [150]) wouldn't be applicable as glomerular capillaries are much larger than those of the choriocapillaris and as magnification has to be as high as 30 000 to be able to quantify the fenestrations. The bowman capsule can be easily identified even by inexperienced observers (see Figure 22) and represents the end of each line of the SURS protocol. The Zeiss EM 900 possesses two operation units to select sample areas: a trackball for fine steps and X and Y grid position control keys for large steps. To perform this systematic uniform random sampling protocol (SURS) the second mentioned operation unit is indispensable as has already been proposed by other authors [145].

With the method performed, a high number of pictures are taken in a time-efficient way, which protects the samples from major damage and permits re-evaluating if necessary, and the taking of the multiple image arrangements (MIAs) in order to provide an overview of the entire glomerulus. In order to maximize the chance to unequivocally identify the fenestrations of the endothelium, first the pictures for the counting analysis were taken, then those for the overlapping MIA's. This compromise can be seen in the montage images (for details see figures 20-26 and Results section below).

But the even more important aspect of the SURS analysis method performed is

that it is left to chance as to whether the fenestrated endothelium is captured or not. This feature makes the examination method observer-independent. Moreover, the method is reproducible even though the results obtained for a single specimen are not as it is technically nearly impossible that a grid is positioned in the grid holder of the electron microscope at the same place twice. This is another point that makes it necessary to perform all planned examination methods at one time on one grid.

MIA's have to be performed to get a good overview of the examined glomerulus. With one glomerulus having a size of about 200 μm [51], the low magnification necessary to capture the whole structure would reach the limits of what is possible with a transmission electron microscope. Moreover, overlapping pictures as performed with the MIA's offer a much higher resolution and thus make it possible to assess possible pathologies.

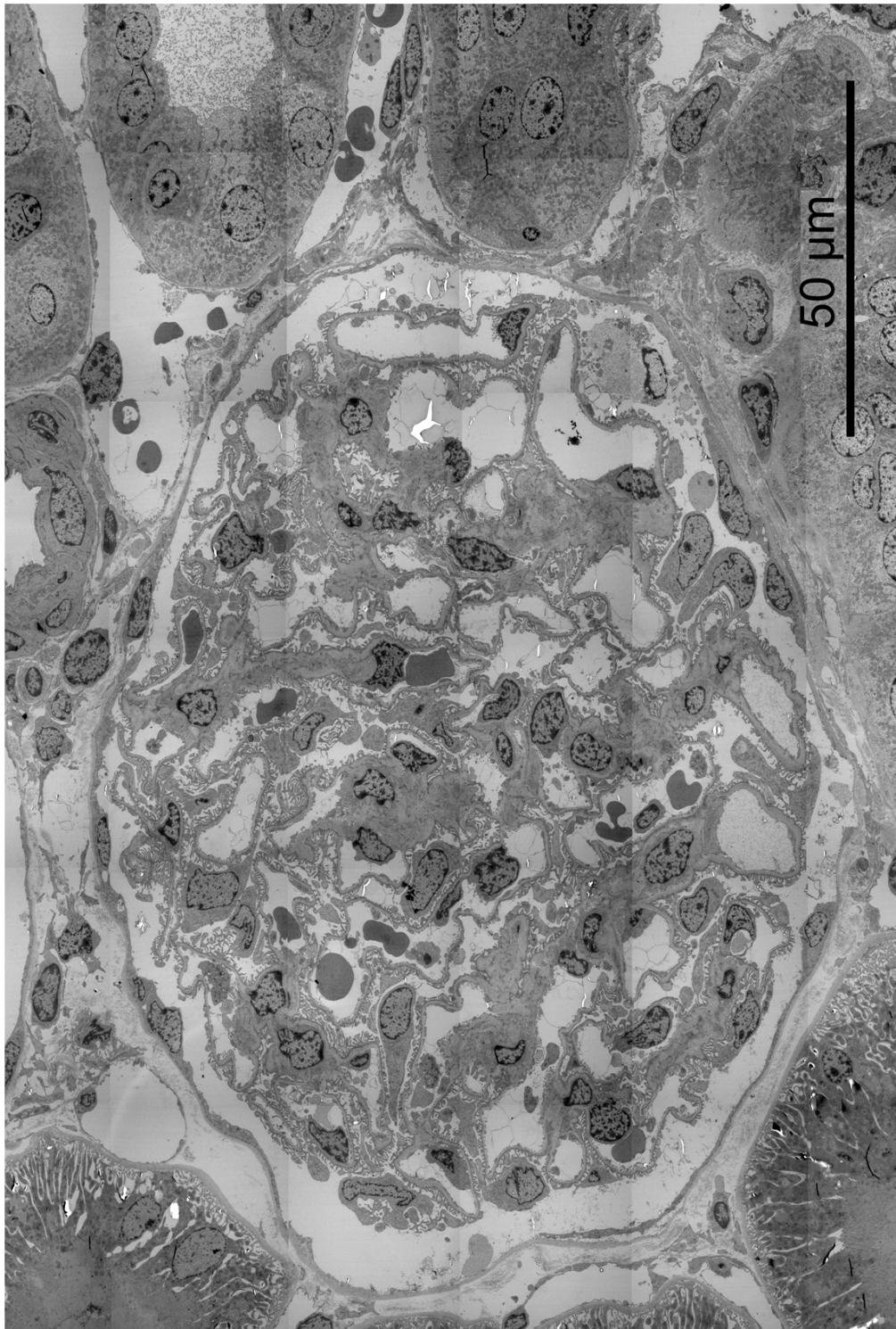


Figure 20: Example of a MIA

„Example of a montage of transmission electron micrographs by using multiple image arrangements (MIAs) in order to provide the entire renal glomerulus. These images were taken using the image analysis software iTEM at the magnification of 63000. Here one day after aflibercept injection“ [42] Note also the proximal and distal tubules and collecting tubules/ ducts can be seen.

Own image, figure and legend published in [42].

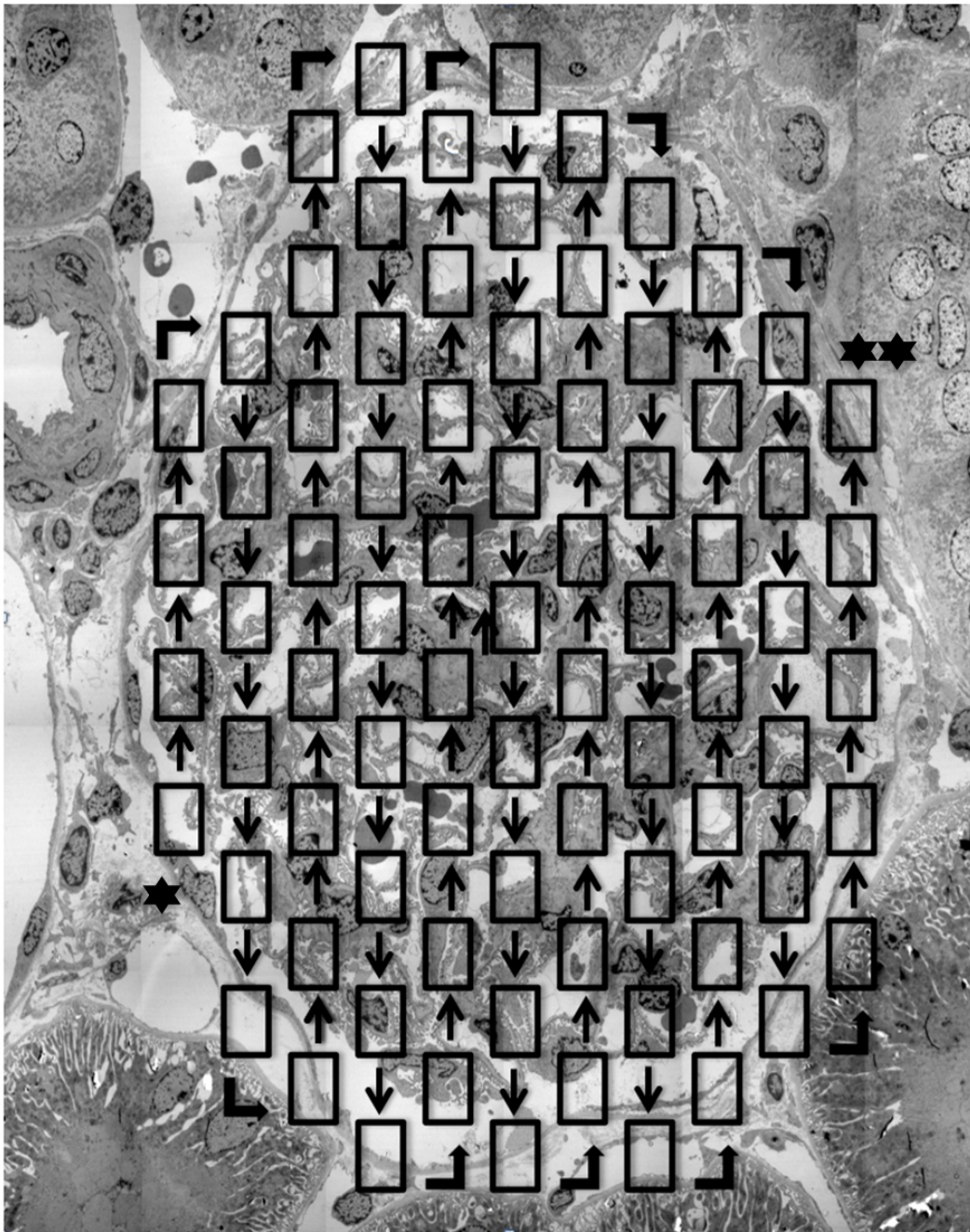


Figure 21: Demonstration of the SURS method on a MIA

“Demonstration of the systematic uniform random sampling protocol (SURS) on a multiple image arrangement (MIA). Transmission electron microscopy, magnification $\times 3000$. Sample: Aflibercept day 1, Glomerulus 1. Asterisk marks starting position (first picture), double asterisks mark end position (last picture), arrows mark direction into which SURS was performed.” [42]
Own image, figure and legend published in [42], modified.

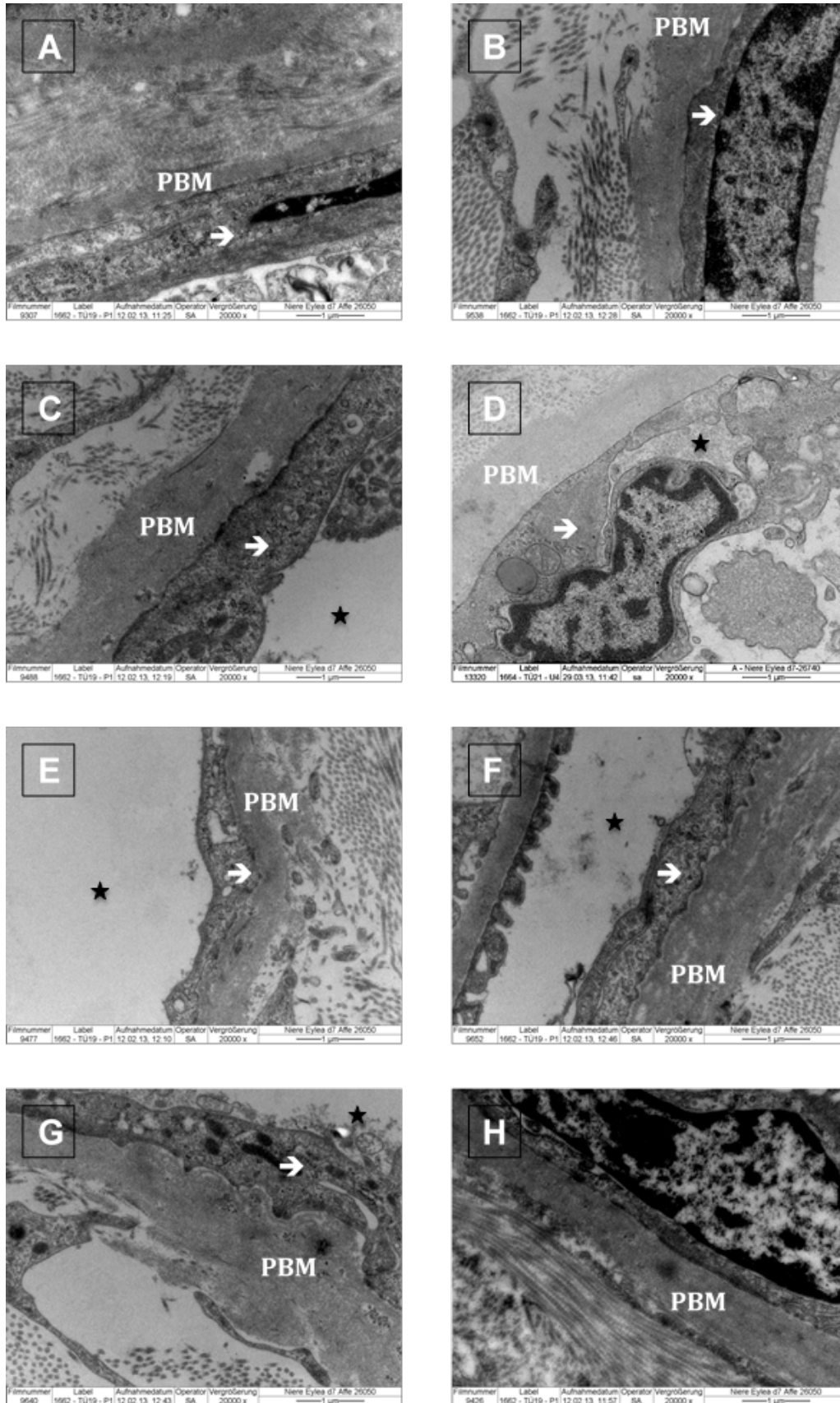


Figure 22: Recognition of Bowman capsule during SURS protocol

The images were taken performing the SURS protocol in glomeruli of Aflibercept day 7, images are uncut. The shown images mark stop points of rows performed in x-direction before moving the grid vertically in y-direction. Once having identified the glomerulus at low magnification (not shown), certain ultrastructural characteristics make it easy to identify Bowman's capsule even for inexperienced observers in spite of the small image section seen at this magnification of x20000:

- the parietal layer of Bowman's capsule (**arrows**) is easy recognizable. In most cases, either pericytes or nuclei can be seen. Note that parietal cells exhibit a cilium and show numerous vesicles and intermediate filaments [51] (see C,D,E,F,G). They have also been described as "parietal podocytes" at the vascular pole of the human glomerulus by Gibson *et al.* [175] as they resemble visceral podocytes
- also, the urinary space/capsular space (**asterisks**) separating the parietal and visceral layers of Bowman's capsule can easily be seen
- the basement membrane of the parietal endothelial cells (**PBM**=Parietal basement membrane) is considerably thicker than the glomerular basement membrane
- in contrast to the GBM (consists of lamina rara interna, lamina densa, lamina rara externa), the PBM contains an outer lamina reticularis with a high amount of reticular fibers. Moreover, collagen is seen in the interstitial space below the PBM. These fibers are a very good marker no matter if they are cut longitudinal or transverse. As soon as a high amount of collagen fibers is seen close to the glomerulus, the direction of the SURS protocol can be changed with fibrosis being excluded by former ultrastructural analyses of the interesting areas

If in a rare case the image does not hit Bowman's capsule and is taken further laterally, no parts of the glomerulus are identifiable. Then the tubular basement membrane can be seen as the glomerulus is always accompanied by proximal and distal tubules.
Own images, sample: aflibercept day 7, three different glomeruli.

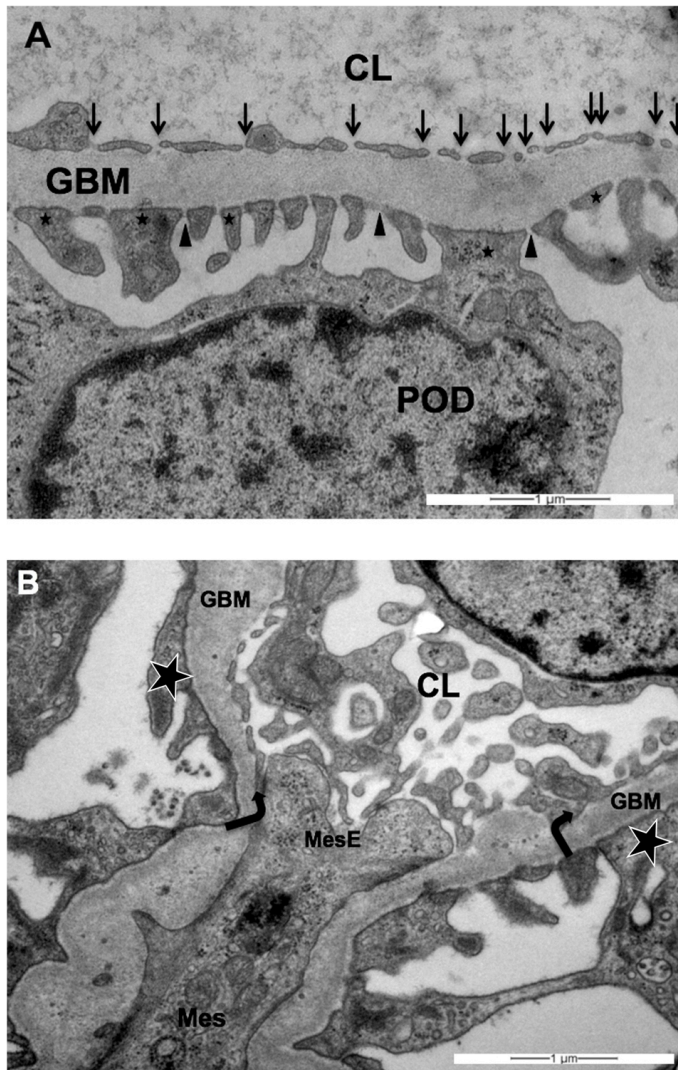


Figure 23: TEM Example to distinguish between peripheral and mesangial portions

„Examples of representative transmission electron micrographs of (A) a fenestrated glomerular endothelium and of (B) peripheral *versus* mesangial portions of the glomerular endothelium (both one day after aflibercept injection).

(A) Blood lumen on the upper part, urinary space on the lower part of the image. The healthy glomerular filtration barrier consists of three layers [67]: the fenestrated glomerular endothelial cells, the intervening glomerular basement membrane and the podocyte processes and slit diaphragm. GBM= glomerular basement membrane, CL= capillary lumen, POD= podocyte. Arrows mark glomerular endothelial cells fenestrae (note the absence of diaphragm), asterisks mark podocyte foot processes, arrowheads mark podocyte slit diaphragm.

(B) At this magnification, podocyte foot processes (asterisks) allow the clear identification of the capillary lumen (CL). In accordance with our definition, the peripheral portion begins where the endothelium and the glomerular endothelial basement membrane (GBM) run approximately parallel (marked by arrows). Arrows mark the direction into which the peripheral endothelium begins. In between the arrows the mesangium (Mes) and the mesangial portion of the capillary endothelium (MesE) is located. Note that in the mesangial portion there is no GBM adjacent to the fenestrated endothelium so that the counting method described is not applicable and the endothelium does not show the typical single-layered configuration. Magnification $\times 20000$.“ [42] Own images, figures and legends published in [42], modified.

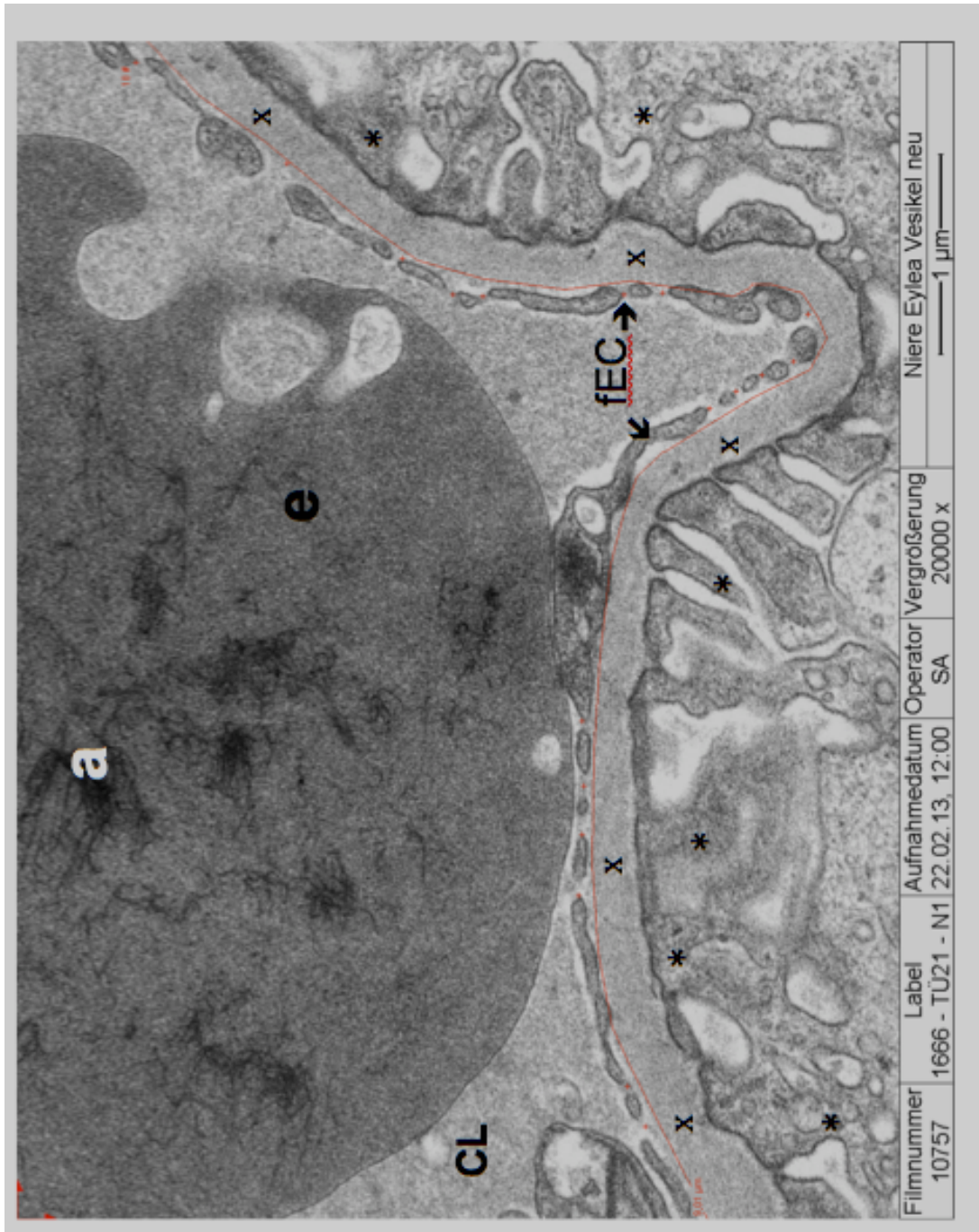


Figure 24: Demonstration of the estimation of the ratio fenestrae per μm

Demonstration of the estimation with the counting tool of the iTEM software

The red line is manually drawn along the lamina rara interna of the endothelial basement membrane adjacent to the fenestrated endothelium. A single observer under standardized conditions counts fenestrations manually (red crosses). Here: 18 fenestrations per 9,01 μm endothelial length. Then the program calculates the ratio fenestrae per μm automatically and provides a table and a statistic. **Asterisks** mark primary and secondary podocyte processes, **X** marks glomerular basement membrane, **e**= erythrocyte, **fEC** and **arrows**= fenestrated endothelial cells, **CL**=capillary lumen, **a**= artifacts.

Own image, sample: aflibercept vehicle, glomerulus 1.

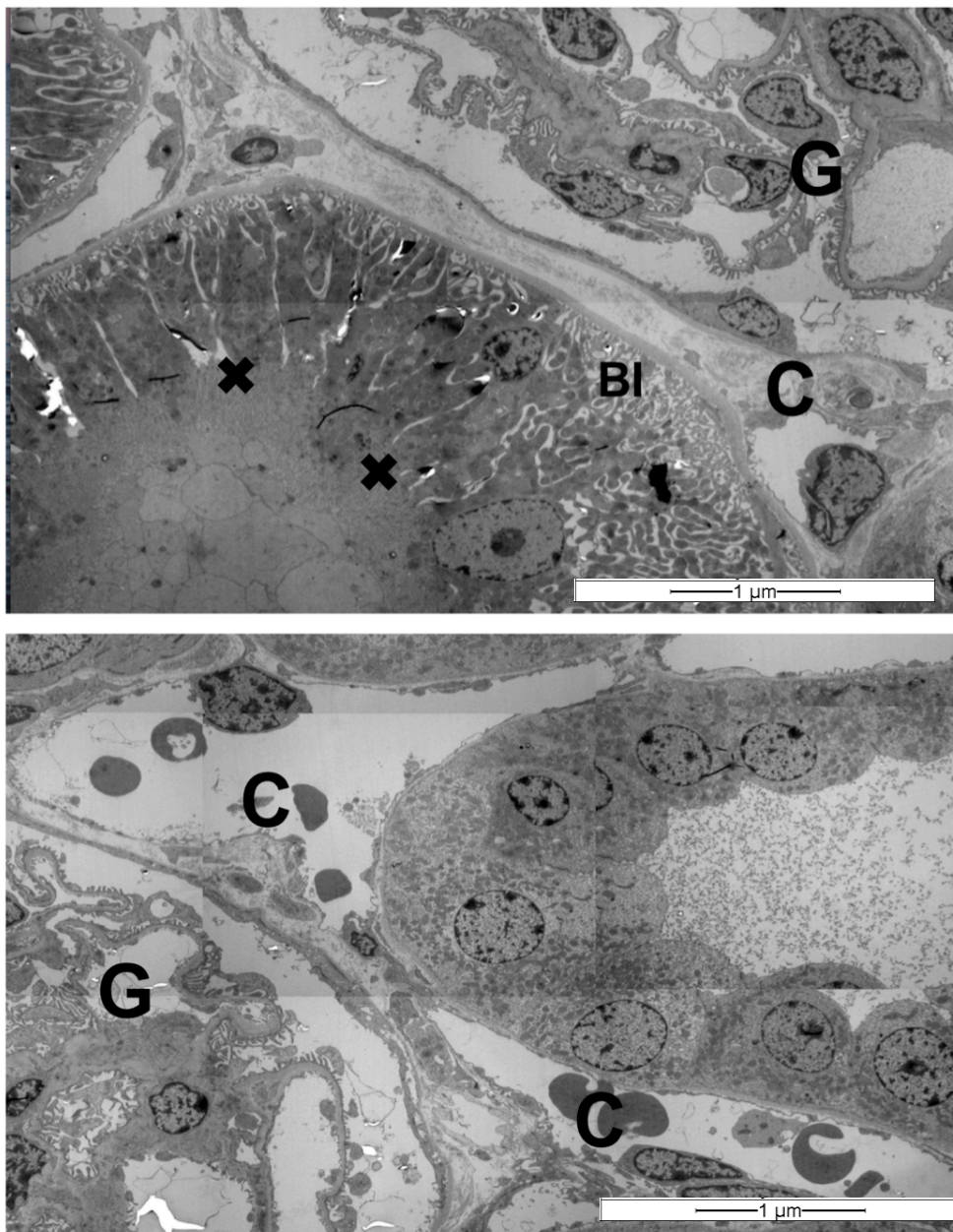


Figure 25: Examples for surrounding structures of the glomerulus

First image: Magnification/ detail image of figure 20 (bottom left part):

Part of a proximal tubule with typical brush border (**crosses**) and basal infoldings (**BI**) with a high amount of mitochondria.

Second image: Magnification/detail image of figure 20 (upper right part):

Part of a distal tubule. Note that there is no brush border, the diameter is apparently smaller and the epithelium lower than in A. Also, the lumen appears larger and cell borders are better recognizable than in the proximal tubules.

Note also the interstitial /connective tissue between the tubules and between tubules and glomerulus (**G**) with peritubular capillaries (**C**) (partly with erythrocytes)

Own images, detail images of figure 20 (MIA), sample: Aflibercept day 1, magnification x3000.

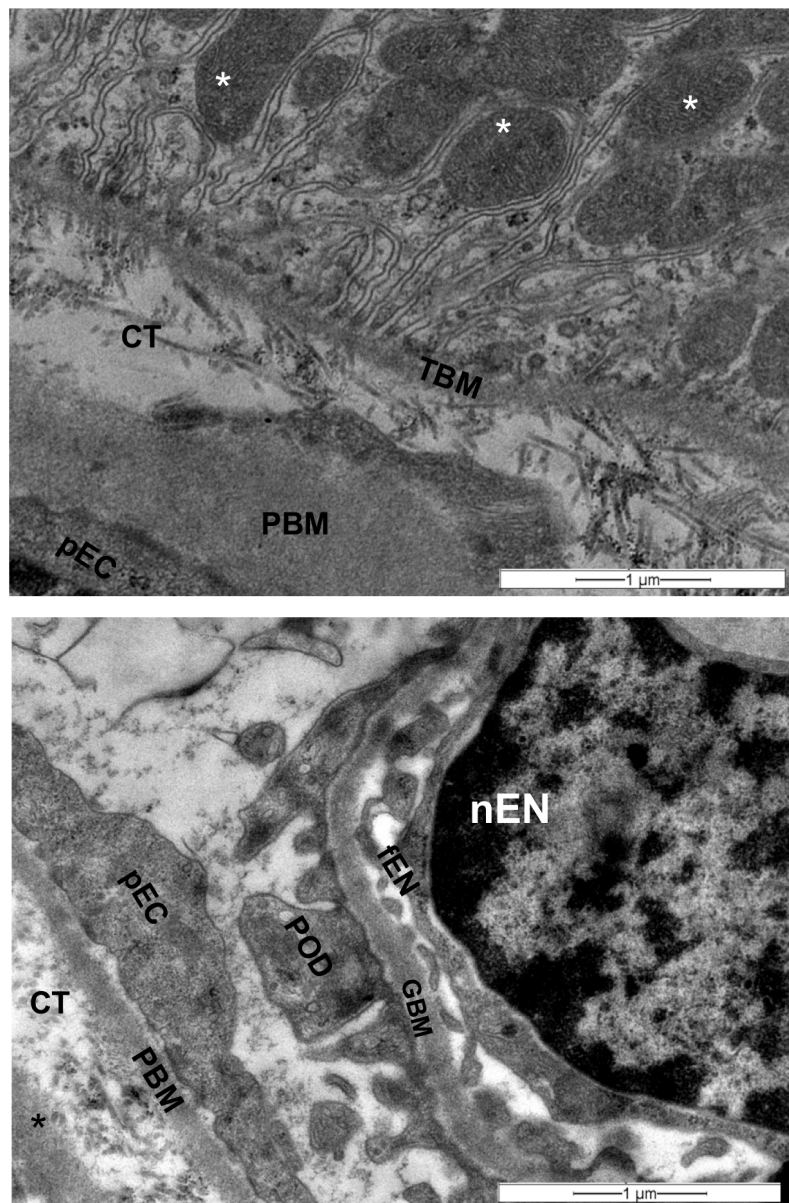


Figure 26: Details of surrounding structures and Bowman's capsule at higher magnification

First image: transition zone of the glomerulus(bottom) to a proximal tubule (top). Note the multiple basal infolding of the basement membrane of the proximal tubule (**TBM**) and the high amount of mitochondria (**asterisks**). Also, parts of connective tissue (**CT**) and the basement membrane of the parietal layer of bowman's capsule (**PBM**) can be seen.

Own picture, sample: Aflibercept day 1, magnification x20 000

Second picture: another example of the transition zone. Here, part of a glomerular capillary with podocyte foot processes (**POD**), glomerular basement membrane (**GBM**) and fenestrated endothelium (**fEN**) as well as a part of a prominent nucleus of an endothelial cell (**nEN**) can be seen. On the lower left part of the picture the parietal portion of Bowman's capsule (parietal epithelial cell =**pEC**, parietal basement membrane= **PBM**) and connective tissue (**CT**) as well as the basement membrane of the following structure (**asterisk**) can be seen.

Own image, sample: Aflibercept day 1, magnification x20 000.

9. Statistical analyses of fenestrae per μm

„The ratio of fenestrae per μm was calculated using Microsoft-Office-Excel for each image considered. Statistical significances for the evaluation of the (number of) fenestrae per μm of the glomerular capillaries and for the quantification of VEGF as well as ranibizumab/aflibercept were determined by using the Student's t test from the JMP10 statistical program (SAS, Heidelberg, Germany). $P < 0.05$ was considered statistically significant.“ [42]

The image analysis software (iTEM, Olympus Soft Imaging Solutions, Muenster, Germany) automatically calculates the ratio of fenestrae/ μm when the analysis is manually performed with the counting tool. These data were exported to Microsoft Office Excel 2011 and to the JMP statistical program (SAS, Heidelberg, Germany, Versions 10 and 13). Charts were generated using JMP software. For descriptive statistics, common values (arithmetic means, medians, standard deviations, standard errors, confidence intervals) were calculated and distributions of values were analyzed via histograms. For statistical evaluation of data and especially comparison of groups, analysis of variance (ANOVA), Student's t-test and Tukey Kramer HSD test were performed with the level of significance conventionally set at $\alpha = 0.05$. Also, power and sensitivity of the tests were calculated and critically regarded as well as the study design and sample collection and size. In the following, the applied statistical terms and techniques are briefly summarized..

One aim of statistical analysis is to estimate the population mean. For this purpose, different values can be calculated. **The arithmetic mean** is the average of a collection of values. It is calculated as the sum of the values divided by their number [176]. Another statistic that can be calculated is the **median**. The median is the one observation which divides the sample into two equal groups with at most half of the values falling below and at most half of the values above it [177]. There are two important differences between these two values: In a normal distribution (see below), the variance of the mean is smaller than the variance of the median resulting in a higher precision of the mean. On the other hand, the mean can be more greatly affected by outliers than the median [176].

Variance, Standard deviation, standard error

“Variance is the expected squared deviation of a random variable from its expected value [...] standard deviation is the square root of the variance” [176].

Standard error is an estimation for the standard deviation of the mean [177].

Box Plots

„The box part [...] surrounds the middle half of the data. The lower edge of the rectangle represents the lower quartile, the higher edge represents the upper quartile, and the line in the middle of the rectangle is the median [...] the lines extending from the box show the tails of the distribution [...] these lines are also sometimes called whiskers [...] points farther away are shown individually as outliers” [176].

Gaussian distribution

This distribution, also called normal distribution is often applied to describe the dispersion of data, especially the natural variability [177]. The dispersion around the average value is here a consequence of a variety of independent factors with an additive influence on each other [177]. Also, normal distribution of values within a sample is the basis for mathematical terms of numerous analytic methods (for example analysis of variance, T-test) [176].

As is necessary for a qualified scientific analysis, as many factors as possible influencing and deranging the result were eliminated with the aim of seeing the influence of the only variable of interest: the injected drug. Choosing comparable monkeys, housing them under standardized conditions and the coincidental assignation to the aflibercept, ranibizumab or control group achieved this. In addition, the injection and examination procedures of the animals followed a strict protocol and were performed at the same time points. Concerning the preparation and analysis of the samples, they were technically all treated the same way following the protocol of our work group (see figure 18) and images were randomly taken following the SURS protocol (see figure 21) and analyzed following distinct criteria.

The greater the dispersion, the flatter the distension of the bell-shaped curve

[177]. On its left and right, the curve asymptotically approaches the x-axis. The peak value of the curve is the expected value, the two points of inflection of the curve are located one standard deviation from the expected value [177].

Confidence interval

The confidence interval is a tool to indicate how exactly the expected value can be estimated by the arithmetic mean. The confidence interval is computed from a sample and is a range which contains the expected value with a given probability. This probability is generally 95 % and the confidence interval thus as large to contain the expectation value with the probability of 95 % [177]. If the sample is small, the estimation of the expected value underlies high imprecision. Hence, the confidence interval has to be larger [177]. The smaller the confidence interval can be set, the more precise is the estimation of the expected value.

P value

This value is used in statistical programs like the SAS JMP statistical program and is used for inferential analysis.[177]. The p-value can be declared as “the probability of being wrong if you declare an effect being non-null” [176] or the “significance probability” [176]. P-values below the set alpha-level (in my case alpha was set 0,05 as generally accepted) reject the null hypothesis, meaning that the probability of having an effect is very high [176] or the probability of being wrong when deciding for a non-null-effect is below 5 %. In terms of statistics, a p value less than 0,05 is thus regarded as significant [176].

Analysis of variance (ANOVA)

One method to compare means of different groups is the ANOVA analysis (short for: “one way analysis of variance”), with the F test as its main element. It is usually used when more than two groups are compared [176]. The chart of this analysis (see Results section) displays the group means and the 95% confidence intervals as diamonds [176]. If these diamonds „do not overlap, the groups are significantly different“ [176]. For further determination of the difference of the group means, an analysis of variance and a t-test have to be

performed.

The analysis of variance leads to an F ratio and determines whether the “separate-means model” or the “grand-mean model” fits better meaning in which estimation of the mean (groups separately or overall mean of all the values) the variance is larger. If the F ratio is around 1, both means are equal. If the F ratio increases, the separate-means model fits better [176]. If the p-value associated with this test is smaller than the set alpha level (here 0,05), one can say that there is indeed a statistical significant difference in the means of the groups though without specifying about which means are different [176].

Student’s t-test

Student’s t-test is based on the Gaussian distribution. The more degrees of freedom for error (number of observations minus the number of parameters estimated) are added, the more precise the t-test works [176]. Additionally to the normal distribution, the t-test requires the two group variances to be equal. However, it can be used with unequal variances as well when Welch’s correction is applied [176]. It can either be used to test whether a mean differs significantly from a hypothesized value [176] or “*whether the difference of two means is significantly different from the hypothesized value of zero*” [176].

Following general definition, the specimens in this study can be considered to be independent groups [176]. Student’s t-test can be applied to compare many means by comparing each pair when the data is unbalanced (with a different amount of observations in each group) [176].

Tukey-Kramer-HSD

For finding pairwise differences between the groups, a Tukey-Kramer-HSD (Honestly Significant Difference) is carried out. The method compares any two groups for significant mean differences while correcting the significance level for multiple testing. This test is supposed to decrease the possibility of committing a Type I error, which is likely to happen when multiple comparisons are made and includes a protection from falsely declaring significance [176] which is not included in student’s t-test.

Sensitivity of the test

To make sure that non-significant results are interpreted correctly, the sensitivity of the test has to be evaluated. Otherwise no distinction can be named between an experiment having too little data to make a conclusion and an analysis simply not being able to detect an actual difference present between values [176]. The estimation of the Least Significant Number (LSN) and the Least Significant Value (LSV) give an indication as to “how many more observations would make the reported difference become significant” [176] and “how small a difference could the significance test in this example detect” [176].

Power

The term statistical power defines how probable it is that an effect is detected if it is there [176]. It increases with the amount of data available, the less random variation is present, the more sensitive the statistical method [176]. There are two important errors in statistics: Type I error (often represented as alpha) means that the null hypothesis is rejected though it is true, Type II error (often represented as beta) means that an existing difference is not detected [176]. Power is 1 minus beta or in other words: the probability of detecting a difference [176].

III) Results

1. Immunohistochemistry- Ranibizumab/aflibercept fluorescence staining, quantification and normalization

Apart from the weak autofluorescence of erythrocytes, no specific staining of glomeruli was seen in samples of the control animal with either of the two antibodies (against the anti-human IgG-Fc fragment or against the anti-human Fab fragment of IgG) used [42]. This pattern changed in samples one day after aflibercept injection, where *“the endothelium cell layer and material within the capillaries of many glomeruli were highly fluorescent [...] Occasionally, glomeruli in which only the endothelium was stained were localized close to others that contained high amounts of IgG-Fc reactive material within the capillaries [...] Erythrocytes within the glomeruli were highly fluorescent [...]”*[42] Examining the samples of the monkey injected with aflibercept seven days after injection, less fluorescent material within the capillaries was seen and the fluorescence was less intense [42]. Similar observations were made with ranibizumab samples. *“One day after ranibizumab injection, the endothelium cell layer and erythrocytes of most glomeruli became fluorescent after labeling with an antibody against the human Fab fragment of IgG [...] However, the specific fluorescence was nearly lost seven days after injection of ranibizumab.”* [42] (for figures, also see [42]).

Then after glomeruli were defined as areas of interest (aoi) and stainings were quantified and normalized as described above and in [42], statistical analyses were performed of the obtained ratio “stained area/cell count”. T-tests comparing mean values of immune reactivity of the areas of interest in the different groups were performed. *„Immune reactivity against aflibercept or ranibizumab was only detected in aflibercept- or ranibizumab-treated animals respectively and did not show any significant differences between days one and seven“* [42]. But the detected differences in mean values between the controls and the treated animals were highly significant (highly significant at the $p < 0,0001$ level for t-test of aflibercept day 1 and aflibercept day 7 against control; highly significant at the $p < 0,001$ level for t-test of ranibizumab day 1

and ranibizumab day7 against control)[42]. The corresponding controls are samples of the untreated monkey, “*respectively after staining with the anti-Fc-fragment antibody for aflibercept and the anti-Fab fragment antibody for ranibizumab immune reactivity analysis*” [42].

2. Immunohistochemistry- Quantification and normalization of VEGF staining

Also for anti-VEGF stained samples, the ratio of stained area to counted cells was estimated for the glomeruli representing the aoi. T-tests comparing each group as well as t-tests against the untreated control were performed.

Concerning t-test against controls, differences between the aflibercept- and ranibizumab-treated samples can be seen: For ranibizumab-treated animals (days 1 and 7), “*no significant changes at any of the analyzed time points [...] compared to the untreated control-animal samples*” [42] were seen. “*However, the stained area to cells ratio of the tissue-samples of the aflibercept-treated animals showed a significant decrease one day [...] after treatment ($p < 0.05$) and an even stronger decrease seven days [...] after treatment ($p < 0.0001$) compared to the untreated control-animal samples*” [42].

Comparing mean values of the different groups, differences were significant comparing animals treated with the two different drugs at the same time point: “*The levels of VEGF were found to be significantly lower in the aflibercept-treated animals on days one ($p < 0.05$) and seven ($p < 0.0001$) after treatment as compared to the corresponding ranibizumab-treated ones*” [42]. Also in aflibercept-treated samples only, “*The decrease of the VEGF level from day one to day seven after treatment was also found to be significant ($p < 0.0001$)*” [42] (also see figures in [42]).

In conclusion, significant differences were found between the mean values of the ratio stained area/cell count the following groups: Concerning aflibercept/ranibizumab staining, means of samples obtained from the monkeys treated with both drugs and sacrificed one and seven days after injection differed significantly from control samples. Concerning VEGF staining, samples obtained from monkeys injected with aflibercept on days 1 and 7 differed

significantly from controls. Also, significant differences were seen between means of the monkeys injected with the two different drugs and sacrificed at the same time points (Aflibercept day 1/ Ranibizumab day 1 and Aflibercept day 7/ Ranibizumab day 7). Moreover, the difference between Aflibercept day 1 and 7 was significant in contrast to the not significant difference between Ranibizumab days 1 and seven (please see also table 3).

Table 3: Significant differences between means of groups in staining of drugs and VEGF

Analyzed with the JMP software by Alexander Tschulakov, own table

	Significant difference between	group means
Ranibizumab/ aflibercept staining	Control	Aflibercept day 1
	Control	Aflibercept day 7
	Control	Ranibizumab day 1
	Control	Ranibizumab day 7
VEGF staining	Control	Aflibercept day 1
	Control	Aflibercept day 7
	Aflibercept day 1	Ranibizumab day 1
	Aflibercept day 7	Ranibizumab day 7
	Aflibercept day 1	Aflibercept day 7

3. Measurement of VEGF-A¹⁶⁵ plasma levels

The detectable limit of the assay was 30 pg/ml. Our doses were below this limit (figure 27).

Quantification of VEGF-A¹⁶⁵ plasma concentrations

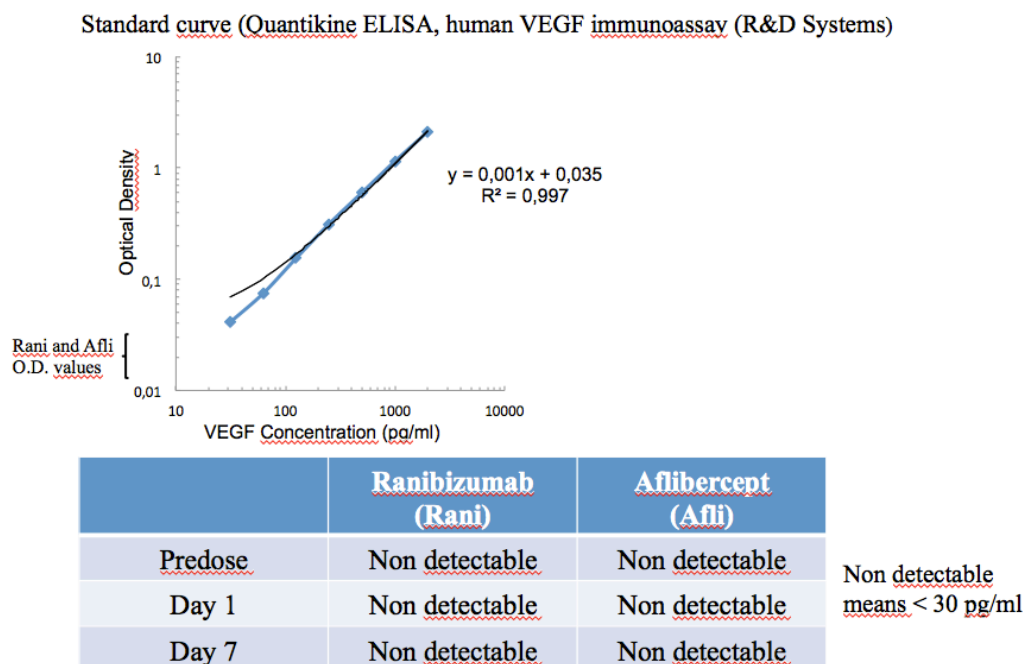


Figure 27: Quantification of VEGF-A₁₆₅ plasma concentrations in EDTA blood samples

Samples of all monkeys collected in the predose phase and on day 1 or 7, respectively. Quantikine ELISA human immunoassay (R&D System). Graph shows VEGF Concentration versus Optical Density. All of the doses were below the detectable limit of the assay. Figure with kind permission from Sylvie Julien-Schraermeyer, own legends.

4. General examinations by light and transmission electron microscopy

“The biopsies of all the kidneys were first studied by light microscopy and also by TEM with increasing magnification in order to scan the specimens on artifacts and pathologic features (figures 28-35). None of the glomeruli was sclerotic. The podocyte foot processes were well-formed and did not show effacement, and a continuous slit diaphragm could be observed. The glomerular basement membrane (GBM) was of normal thickness and did not show duplication in all specimens without widening of the subendothelial space or cellular interposition. The well-defined glomerular endothelium was flattened though there were slight variations in thickness without endotheliosis. In all samples, it was mostly adjacent to the GBM.

The capillary loops were filled with more or less electron-dense serum. The

density difference could be observed in glomeruli of all of the kidneys. “ [42] (see figure 28).

For an overview, overlapping x3000 TEM pictures were taken and MIA's were prepared with the iTEM software as described above. This procedure allows an easier comparison of the general histology of the different specimens. It should be noted that the program limits the possible amount of pictures to create one MIA. Thus, if the diameter of the glomerulus is larger or if the MIA is started too far in the periphery or too close to the capsule of the glomerulus, it might not fit completely on one arranged picture. As already mentioned, the electron beam might destroy or at least reduce the contrast of the ultrathin cut specimen if a section is viewed for more than a couple of seconds. As a good quality of the higher magnification pictures (x20 000) for quantification of endothelial fenestration must be guaranteed, there was only one attempt to obtain a MIA of each glomerulus. This worked very well for one glomerulus of aflibercept day 1 (see figure 20, also published in [42]). Further examples of MIA's can be seen below).

Prof. Dr. Markus van der Giet from the Division of Nephrology at the Charité University Berlin checked my light and electron microscopic pictures of the monkey kidneys and confirmed that there are no abnormalities detectable.

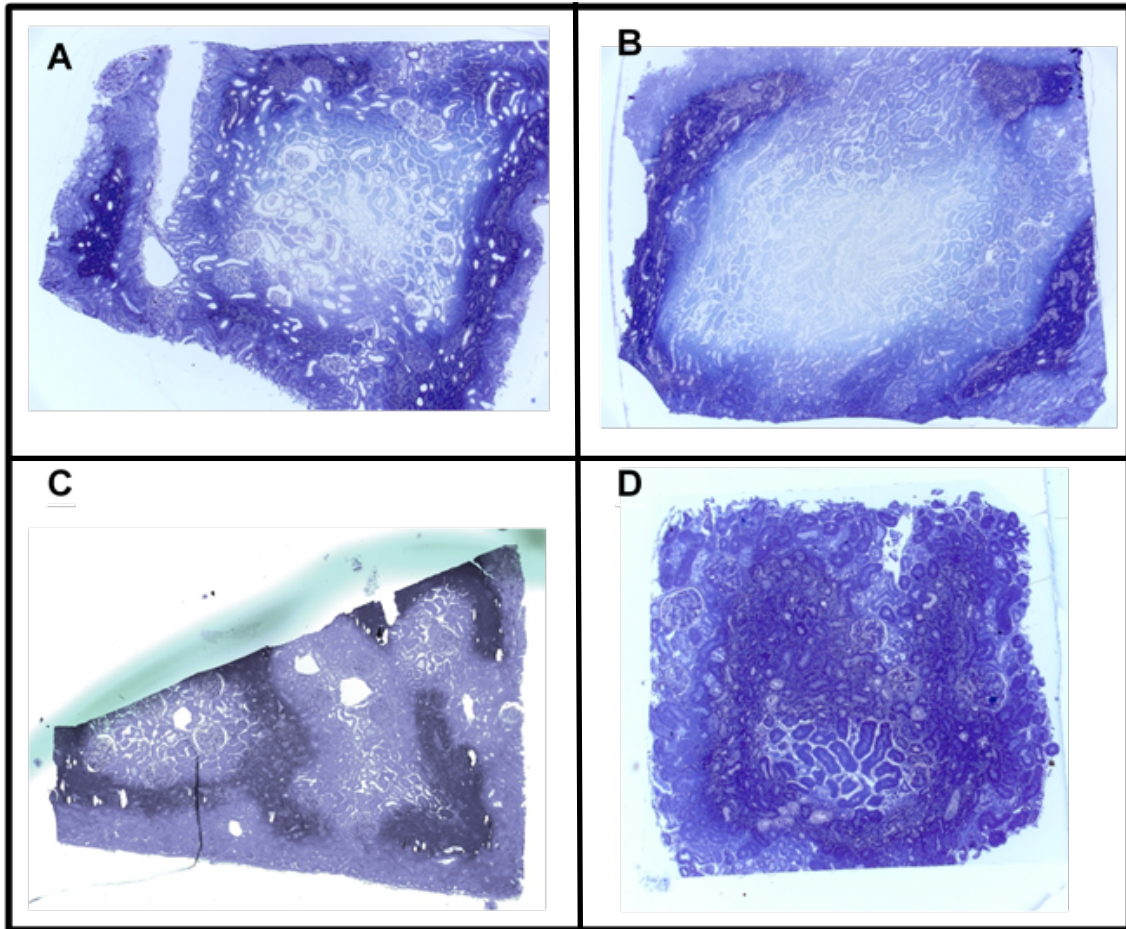


Figure 28: Overview over semithin sections

Sections were stained with Toluidine Blue and prepared for light microscopic examination. In this step regions of interest containing glomeruli with a medium to large diameter and intact Bowman's capsule can be chosen and prepared for electron microscopy

Samples: **A:** Aflibercept day 1, **B:** Aflibercept day 7, **C:** Aflibercept day 1, **D:** Aflibercept day 7, own images.

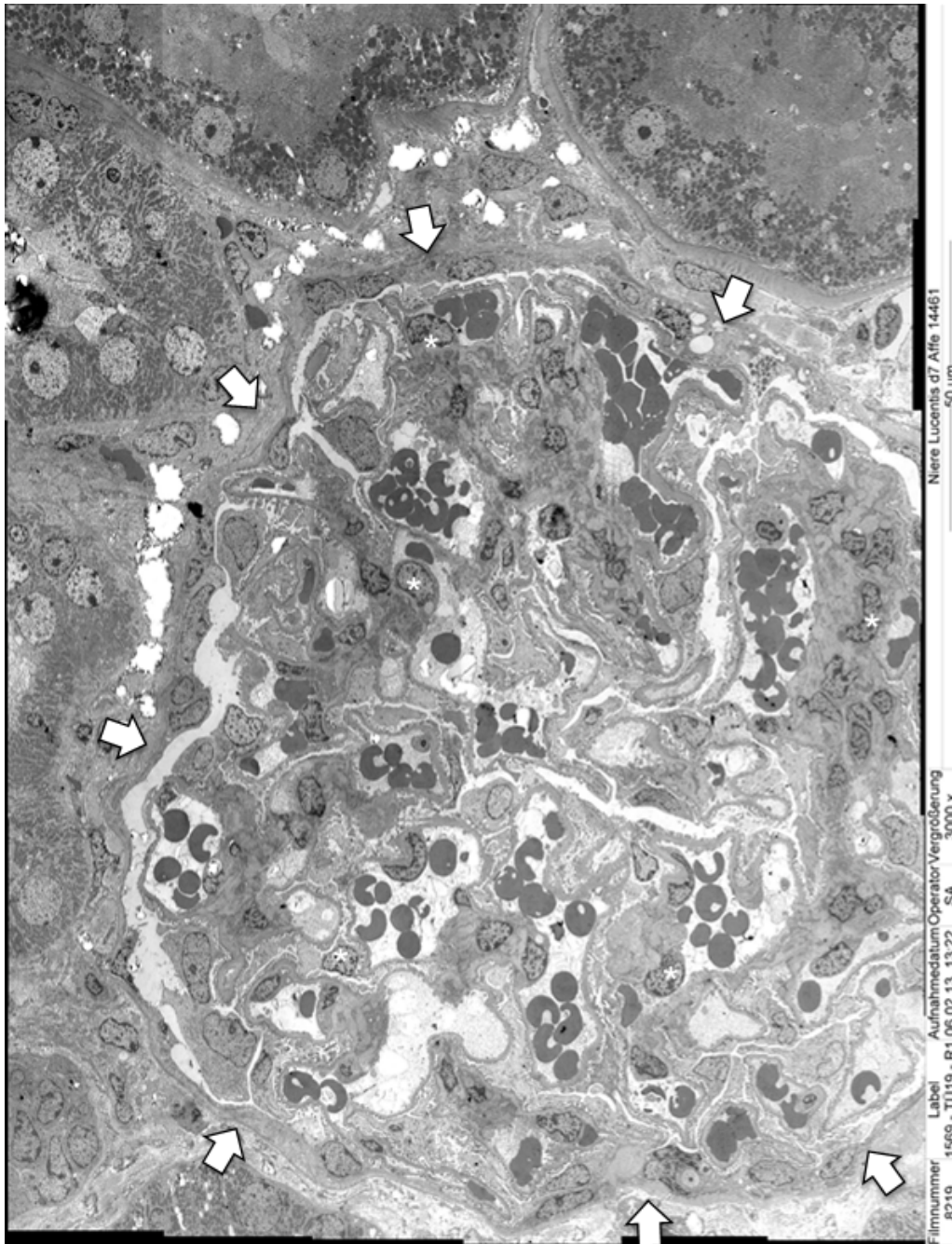


Figure 29: MIA of ranibizumab day 7

Another overview montage image (MIA) of a kidney glomerulus (incomplete). Bowman's capsule (**arrows**) is intact but the Bowman's space is not uniform; capillaries are filled with erythrocytes, no hemolysis. **Asterisks** mark prominent nuclei of mesangium cells. For a more detailed examination and for quantification of endothelial fenestrations, high magnification (x20 000) was used. TEM, magnification x3000.

This MIA is incomplete due to the large diameter of the glomerulus and the fact that the capacity of pictures which could be composed to one multiple image arrangement were limited by the program used. For quantification of glomerular endothelial fenestrations, the whole glomerulus was scanned through performing the SURS protocol (see above). Own image.

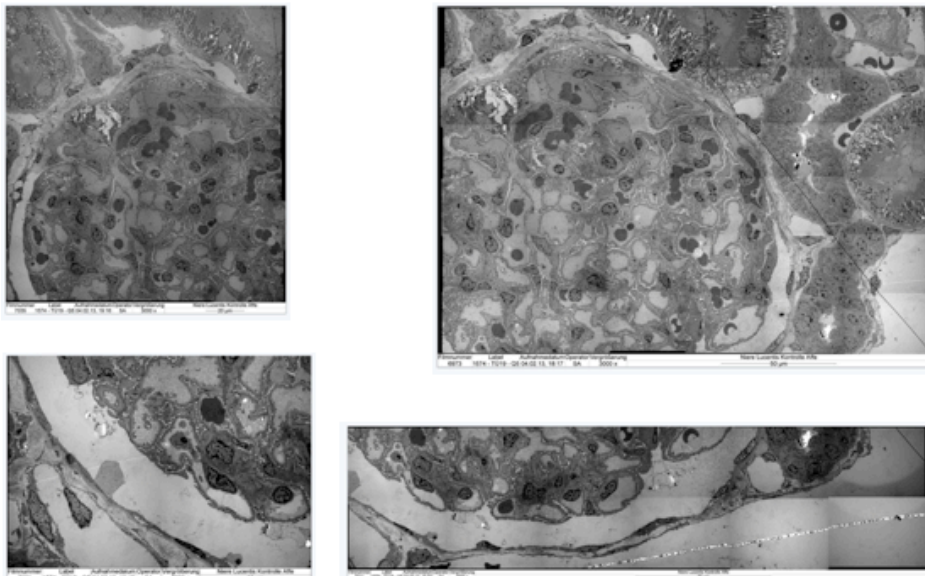
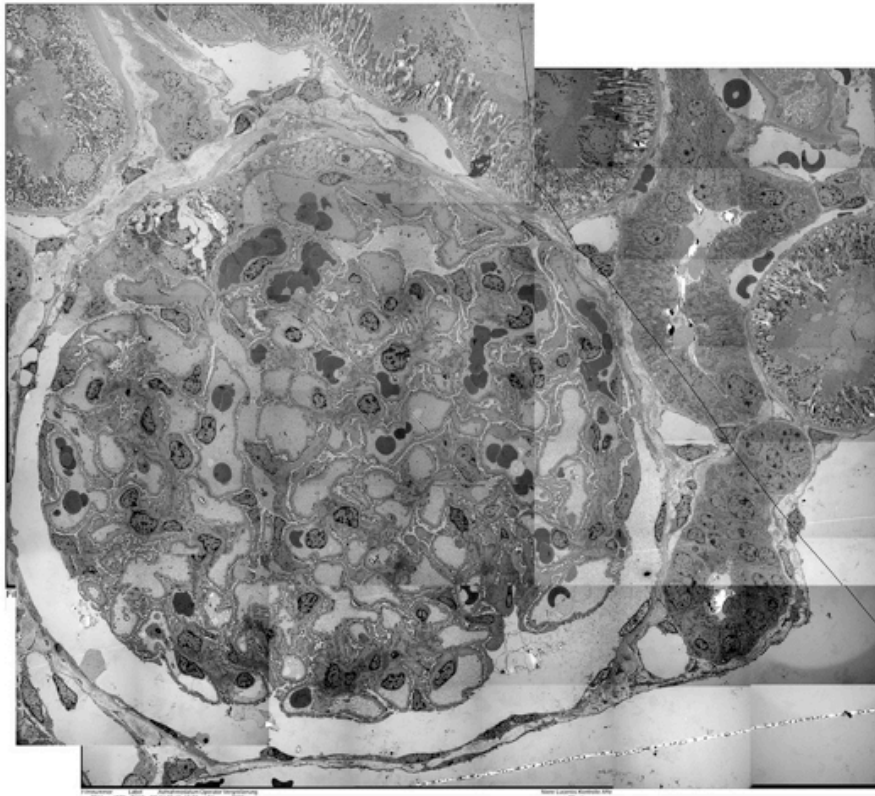


Figure 30: MIA of untreated control

Another example of an MIA (on top) and the 4 crude partial MIA's of which it was manually composed (bottom) in Adobe Photoshop, TEM, magnification x 3000.

In this case, the glomerulus chosen was too big for the iTEM program to produce a single MIA. Note the lower quality compared to the automatically produced MIA due to the contrast and size differences of the different components.

Own images.

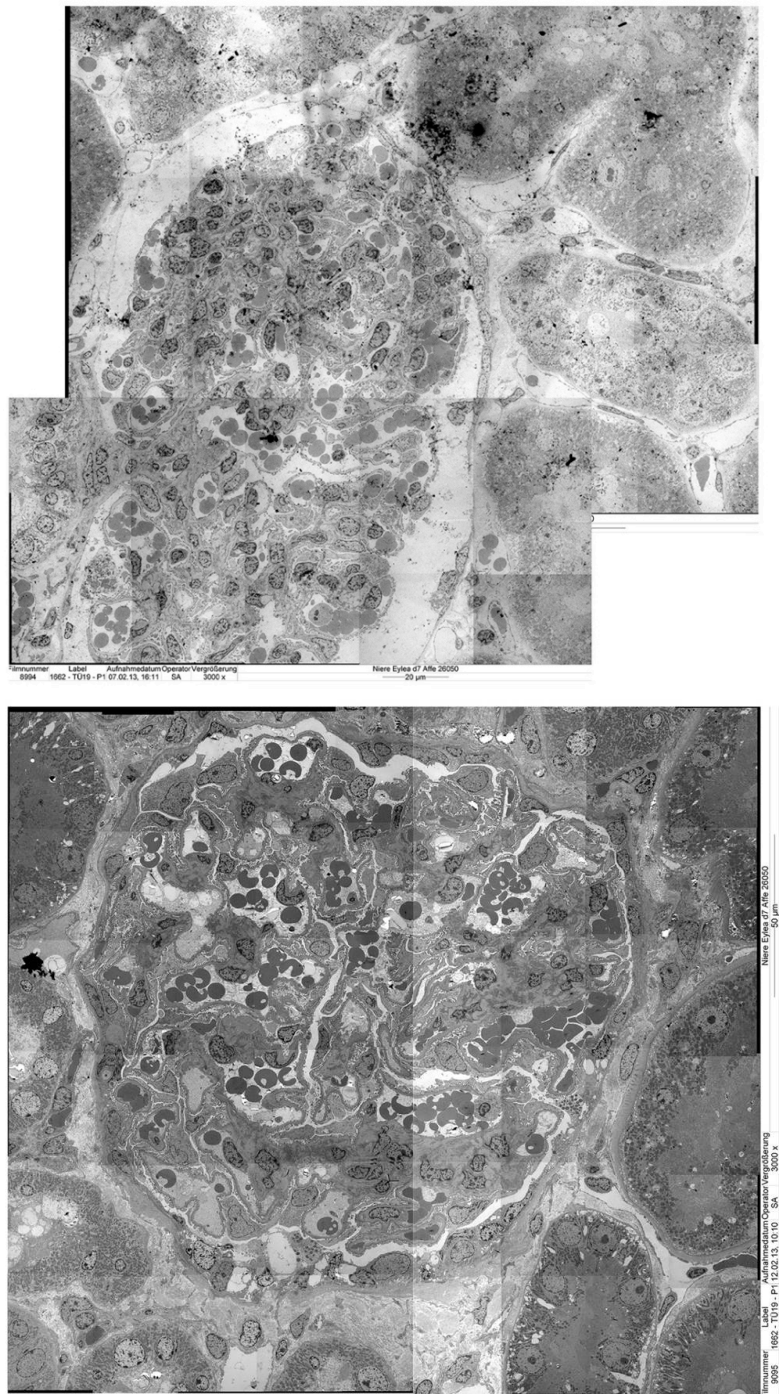


Figure 31: 2 MIA's of two glomeruli of aflibercept day 7, incomplete

Here the MIA's were started at a position too far from the center of the glomeruli resulting in incomplete overviews. On the upper picture, the typical contrast reduction as well as traces of the previously performed attempt can be seen. Note the different width of the lumen of Bowman's capsule without pathological importance.

Both MIA's were manually composed of two partial MIA's each with Adobe Photoshop. TEM, magnification x3000.

Own images.

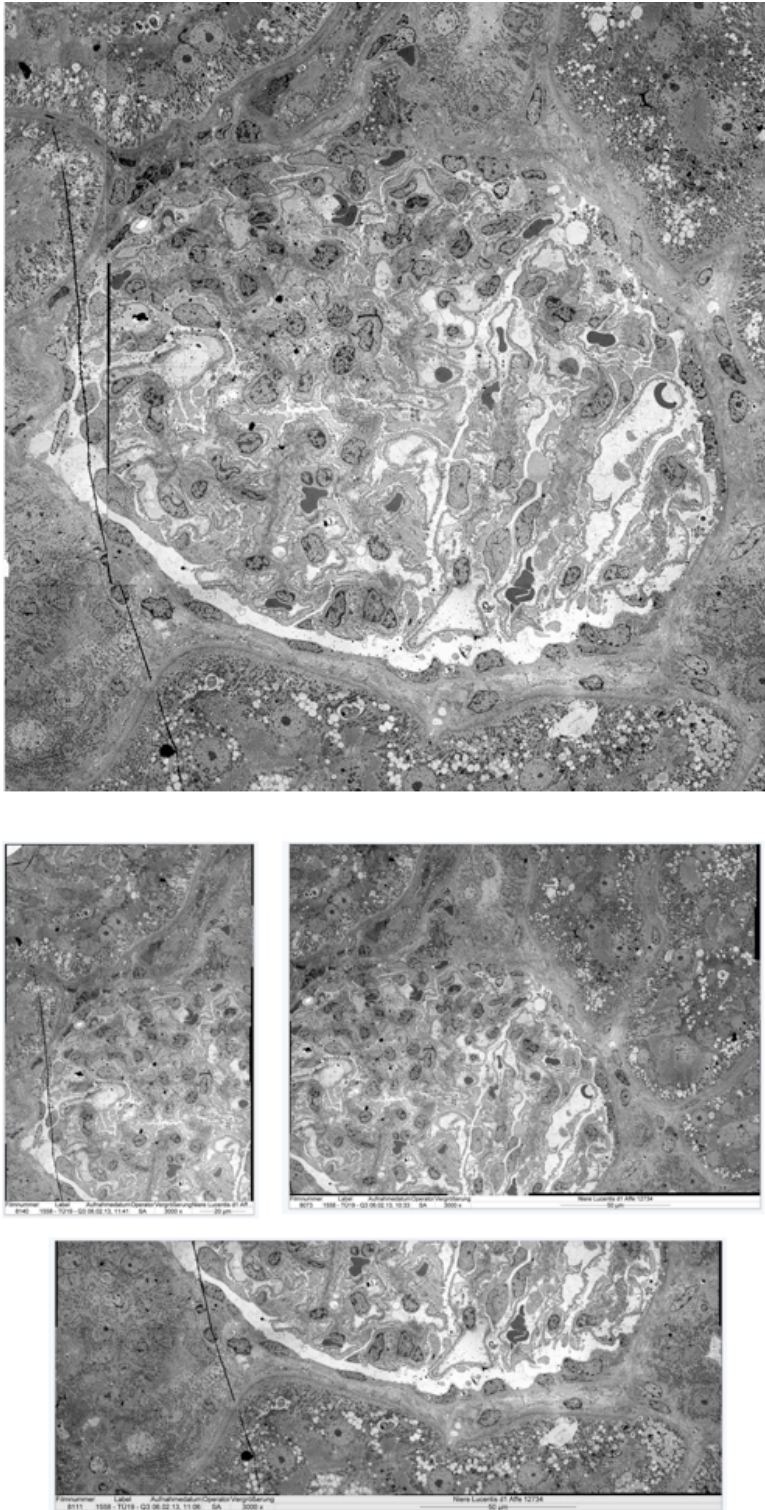


Figure 32: MIA of a glomerulus of ranibizumab day 1

Top: the manually composed MIA (Adobe Photoshop), TEM, magnification x3000.
Bottom: the 3 partial MIA's taken with the iTEM software
Own images.

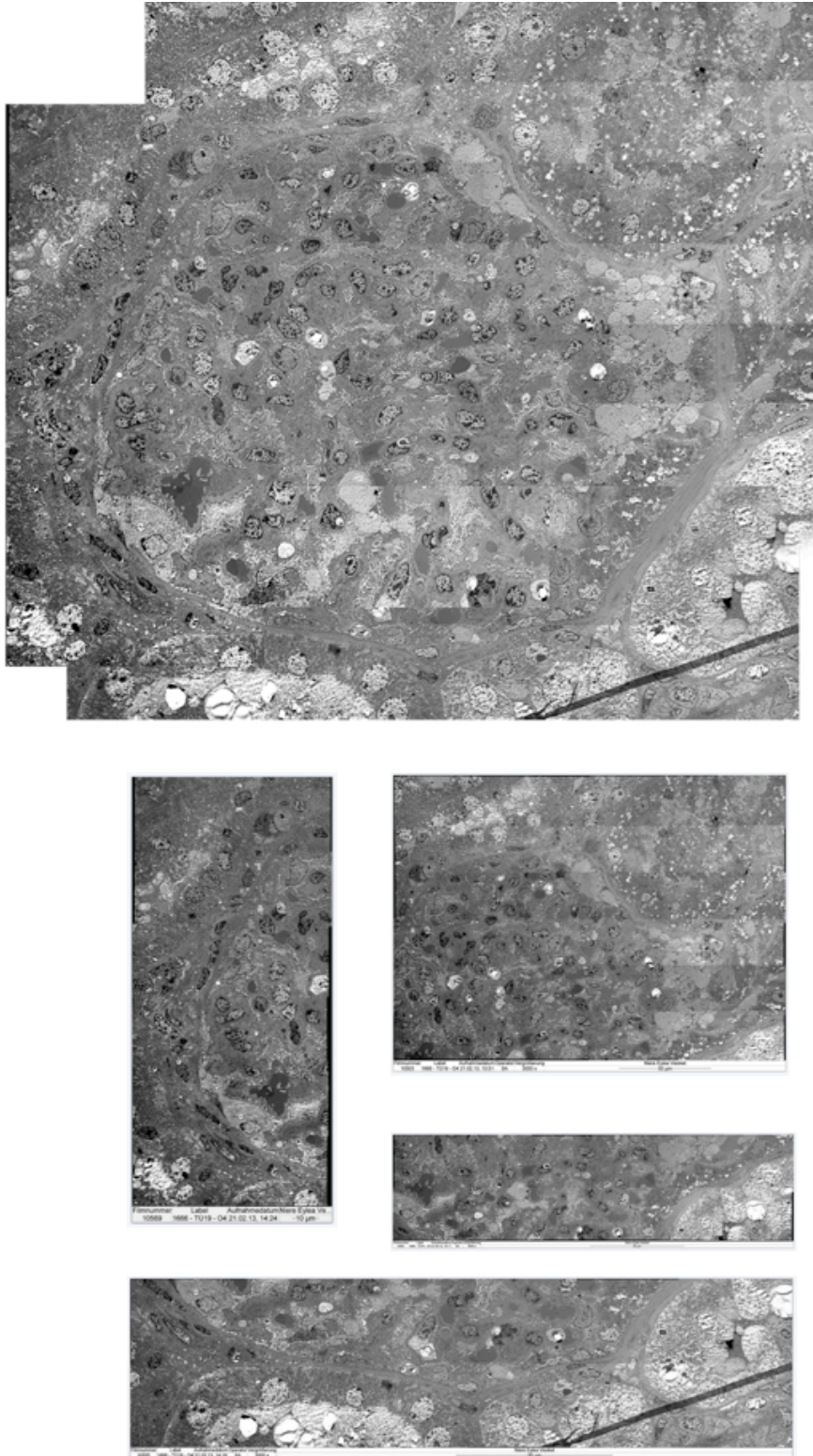


Figure 33: MIA of aflibercept vehicle

Another example of an MIA (on top) and the 4 partial MIA's of which it was manually composed (bottom) in Adobe Photoshop, TEM, magnification x 3000.

Here also the quality is a bit lower than of compared arrangements due to distortions. Own images.

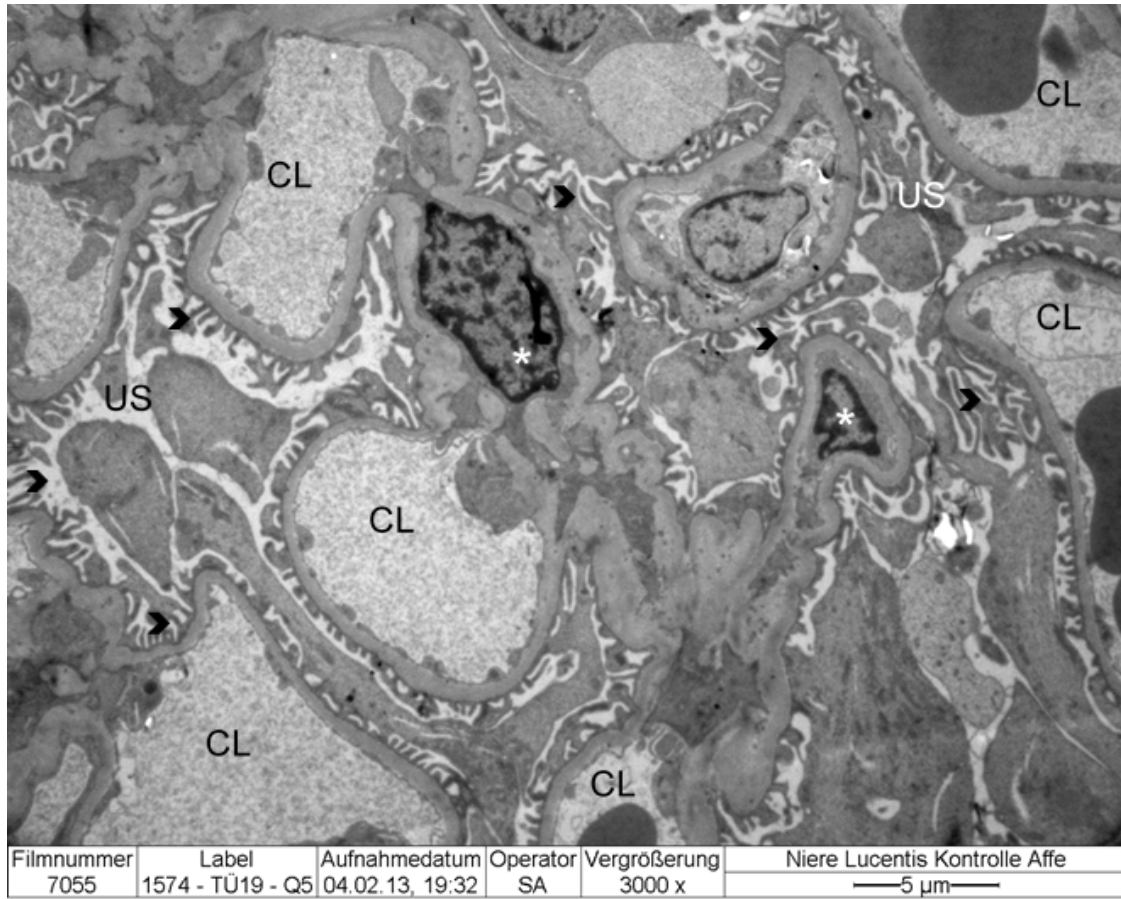


Figure 34: Detail of glomerular electron microscopy

Densely packed capillary loops surrounded and held by mesangium (mesangium cells and extracellular matrix). Note that mesangium and endothelial cell nuclei (asterisks) are very prominent and that podocyte foot processes can be easily identified and are an important marker to identify the urinary space of the glomerulus. The capillaries lined by fenestrated endothelium represent the blood space. Erythrocytes do not show lysis and are only found in the capillaries, podocytes are well-formed, no sclerosis is seen. Glomerular basement membrane is of even thickness without duplications and the glomerular endothelium is flat and adjacent to the glomerular basement membrane. These details can be better observed in higher magnifications as used to quantify endothelial fenestrations (see beyond).

US= urinary space, **CL**= capillary lumen, **arrowheads** mark podocyte foot processes, **asterisks** mark nuclei of mesangium and endothelial cells

TEM, magnification x3000

Sample: Untreated, own images.

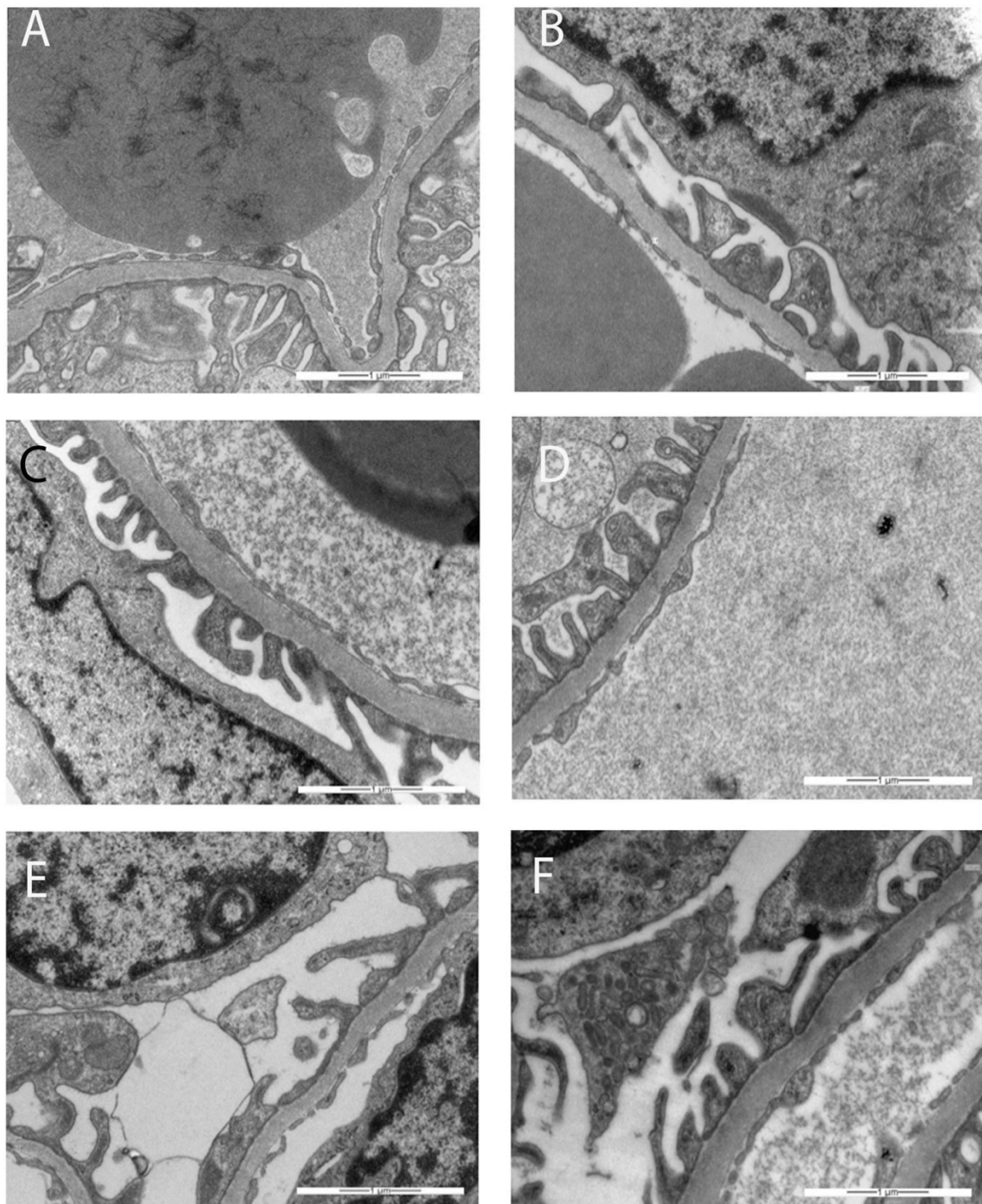


Figure 35: Examples of TEM used for the quantification of fenestrations

Images to compare and verify at a higher magnification that there are not any pathologies in any of the samples at any time point. Here, capillary endothelium, glomerular basement membrane and podocyte foot processes can be better assessed and the quality of electron microscopy appears: even organelles can be distinguished.

(Annotation: The scale shown in the lower right corner of each picture is 1 µm)

Examples of transmission electron micrographs used for the quantification of the glomerular endothelial cells fenestrations.

(A) after injection of the vehicle; (B) in the untreated monkey; (C) one day after injection of ranibizumab; (D) seven days after injection of ranibizumab; (E) one day after injection of aflibercept; (F) seven days after injection of aflibercept. Magnification $\times 20000$." [42],

Figures and legends (partly) published in [42], modified ;own images.

5. Quantification of the glomerular endothelial cells fenestrations

Kidney samples of eight monkeys of the aflibercept and the ranibizumab group, respectively, taken on days one and seven after injection and one untreated monkey as well as one monkey treated with aflibercept's vehicle were examined. The obtained values of the number of fenestrations per μm of each group were statistically analyzed.

Note that for simplification, values obtained from the kidneys of the different monkeys will be named "groups" and addressed with the name of the group spelled with a capital letter (e.g. "Untreated" for the group of values obtained from the untreated monkey, "Aflibercept day 1" for the group of values obtained from the two monkeys treated with aflibercept and sacrificed on day 1).

5.1. Descriptive graphs and statistics

Table 3 shows important statistical values of this analysis. Alpha was set 0,05, the confidence interval (1- alpha) thus 95 percent. Also, statistics of pooled controls (the groups Untreated and Aflibercept Vehicle summarized) are shown. This will be justified below.

Table 4: Statistical values of the distribution analysis of the number of fenestrations per μm , all values and groups separately

N= Number of observations

MV= Mean value

M= Median

SD= Standard deviation

SE = Standard error of mean value

Calculated with SAS JMP 13.

	N	MV	M	SD	SE
All	1382	1,332	1,26	0,741	0,020
Untreated	117	1,317	1,25	0,684	0,063
Aflibercept Vehicle	132	1,217	1,12	0,727	0,063
Controls pooled	249	1,264	1,17	0,708	0,045
Aflibercept day 1	231	1,522	1,46	0,821	0,054
Aflibercept day 7	317	1,233	1,165	0,716	0,040

Ranibizumab day 1	297	1,324	1,28	0,671	0,039
Ranibizumab day 7	288	1,355	1,28	0,773	0,046

The total number of observations is very high at 1382. The sample size of treated animals is higher (about double in each group) than the size of the single control groups (Untreated and Aflibercept Vehicle). This is due to the fact that there were two animals for both time points for both drugs whereas there were only two animals serving as controls of which one was sacrificed one day and the other one seven days after intravitreal injection.

Regarding the means and medians, tendencies can be seen: The values of the group Aflibercept day 7 are lower than the corresponding values one day after injection of the drug. This trend is not seen for ranibizumab- treated samples where means are about equal and medians are exactly the same. One day after treatment, the values are by trend higher than in control samples (especially compared to means and median of the untreated monkey)- a tendency that is more distinct for Aflibercept day 1 than for Ranibizumab day 1. Also, values one day after injection of aflibercept are clearly higher than one day after ranibizumab injection. The values of the two treated groups which were sacrificed seven days after injection are very similar and still seem to be slightly higher than in control groups. The two control groups (Aflibercept Vehicle and Untreated) seem to be very similar concerning means and medians. Standard deviations and standard errors are very low in all groups. Moreover, the means and medians of all groups combined are very similar with corresponding values of the untreated monkey and also close to the values of the groups Ranibizumab days 1 and 7.

The described characteristic can be visually comprehended in the following histograms and box plot (see figures 36 and 37) and will be further analyzed in the following.

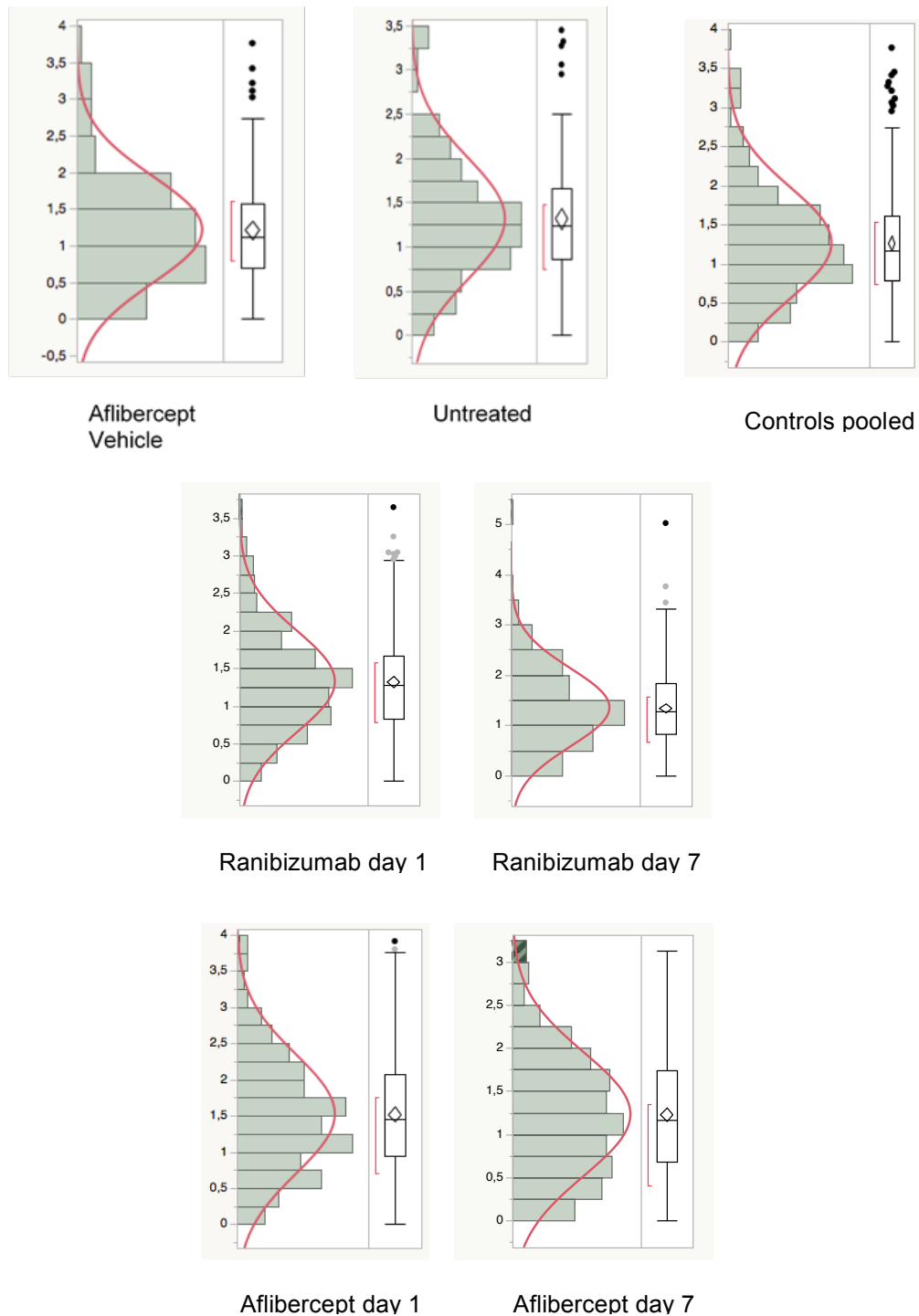


Figure 36: Histograms of the distribution of the number of fenestrations per μm in the different independent groups

The red line superimposed on the histogram represents the normal density corresponding to the mean and standard deviation in the sample (all observations). Also shown: distribution of values when control groups (Untreated and Aflibercept Vehicle) are pooled.

The diamond shows the mean and its 95% confidence interval. The red bracket indicates the shortest half meaning the shortest interval containing half the data [176].

Software: SAS JMP 13.

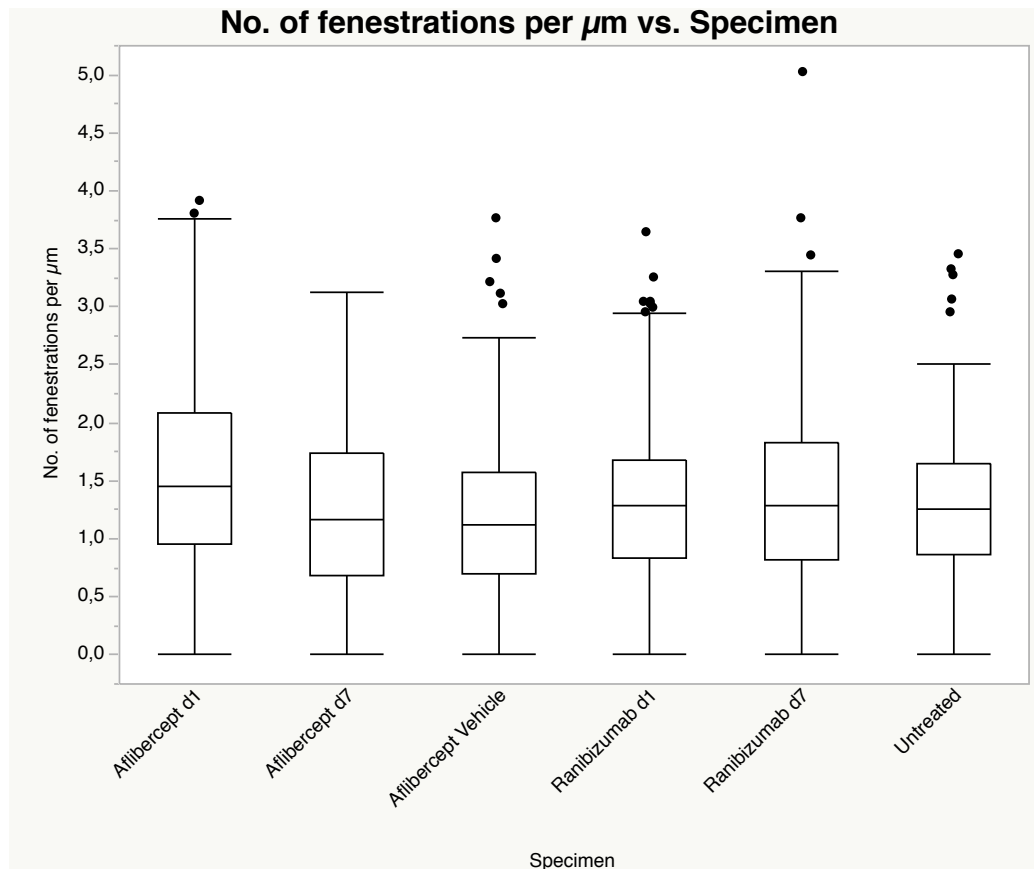


Figure 37: Box plot representation of the quantification of the number of fenestrations per μm depending on the treatment and its duration, Version 1

same groups as in figure 36. Samples of Afibercept's vehicle and the untreated monkey NOT pooled.

Software: SAS JMP 13.

The form of the box plots also gives an indication of the existence of a normal distribution if there is a good parallelism of the marks and the spaces of the upper and lower quartiles are at about the same distance from the median [176]. This is approximately the case in all of the samples; the boxes also show good symmetry. A normal distribution of values can be assumed regarding the histograms in figure 36 and this is also confirmed by the illustration of the normal quantile plots with the JMP software, which tend to follow a straight line (not shown). Moreover, performing the Shapiro-Wilk Test (W statistic) to test the distribution for normality shows no significance in any of the groups indicating that the distributions are all close to normal (not shown).

5.2. Pooling of control samples

As already mentioned, sample sizes of treated animals are clearly higher due to the double amount of animals per time point for treated animals compared to the two animals serving as controls for both time points. For statistical analyses, equal sample sizes are advantageous, thus approaching a so-called balanced data design [176].

Thus, equalizing of sample sizes has to be considered by uniting data obtained from the untreated monkey and the monkey treated with aflibercept's vehicle. For medical reasons, this consideration can be justified. Injection of a saline solution may induce stress in the treated animal and may have influence on the treated eye, but not have any influence on the kidney. This assumption is supported by the obtained values in table 3 and by the fact that my morphological observations revealed no differences between the kidneys of these two monkeys. As a condition for pooling of the two samples, there must not be a significant difference when comparing means. The performed t-test for independent samples resulted in $t=1,1117$ and a p-value of $p=0.265$. There is thus no significant difference between these two groups.

The sensitivity and power analysis of this t-test shows that a difference of 0,177 (LSV= least significant value) would have been needed to be measured in order to detect a significant difference at an alpha level of 0,05, whereas the actual measured difference in the mean of the number of fenestrations per μm was $1,317 - 1,217 = 0,1$. The actual sample size of these two groups was 249, the least significant number is 774, meaning that with the given variances and differences, a sample size of 774 would be necessary to detect a significant difference (at a probability level of at least 50 % [176]).

In conclusion, no significant difference between group means was seen and as this is also plausible as regards content, observations obtained from the two samples Untreated and Aflibercept Vehicle were pooled. Figure 38 shows the box plot similar to figure 37 with the newly formed control group and approximately equalized sample sizes.

5.3. Statistical analysis comparing group means, controls pooled

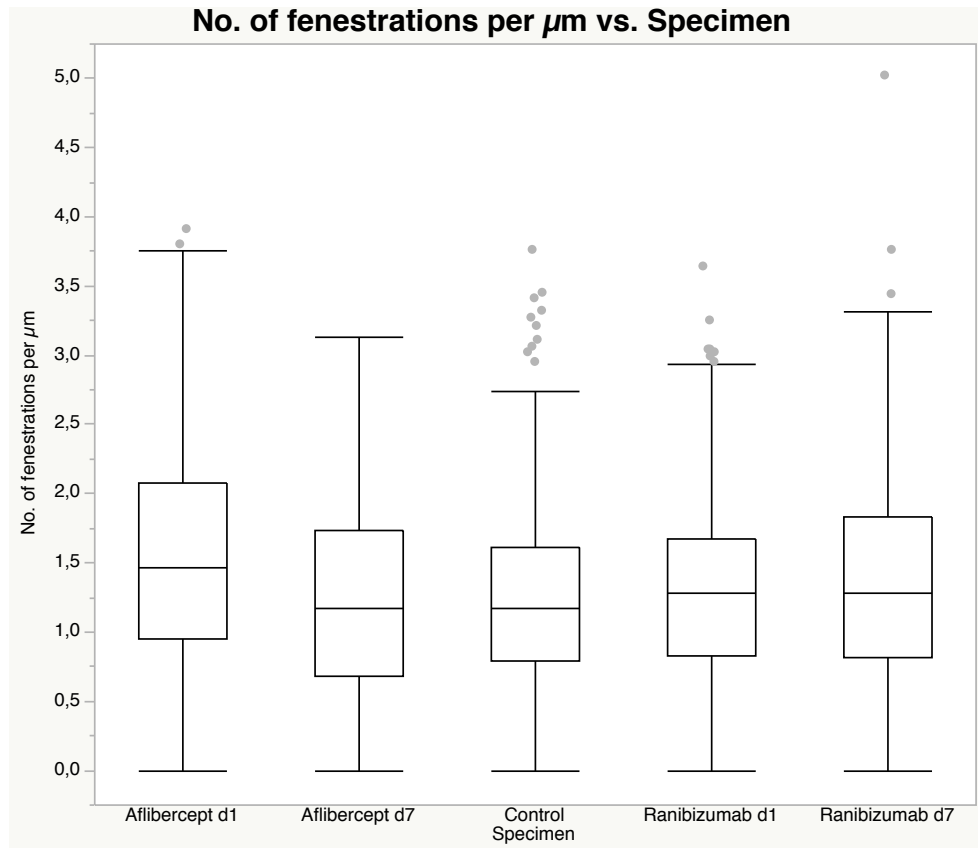


Figure 38: Box plot representation of the quantification of the number of fenestrations per μm depending on the treatment and its duration, Version 2

Samples of the monkey treated with aflibercept's vehicle and the untreated monkey pooled.
Software: SAS JMP 13.

The visual analysis of this box plot shows the following trends of which most are comparable to those seen in figure 37: a higher mean of the group Aflibercept day 1 compared to all the other groups including the group Control. Also the decrease from day 1 after treatment to day 7 is seen, which is clearly more distinct for the aflibercept-treated samples. Comparing the two groups injected with the different drugs and sacrificed at the same time points, the means of the aflibercept-treated samples seem to be higher than those of the ranibizumab-treated groups one day after injection and means seem to be about equal seven days after injection of the two drugs. Comparing mean values of the groups seven days after injection of ranibizumab and the group mean of the

control, roughly no difference is visually recognizable.

The form of the newly formed box plot of the group Control is comparable to those of the groups Aflibercept Vehicle and Untreated in figure 37 with very good symmetry.

One way ANOVA analysis of number of fenestrations/ μm versus specimen, analysis of variance

To estimate if the group means of the five independent samples differ significantly, a one way ANOVA analysis of the ratio number of fenestrations/ μm was performed. The preconditions for this analysis are: the existence of a Gaussian distribution in all samples and the homogeneity of variance in all samples [176]. The fulfillment of these conditions can be assumed as there are no big differences in the standard deviations (see table 3) and as the visual assessment of the histograms in figure 36 as well as the W statistics indicate a normal distribution of values with values roughly in the range between 0 and 4.

The chart of the ANOVA analysis can be seen in figure 39. $F=5,911$, the corresponding p-value is highly significant with $p= 0,0001$. This indicates that there is indeed a statistically significant difference between the group means, but which groups differ is not specified in this analysis. Thus, to further investigate these differences, multiple comparisons performing the Tukey-Kramer-HSD test have to be made. The results can be seen in figure 40.

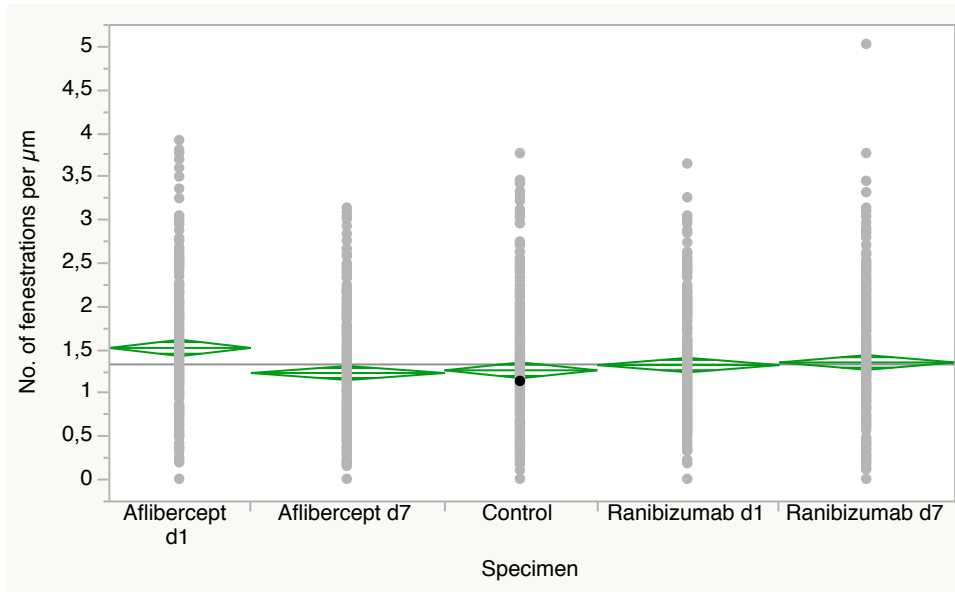


Figure 39: One-way ANOVA analysis

Chart of the one-way ANOVA analysis to estimate differences between the mean values of groups. Each group is formed by the values of the number of fenestrations per μm of two monkeys, the groups Untreated and Aflibercept Vehicle are pooled as “Control”.

The diamonds represent the 95% confidence interval around the group means (center lines of the diamonds), “The line across the middle is at the grand mean” [176].

Also note the similar sample size illustrated by the distance the diamonds cover along the x axis.

software: SAS JMP 13.

Kategorie	- Kategorie	Differenz	Std.- Fehlerdiff.	p-Wert
Aflibercept d1	Aflibercept d7	0,2897511	0,0637265	<,0001*
Aflibercept d1	Control	0,2585161	0,0672498	0,0012*
Aflibercept d1	Ranibizumab d1	0,1981433	0,0645816	0,0186*
Aflibercept d1	Ranibizumab d7	0,1677215	0,0650720	0,0751
Ranibizumab d7	Aflibercept d7	0,1220296	0,0600275	0,2508
Ranibizumab d1	Aflibercept d7	0,0916077	0,0594956	0,5367
Ranibizumab d7	Control	0,0907947	0,0637555	0,6121
Ranibizumab d1	Control	0,0603728	0,0632550	0,8753
Control	Aflibercept d7	0,0312349	0,0623817	0,9873
Ranibizumab d7	Ranibizumab d1	0,0304219	0,0609345	0,9874

Figure 40: Sorted list of differences between the means of the groups, Tukey-Kramer-HSD test

The groups Untreated and Aflibercept Vehicle are pooled as “Control”. Note that only differences between the first 2 couples are significant at an alpha level of 0,05. The value in the middle of the table marked red is on the edge of being significant.

Software: SAS JMP 13, German.

The one-way ANOVA analysis shows that the confidence intervals of some of the different groups shown by the diamonds in the chart (figure 39) do not overlap. This means that the groups are significantly different [176]. Here, the

95% confidence interval of the group Aflibercept day 1 does not overlap with the confidence interval of the groups Aflibercept day 7, Control and Ranibizumab day 1. This assumption has to be further followed. On the other hand, all the other confidence intervals do overlap. Thus, it has to be evaluated to which extent these means are different with the help of the p values and analyses of variance. As the F ratio with 5,911 is considerably larger than 1, the analysis of variance reveals that the separate-means model of the different groups fits better than the one-mean model summarizing the mean of all the values [176]. This fact together with the p-value associated with the F ratio in the analysis of variance that is smaller than 0,05 ($p < 0,0001$, highly significant) leads to the conclusion that *“the variance around the group mean is (highly) significantly less than the variance around the grand mean”* [176]. Thus, there is indeed a difference between the group means; the groups do differ but it is not yet known which means are different.

To find out more about the differences between the means of the particular groups, student's t- test comparing each pair can be performed. But as already mentioned, the Tukey-Kramer-HSD test is more effective in preventing false declarations of significant differences than the t-test and is thus more suitable for performing multiple comparisons [176]. The list of sorted differences of the Tukey-Kramer-HSD test (see figure 40) indicates a significant difference between the animals treated with the same drug one and seven days after treatment concerning aflibercept but not ranibizumab. Also, only Aflibercept day 1 differs significantly from the control and the difference between Aflibercept day 1 and Ranibizumab day 1 is on the edge of being significant. Of interest, means of Aflibercept day one are not only significantly different but also higher than means of other groups. (Annotation: In student's t-test comparing each couple (not shown), the difference between means of Aflibercept day 1 and Ranibizumab day 1 is significant.)

In the article published in PloS One [42], the untreated monkey was the only animal serving as control. This is based on the assumption that only one animal was truly “untreated” (the other animal which also served as control in the previous analysis was injected with a saline solution). Equally to the previously

described considerations, sample sizes should again be approximately equal. Thus, only about half the data obtained from each group of treated animals was taken into account for statistics. Therefore, values from three out of six glomeruli evaluated (from two monkeys in each group) were randomly chosen (see “A” and “B” in table 5). For statistics see [42]. The results are in accordance with those described in this work.

table 5 shows the total number of pictures evaluated. It must be pointed out that the amount of pictures evaluated cannot be equalized with the amount of observations for the number of fenestrations per μm available. In one picture, several measurements are performed when there are multiple parts of glomerular endothelium seen. Thus, the total amount of observations (ratio of number of fenestrations per μm) is at 1382 (see table 3) correspondingly higher than the total amount of pictures evaluated.

“The total amount of pictures taken was 4855 of which 1327 (27.3%) were evaluated” [42]. On average, 486 pictures per procedure (A or B, respectively, with three glomeruli evaluated per procedure per time point) were available of which on average 132,7 were analyzed. Regarding a single glomerulus, on average 162 pictures were taken and 44,2 analyzed. Considering all the pictures evaluated for the treated animals (not the two controls), 809 pictures per modality (1002,3 when the two controls are not considered) were taken of which 221,2 (269,5 without controls) were evaluated (27,2 % /26,9%). Overall, the ratio of evaluated pictures/ pictures taken was about the same for each monkey/time point (24,7% to 33,8%). The amount of pictures evaluated was then also comparable with the control groups (Aflibercept Vehicle and Untreated) pooled (230 for Aflibercept day 1, 266 for Aflibercept day 7, 298 for Ranibizumab day 1, 284 for Ranibizumab day 7, $132+117=249$ for controls).

Table 5: Numbers of images taken and evaluated for the first and second statistical analysis

Numbers and percentages of evaluated images with and without controls. Data shown per glomerulus, per procedure (A for article published, A + B for statistics of this work) and per time point (2 monkeys for treated animals, 1 monkey for controls)

A: Glomeruli randomly chosen for the analysis published in [42], with 3 glomeruli per time point
A+B: complete data used for the statistical analysis in this thesis, observations from 2 monkeys (6 glomeruli) per time point for treated animals

Software: Microsoft Excel for Mac 2011.

	PER GLOMERULUS			PER PROCEDURE			PER TIME POINT		
	taken	evaluated	percentage	taken	evaluated	percentage	taken	evaluated	percentage
Aflibercept d1 A G1	68	36	52,9%	241	100	41,5%	764	230	30,1%
Aflibercept d1 A G2	76	27	35,5%						
Aflibercept d1 A G3	97	37	38,1%						
Aflibercept d1 B G1	193	60	31,1%	523	130	24,9%			
Aflibercept d1 B G2	199	40	20,1%						
Aflibercept d1 B G3	131	30	22,9%						
Summary for Aflibercept d7									
Aflibercept d7 A G1	175	49	28,0%	539	150	27,8%	1078	266	24,7%
Aflibercept d7 A G2	182	49	26,9%						
Aflibercept d7 A G3	182	52	28,6%						
Aflibercept d7 B G1	197	37	18,8%	539	116	21,5%			
Aflibercept d7 B G2	148	35	23,6%						
Aflibercept d7 B G3	194	44	22,7%						
Summary for Ranibizumab d1									
Ranibizumab d1 A G1	199	42	21,1%	474	113	23,8%	1016	298	29,3%
Ranibizumab d1 A G2	140	34	24,3%						
Ranibizumab d1 A G3	135	37	27,4%						
Ranibizumab d1 B G1	153	53	34,6%	542	185	34,1%			
Ranibizumab d1 B G2	198	76	38,4%						
Ranibizumab d1 B G3	191	56	29,3%						
Summary for Ranibizumab d7									
Ranibizumab d7 A G1	199	46	23,1%	554	130	23,5%	1151	284	24,7%
Ranibizumab d7 A G2	198	59	29,8%						
Ranibizumab d7 A G3	157	25	15,9%						
Ranibizumab d7 B G1	199	47	23,6%	597	154	25,8%			
Ranibizumab d7 B G2	199	53	26,6%						
Ranibizumab d7 B G3	199	54	27,1%						
Summary for Aflibercept Vehicle									
Aflibercept Vehicle G1	175	37	21,1%	500	132	26,4%	500	132	26,4%
Aflibercept Vehicle G2	198	58	29,3%						
Aflibercept Vehicle G3	127	37	29,1%						
Summary for Untreated									
Untreated G1	163	70	42,9%	346	117	33,8%	346	117	33,8%
Untreated G2	88	18	20,5%						
Untreated G3	95	29	30,5%						
TOTAL AMOUNT	4855	1327		4855	1327		4855	1327	
Mean Value	162	44,2		486	132,7		809,2	221,2	
MV without controls	167	44,9		501,1	134,8		1002,3	269,5	

5.3 Exclusion of errors of measurement

To avoid gross errors, fixation and preparation of samples was documented and performed with the same detergents following a standardized protocol (see figure 18). Preparation and fixation procedures were performed by a single person from our work group (Tatjana Taubitz) within one week.

In my analyses, variability between measurements might occur mainly due to the fact that the line along the endothelium is manually drawn in the software program and due to the recognition or not of fenestrations by the observer. The number of images chosen for analysis did not vary on a big scale as criteria were very clear nor did the other named criteria as there was only one observer. Also, differences in picture quality with a possible influence on the recognition of fenestrations have to be taken into account.

To minimize the random error of measurement, the mean value of repeated measurements can be calculated. The more measurements are performed the lower the error [177]. As the number of images taken was very high at 4855 and so accordingly the number of evaluated images (1327), the evaluation of three glomeruli per kidney/ time point can already be considered to be a repeated measurement reducing the random error. Moreover, in total up to 6 glomeruli per time point were evaluated for all the treated animals (and control animals when pooled).

The statistical power can be assumed to be high due to the high number of observations. Moreover, the assumption of normality was inspected, with the result of all groups being approximately normally distributed.

Test on equal variances

Also, means were tested with the JMP 13 program for equality around the groups. Small p values as results of the test on equal variances suggest that the variances are indeed not equal in the groups. Hence, the Welch Anova F-test was applied in addition. In this variance-weighted test F was 12,584 for analysis number 2 compared to an F value of 15,851 in the unweight Anova analysis. As the F value was highly significant in both cases and as being zero or larger than zero (not the exact value) is the only informative value of the test [176], inequality of variances was excluded as a major source of error.

Moreover, as a prevention of falsely declaring significance, more attention was placed on the Tukey-Kramer- HSD test than on the t-test.

6. Conclusion of Results

The samples of the untreated animals as well as those of the animals treated

with aflibercept and ranibizumab one and seven days after injection were examined regarding three criteria: the histology (microscopically and ultra-structurally), the immunohistochemistry and the ratio fenestrae/ μm of the glomerular endothelial cells. Also, a measurement of VEGF-plasma levels was performed but all doses were below the detectable limit of the assay.

In histological analyses, no abnormalities were seen in any of the samples in either light or transmission electron micrography.

The anti-VEGF staining as well as the evaluation of reactivity against ranibizumab and aflibercept revealed that no reactivity against the injected drugs was detected in controls. However, differences in reactivity against the drugs were significant between controls and all treated animals in terms of higher values for treated animals.

Concerning anti VEGF-stainings, mean values of the aflibercept-treated samples were significantly decreased compared to controls in contrast to ranibizumab-treated samples where no significant differences were observed. Also, mean values of samples treated with aflibercept were significantly lower one day as well as seven days after injection compared to ranibizumab-treated samples at the same time points. The decrease in the level of VEGF from day one to day seven was found to be significant for aflibercept-treated but not for ranibizumab-treated animals.

The statistical analysis of the number of fenestrations of glomerular endothelial capillaries was complexly regarded. The distribution of values is always close to normality no matter which group is considered. Great effort was put into reducing errors of measurement and data was censored critically. Moreover, the sample size was very high considering the small number of monkeys in this pilot study. But as always advisable when data is statistically edited, the most cautious and assured conclusions are presented. The values obtained from the monkey treated with aflibercept and scarified one day after injection differ highly significantly from all values obtained from any other monkey (Anova, student's t-test and Tukey-Kramer-HSD test) in the sense of having a higher number of fenestrations per μm than all the other groups.

Also, significant differences were observed comparing the different time points

(days one and seven after injection) of the two animals injected with aflibercept, but not with ranibizumab when controls (the untreated monkey and the monkey injected with aflibercept's vehicle) are pooled. Comparing the same time points and the two different drugs, significant differences comparing the means of the groups Aflibercept day 1 and Ranibizumab day 1 are evident. Seven days after injection, comparing the two monkeys injected with the two different drugs (Aflibercept day 7 and Ranibizumab day 7), the difference between mean values is not significant at the set alpha level of 0,05.

In conclusion, it is evident that mean values of the group Aflibercept day 1 differ significantly from all other groups and control animals in the sense of higher group means. For other conditions, tendencies have to be kept in mind: The trend in the number of fenestrations seems to be higher especially one day after injection for the animal treated with aflibercept compared to the ranibizumab-treated monkey. Also, the ratio of fenestrations per μm seems to decrease comparing days one and seven after injection of both drugs- an observation that is statistically significant for aflibercept-treated but not ranibizumab-treated samples.

IV) Discussion

1. Analyses of eye tissue samples

(All the following results were obtained and described by Sylvie Julien-Schraermeyer and her co-authors in [148]).

The results obtained from the ophthalmologic analyses of other members of our study group will be briefly summarized so as to compare the findings to those observed in the kidney. As already mentioned, the same monkeys and treatments were used.

1.1. Ophthalmic examinations

No abnormalities in any of the eyes or time points in funduscopy, FA and SD-OCT were seen [148]. A significant increase in intraocular pressure directly after drug administration and a return to baseline ten minutes after drug administration was observed [148]. Regarding the measurements of intraocular pressure one day after injection of the two drugs, a significant decrease was seen. This decrease was only statistically significant for ranibizumab-treated but not for aflibercept-treated samples [148]. On day 7 after aflibercept injection, a significant IOP reduction compared to the untreated animal was seen. In contrast, the IOP of ranibizumab-treated animals normalized and reached baseline values 7 days after drug administration [148].

1.2. Immunohistochemistry of retina and choroid

Distinct distribution patterns of immune reactivity were already observed one day after intravitreal injection of the drugs. These distributions evidently differ between ranibizumab and aflibercept: *„Ranibizumab permeated the retina via intercellular clefts [...], whereas aflibercept was taken up by ganglion cells, cells of the inner and outer retinal layers and the RPE [...] Local accumulation in retinal and choroidal vessels was observed for both drugs [...] Ranibizumab immune reactivity was reduced after 7 days compared with day 1 [...] while aflibercept [...] showed no changes.“* [148]. Further immunohistochemical stainings indicated a mild activation of Mueller cells in the retina 1 and 7 days

after drug injections compared to controls [148]. Light microscopy revealed localized thrombocyte activation and fibrin formation in deeper choroidal vessels at day one and occasional stasis and hemolysis on day 7 after ranibizumab injection [148]. These findings were seen to a much greater extent in aflibercept treated samples where stasis and haemolysis occurred widely in the choriocapillaris samples examined [148]. Moreover, RPE was hypertrophic only in aflibercept treated samples and indications of RPE cell death were also found exclusively in these samples but on the other hand, photoreceptors did not seem to be affected [148]. Quantification of the area occupied by the choriocapillaris and of free haemoglobin revealed that the choriocapillaris area was reduced one day as well as seven days after injection of both drugs compared to untreated controls [148]. Also, a significantly higher amount of haemolytic plasma was seen in the choriocapillaris one and seven days after aflibercept injection compared to corresponding ranibizumab samples (Wilcoxon test) was seen [148].

1.3. Quantification of choriocapillaris endothelial cell fenestrations and measurement of endothelial thickness

The statistical analysis (Wilcoxon test) revealed a significant reduction in the number of fenestrae in the choriocapillaris after treatment with both aflibercept and ranibizumab compared to control samples [148]. Moreover, comparing the two drugs, the reduction in the number of fenestrations was significantly more predominant after aflibercept treatment at both time points [148]. The mean thickness of the endothelial wall decreased significantly when comparing treated animals and the control [148]. This effect was higher for aflibercept-treated animals [148] and the effect seems to be higher by comparing specimens of aflibercept days 1 and 7 [148].

1.4. Discussion of retina and choriocapillaris analyses

The possibility of an increase of the intraocular pressure after intravitreal anti-VEGF injection can be discussed. The normal intraocular pressure in human eyes is between 10-21 mm Hg, fluctuating during the day [148]. In the performed experiments, circadian fluctuations can be excluded due to regular

performances of measurements. A short term reversible increase in IOP is a well-known phenomenon after intravitreal injections [178], mainly due to an increase of intraocular volume [148]. The amount of aqueous humor determines intraocular pressure.

The ophthalmic examinations described show no detectable damage after a single intravitreal injection when funduscopy, FA and SD-OCT are performed, as it is clinical practice. We noted that there were no significant alterations of clinical observable parameters (of course, vision loss or gain could not be determined in a monkey experiment).

Only with the more specific histological, immunohistochemical and ultrastructural methods, early appearing effects of the drugs aflibercept and ranibizumab on the retina and choroid of these monkeys could be observed [148]. The study could provide evidence that the drugs permeate the retina in different ways: ranibizumab actively via intercellular clefts, aflibercept via uptake by ganglion cells, cells of the inner and outer retinal layers and the retinal pigment epithelium [148]. But further differences concerning the interaction of the drugs with the retinal tissues were seen. Particularly after aflibercept's treatment more frequent stasis and haemolysis were seen with the consequence of hypertrophy and death of individual RPE cells [148]. Also, the thickness of the endothelium of the choriocapillaris and the number of its fenestrations was reduced and haemolytic areas were more prominently seen after treatment with aflibercept although similar effects were seen for ranibizumab treated samples [148].

It has to be discussed if these findings are related to the Fc domain or other aflibercept-specific characteristics [148]. Especially the observed protein complex formation induced by aflibercept [148] is similar to processes previously described for bevacizumab [86, 131, 134, 179-181]. It can be speculated that phenomenon occurring under aflibercept treatment can be attributed to the fact that –in contrast to ranibizumab- it also contains the Fc domain of human IgG1 [148]. Also, binding affinities differ between drugs used for intravitreal injections [148]. In detail, one molecule of bevacizumab binds two VEGF-dimers. For ranibizumab, the contrary is the case with two molecules

needed to bind one VEGF-dimer. One molecule of aflibercept binds one molecule of VEGF-A or placental growth factor, respectively [182], [148]. Two hypotheses of the interaction of aflibercept and bevacizumab with proteins are presented in [148], one of them assuming that a part of the VEGF is still accessible allowing protein complex formation in spite of aflibercept forming a VEGF trap [148].

Due to differences of drug production (in Chinese hamster ovary (CHO) cells) [148], aflibercept and bevacizumab contain sugar residues whereas ranibizumab is produced in bacteria (*Escherichia coli*) and lacks these residues [148]. An interaction of these sugar residues and aflibercept's Fc domain might lead to red blood cell death through complement-activation [148], which is a possible explanation of the increased haemolysis found in the choriocapillaris in aflibercept-treated animals [148].

The role of VEGF in the maintenance of the choriocapillaris was previously described [183]. Consequently, a reduction of fenestrations as well as vessel occlusion is not surprising and has previously been investigated for bevacizumab [86] and also in the presently described study for the drugs aflibercept and ranibizumab, though with aflibercept having a stronger effect [148]. Also, free haemoglobin is proven to be toxic [184] and it can be hypothesized that it can have an effect on retinal pigment epithelium and endothelial cells [148].

In summary, the most striking changes of these analyses were a reduction of the lumen of the choriocapillaris, haemolysis, microangiopathy, formation of protein complexes, RPE hypertrophy and cell death [148] with all of the changes mentioned, apart from the lumen reduction, being more distinct or even only present after aflibercept treatment [148]. Thus, the authors recommend observation of the interaction of aflibercept and especially its Fc fragment with other molecules and cells and further investigation of the clinical significances of these findings [148].

1.5. Analysis of ciliary body and iris

(All the following results were obtained by Maximilian Ludinsky and analyzed,

described and discussed by me and Maximilian Ludinsky to the same degree in [150]; also see the declaration of personnel contribution on page 137 and appendix.)

Apart from the retina and choriocapillaris, the ciliary body and iris of the monkeys were also examined. Of special interest here were the fenestrations of the blood vessels of the ciliary body, which have - similar to those of the choriocapillaris and the glomerulus - a VEGF-dependent fenestrated endothelium [150]. These vessels also nourish the iris [150] and as the aqueous humor produced by the epithelium of the ciliary body is mainly responsible for the maintenance of the intraocular pressure (IOP), the relationship of the number of fenestrations [89] and IOP to VEGF inhibition was also of interest.

1.6. Immunohistochemistry/ light and fluorescence microscopy of ciliary body and iris

Immunohistochemical methods (a goat antiserum to human Fab of IgG and a goat anti-human IgG-Fc antibody and for both a cy3-rabbit anti-goat antibody as a secondary antibody, followed by staining, embedding and inspection with a fluorescence microscope) were used to localize the drugs in the ciliary body [150]. Aflibercept was slightly stronger stained than ranibizumab but both drugs could be localized in the ciliary body with equal distributions and the stainings between days 1 and 7 did not differ [150]. Briefly, strong staining was seen in the blood vessels' walls, some vessel lumen, the surface layer of the epithelium and the connective tissue of the vascular plexus. Other structures like the ciliary muscle and the cytoplasm of the endothelium were more weakly stained [150]. A slight difference was seen in the stroma of the epithelium in the aflibercept-treated samples being more intensively stained in contrast to ranibizumab-treated samples where the staining was more concentrated on the epithelial cells [150].

Also, VEGF was localized in ocular tissues. Therefore, the monoclonal mouse anti-human vascular endothelial growth factor was used as the first antibody, detected (REAL™ Detection System) and inspected by light microscopy [150]. The VEGF stainings were semi-quantified using high magnification light

microscopic images and the colour cube based[^] function in the Image-Pro Plus software [150]. Here, the intensive staining of the pigmented epithelium of the ciliary body that could be seen in control samples was weaker in samples of treated animals (similar at the different time points) [150].

1.7. Quantification of fenestrations in blood vessels of the ciliary body and histology

In specimens prepared for electron microscopy, two different regions of interest per eye/time point and control containing parts of both the ciliary body and the iris were photographed and investigated. The number of fenestrations of all the blood vessels visible were counted and the ratio of the number of fenestrations per 10 μm was statistically evaluated. T-test against the control was performed ($p < 0,05$ considered statistically significant) [150].

Morphological changes were seen in the posterior part of the pigmented epithelium of the iris of aflibercept-treated animals only [150]. The epithelial sections seen in samples of the animals treated with aflibercept and sacrificed on days one and seven contained multiple vacuoles in similar amounts [150]. Concerning the number of fenestrations, a statistically significant decrease was seen in samples of aflibercept on days 1 and 7 and ranibizumab on day 7 compared to control samples [150].

1.8. Discussion of ciliary body and iris analyses

The ciliary body is- besides its lens-related functions- responsible for aqueous humor production and secretion [89] and its drainage [88]- the last named in combination with the trabecular meshwork and the canal of Schlemm [88].

A common disease related to intraocular pressure is glaucoma. If the drainage of aqueous humor is defective, the intraocular pressure rises. If this state persists, the optic nerve can be damaged, leading to progressive irreversible vision loss [185]. Besides this major high-pressure related form of glaucoma, states with decreased or normal intraocular pressure can also cause damage to the optic nerve. These cases are called low pressure or normal pressure glaucoma [185]. This subform is caused by abnormal ocular blood flow [186], whereas the risk dominating the whole group of glaucoma diseases is the

significant death of retinal ganglion cells [185, 186]

As repeatedly discussed, neovascular eye diseases that go along with a pathologically increased formation of new vessels can strike the posterior part and cause wet AMD. But also the anterior part of the eye can be encompassed with the example of rubeosis iridis, a complication of diabetic retinopathy and central vein occlusion [150]. In this disease, neovascularization of the iris may lead to a special form of glaucoma, known as neovascular glaucoma [150]. *“The underlying pathogenesis in most cases is posterior segment ischemia”* [187] followed by the formation of new blood vessels that obstruct aqueous humor outflow [187].

The aim of glaucoma therapy is the lowering of intraocular pressure either by optimizing the drainage of aqueous humor or by reducing its production. Conventionally, topical beta blockers, prostaglandins (currently not so often) or alpha-2 antagonists and topical or oral carbonic anhydrase inhibitors are used [187]. The main therapeutic approach is photocoagulation [187], which in some cases needs to be accompanied by surgical procedures (trabeculectomy, glaucoma drainage devices, surgical carotid endarterectomy and others) [187]. Local anti-VEGF therapy is a comparably new therapeutic approach in the management of neovascular glaucoma diseases. Studies have shown that VEGF-A plays a role in the embryogenesis of the ciliary body as well as in the homeostasis and in the maintenance of the fenestrated phenotype of its capillaries in the adult [89]. In neovascular glaucoma patients, VEGF is mainly produced in the non-pigmented part of the epithelium of the ciliary body [187].

“Bevacizumab has already been used intracamerally and intravitreally for the adjuvant treatment of rubeosis iridis and neovascular glaucoma with promising results [119, 188-190]” [150]. Also, ranibizumab injections for the treatment of these diseases have been published [191-194]. More recently, aflibercept trials were also performed [195]. Lately, Rodrigues *et al.* [187] reviewed all the anti-VEGF treatments performed in this field with the result that its long-term effectiveness in neovascular glaucoma remains to be further evaluated whereas there is evidence that an anti-VEGF pre-treatment before surgery might be helpful [187].

Similarly to the cited studies, our results also show that an effect of the drugs is detectable as the number of fenestrations was reduced in the ciliary bodies of all treated animals. This goes along with the fact that the drugs were also well detectable at their possible sites of action. Also, the VEGF-staining became weaker in treated animals, which can be interpreted as a VEGF-reduction due to the pharmacological effects of aflibercept and ranibizumab. To which extent this effect will help to not only stabilize the IOP but also increase vision and comfort for patients has to be further investigated. Also, the possible side effects of these intravitreal anti-neovascular treatments as well as effects over a longer period of time and after repeated injections need further studies. In the described study [150], no histological changes compared to the controls were seen. Also in previous studies with bevacizumab, this was not observed by other authors either [196].

Another point that has to be discussed is the reduction of fenestrations in the vessels of the ciliary body, the trend being even higher when the animals were treated with aflibercept [150]. In ranibizumab samples, a significant reduction was only detected seven days after injection. Apart from being a desirable effect in the treatment of neovascularization, this issue may have clinical impacts like defects of the pigmented epithelial layer [89], prolonged ocular hypotony and phthisis bulbi [197], [150].

The distribution patterns of the two drugs only slightly differed. In contrast to ranibizumab, which was highly concentrated on the cells of the ciliary body epithelium, aflibercept staining was more prominent in the stroma. It can be discussed if this is a sign of a better penetration of ranibizumab into epithelial cells, which again might be related to the differences in the molecular structures of the drugs.

In particular, the vacuoles found in the posterior pigmented epithelium of the iris of aflibercept-treated animals need to be further discussed. They can hardly be related to physiological ageing processes [150]. In contrast to other morphological changes in ocular tissues [90, 93] vacuoles have not been described. Moreover, the human equivalent age of the study animals is between 13,8 and 16 years [150] making changes due to ageing in these

healthy animals improbable. Looking at pathological conditions, vacuoles filled with glycogen were found regularly in the eyes of diabetic patients [198] but also under malignant conditions (lung, prostate, leukemia) and are also known as microcysts of the iris pigmented epithelium [150, 199]. The observed vacuoles might for example be deposits or signs of oedema [150]. Nevertheless, the content and significance of the vacuoles found in the iris after aflibercept treatment remains unclear. Especially uncertainty remains as it was shown that most evidence of a beneficial effect of pre-surgically administered anti-VEGF drugs in neovascular glaucoma was found for the reduction of hyphema [187]. This fact is contradictory to the assumption that the vacuoles found in the iris are signs of oedema.

In summary, intraocular pressure has to be kept within strict limits although the tolerance might also be individual- dependent. The use of anti-VEGF agents in the treatment of patients with neovascular glaucoma is relatively new and its effectiveness and possible side-effects need to be further investigated. It must be seen whether it can offer a useful addition to proven and tested treatment regimens like photocoagulation and surgery. Future trials will show which of the available drugs is also more effective concerning clinical vision improvement with the least possible side-effects. Patients being treated against wet-AMD or rubeosis iridis/neovascular glaucoma might benefit from the higher affectivity of aflibercept in neutralizing VEGF which was found in this monkey study. However, aspects of this study indicate that further research is advisable to rule out any unexpected side effects [150].

1.9. Conclusion of analyses of eye tissue samples

The VEGF concentration was reduced in the ciliary body pigmented epithelium after treatment with both drugs [150]. This and the significant reduction of fenestrated endothelium in the choriocapillaris [148] as well as in the ciliary body [150] is an indication of the local impact of the drugs [148]. The slightly different distribution patterns of the drugs were not very distinct in the ciliary body where aflibercept's concentration was higher in the stroma in contrast to ranibizumab which was more concentrated on the cells of the ciliary body

epithelium [150]. In other ocular tissues the differences in distribution are more evident. More precisely, concerning the penetration of the retina different physiological processes have been revealed for aflibercept and ranibizumab [148]. As an explanation, the different molecular structures of the drugs may account for this [148].

The drugs could be detected in ocular tissues. Namely these were the ciliary body [150], the retina and the choriocapillaris [148]. Also, an effect of the anti-VEGF drugs in the sense of a reduction of fenestrations in VEGF-dependent tissues like the endothelium of the capillaries in the ciliary body [150] and the choriocapillaris [148] was observed. The number of fenestrations was reduced, with an effect tending to be higher in aflibercept-treated samples [148, 150]. No clinically observable changes in the eyes of the untreated as well as the treated monkeys, apart from a temporary increase in IOP (as described above) were seen. This increase can be explained and thus the additionally found morphological changes revealed by immunohistochemical and ultrastructural analyses have to be further investigated. Especially the significance of the vacuoles found in the posterior pigmented epithelium of the iris of aflibercept-treated animals currently remains speculative.

2. Analyses of kidney samples

2.1. Immunohistochemistry/ fluorescence staining of kidney samples

(analyzed and described by Alexander Tschulakow in [42].)

To evaluate the distribution of VEGF, aflibercept and ranibizumab in the kidney glomeruli of the monkeys, three staining methods were performed. After determining the area of interest, normalization and estimating the ratio of stained area/ cell count, samples from the untreated control animal were compared to treated animals and values of treated animals were statistically compared as well [42].

Staining of samples was carried out with a primary mouse antibody against the human IgG-Fab- fragment and a primary mouse antibody against the human IgG- Fc-fragment to test immune reactivity against ranibizumab and aflibercept, respectively. In addition, a fluorescent staining with corresponding antibodies

for the two drugs was performed [42]. These procedures revealed that the drugs were indeed detectable in the corresponding samples one and seven days after injection whereas there was no immune reactivity against the drugs in control samples [42].

Anti-VEGF staining was performed using primary mouse anti-VEGF antibodies. The analyses of the stained samples showed a significant decrease of VEGF levels in aflibercept-treated but not in ranibizumab-treated animals. Comparing samples from the two drugs at the same time points, VEGF levels were significantly lower in aflibercept-treated samples one and seven days after treatment. Also, the decrease in the VEGF level was only significant for animals treated with aflibercept [42].

2.2. Discussion of Immunohistochemistry/ fluorescence staining of kidney samples

It is not surprising that intravitreally injected anti-VEGF agents reach systemic circulation. But neither was it examined whether these agents also are detectable in distant organs like the kidneys nor if they have a measurable effect on the fenestrations of glomerular capillary endothelia.

Drug clearance from the vitreous might depend on molecular size as small molecules have a terminal half-life ($t_{1/2}$) of several hours when intravitreally injected whereas larger molecules have a terminal $t_{1/2}$ of several days (albumin 4,3 days with a molecular size of 67kDa, the full-length antibody trastuzumab 5,6 days with 148kDa) (reviewed by [200]). Also, the size of the eye might contribute, as clearance is quicker in rabbits than in monkeys and might even be slower in humans [200]. Thus, it can be expected that the antibody fragment ranibizumab with its molecule size of 48 kDa might be cleared more quickly from the eye than aflibercept with 115 kDa.

For ranibizumab, it was shown that once intravitreally injected, it is cleared from the eye into the circulation with a half-life of approximately 3 days in cynomolgus monkeys and with fifty percent of the dose reaching the circulation after 2 days [200]. Nevertheless, serum concentrations can be expected to be very low as a relatively small dose is administered and distributes over the

whole blood volume of the individual where it is probably cleared quickly [200]. Moreover, in our studies the drugs were only administered once whereas repeated monthly or on-demand doses are needed and performed clinically [201].

Studies showed that ranibizumab can be found in the serum but the concentrations detected were considered below the necessary threshold for a sufficient VEGF inhibition [202]. As the serum clearance half-life of ranibizumab is 3 days, our detection of the drug in the kidneys of the treated animals in keeping with these pharmacokinetics. It is possible that the drug already reached systemic circulation one day after intravitreal injection, and referring to this relatively long serum half-life, it is possible that there is also still some inflow into the kidney seven days after injection, offsetting the physiologically appearing elimination. Moreover, since ranibizumab is not protected from serum elimination by an Fc-fragment, it has been suggested that it is rapidly cleared from the circulation via renal elimination [42]. Thus, it can possibly accumulate in the kidney for a certain time whereas its dose in systemic circulation is very low and its systemic anti-VEGF activity is not detectable. This is in keeping with the findings in this study. Both drugs were detected within the glomeruli but VEGF levels in the glomeruli were not significantly affected by ranibizumab. Moreover, one day after ranibizumab injection, the endothelium cell layer and erythrocytes of most glomeruli showed specific fluorescence against human Fab of IgG which was nearly lost seven days after injection of ranibizumab [42]. This process might be almost ended 7 days after injection, which conforms to the determined half-life of ranibizumab of approximately 3 days.

For aflibercept, similar considerations have to be assessed. In order to understand its pharmacological characteristics, it has to be kept in mind that aflibercept is designed as a cytokine trap consisting of two extracellular cytokine receptor domains fused together to form a human immunoglobulin G (IgG) [203]. It has been published that aflibercept, in contrast to bevacizumab, binds VEGF-A in a 1 : 1 stoichiometry [204]. These aflibercept-VEGF complexes remain stable in the systemic circulation [204]. The authors speculated that because of this stoichiometry and the inert nature of the complexes, aflibercept

is not expected to accumulate in renal glomeruli [204] as has been found for bevacizumab. In a rabbit model the vitreous elimination half-life was approximately 4.5-4.7 days (reviewed by [205, 206]). Nevertheless, it has to be kept in mind that rodents have smaller eyes than primates and the eyes of humans are even bigger, and also that the half-life of aflibercept in the human eye has not been determined [206]. Thus, the half life can be expected to be even longer, assuming a long-term VEGF- blockade by aflibercept, which could be attributed to the stronger and prolonged binding of aflibercept to the VEGF-A receptor [205]. Also, experimental studies indicate that aflibercept penetrates all layers of the retina after intravitreal injection (molecular weight~110,000) with the least possible systemic exposure [207].

Considering the mentioned pharmacokinetics that can be expected for aflibercept and especially due to its measured vitreous elimination half-life of approximately 4.7 days in rabbits and its molecular size being more than double that of ranibizumab, our findings are surprising. Already one day after intravitreal aflibercept injection, the endothelium cell layer and material within the capillaries of many glomeruli were highly fluorescent after labeling with an antibody against the Fc region of IgG [42]. We wouldn't have expected a measurable amount of the drug to be able to escape from the eye and accumulate in the glomeruli so quickly. The decrease in intensity of this fluorescence on day seven after aflibercept injection is despite the expected long-term survival and stability of aflibercept-VEGF complexes. It is less surprising as any decrease would be physiological and because the amount of the decrease was not quantified in this study. On the other hand, a theoretically possible cross-reactivity of the injected antibody (a primary mouse antibody against the human IgG-Fc-fragment) with the Fc receptors or other Fc-domains containing proteins of the monkey has to be taken into account.

In anti-VEGF staining, a significant decrease in the mean VEGF level/cell ratio was only seen for aflibercept, but not for ranibizumab samples [42]. This was the case for both time points compared to untreated control-animal samples and to ranibizumab samples. A rationale for this was presented by Al-Halafi [205] who reviewed results of other authors [203, 208] indicating that aflibercept

should have more extended binding activity than anti-VEGF monoclonal antibodies like ranibizumab and bevacizumab. Aflibercept theoretically binds VEGF more tightly than native receptors or monoclonal antibodies [205]. These considerations might explain our findings of an apparently more effective VEGF-inhibition by aflibercept.

In 2012, when the present studies were performed, aflibercept was a new anti-VEGF drug. For safety considerations, two similarly designed, double blind, multi-centre, active-controlled, randomized controlled trials (VIEW 1 and VIEW 2) were about to be performed. They resulted in aflibercept being non-inferior to ranibizumab in efficacy in maintaining vision in treatment-naive patients with wet AMD after one year [209]. The safety profile of the two drugs was considered to be similar and it was assumed that with aflibercept, less frequent injections could be necessary [209]. On the other hand, due to different molecular designs and binding affinities, differences would not be surprising. As already mentioned above, differences in the molecular interaction of the two drugs were also found in examinations of the retina of the same monkeys [148]. They found differences in the molecular interaction of the two drugs with the retinal tissues concerning the penetration of the retina, hemolysis and protein complex formation (see above): "*Ranibizumab permeated the retina through intercellular spaces, whereas aflibercept was taken up by neuronal and retinal pigment epithelium (RPE) cells*" [148]. Aflibercept induced protein complex formation and more hemolysis in the choriocapillaris, leading to individual RPE cell death. The clinical significance and relation of these findings to the Fc domain or to other characteristics of aflibercept remain to be investigated.

Also, differences in the effectiveness of VEGF elimination and reduction of fenestrations were seen between the two drugs in the sense of a higher effect with aflibercept [148, 150]. Moreover, the formation of vacuoles in the iris after aflibercept- treatment in these monkeys currently remains unexplained [150]. As already mentioned above, the origins of the observed differences of the drug's effects as well as possible clinical impacts need to be further investigated.

2.3. VEGF-A plasma levels

As we expected the two intravitreally injected drugs to escape the eye and reach systemic circulation, the aim of this analysis was to determine whether VEGF-A plasma levels were affected compared to control samples. For this purpose, EDTA blood samples of all monkeys were collected before intravitreal injection (predose) and on days one and seven after injection of anti-VEGF agents. Plasma was prepared by centrifugation and the blood samples were analyzed using commercially available ELISA kits for human VEGF-A (DVE00) (R&D Systems, Minneapolis, Minnesota) [42]. This kit uses human VEGF-A specific antibodies and an enzyme-linked polyclonal antibody specific for human VEGF-A and a substrate solution employing the quantitative sandwich enzyme immunoassay technique. Color develops in proportion to the amount of VEGF bound in the initial step. The color development is stopped and the intensity of the color (Optical Density) is measured by photospectrometry and VEGF concentration is calculated. The lower detection limit of VEGF-A of this array is 30 pg/ml (for more details see [42, 155]).

We were unable to measure plasma VEGF levels since the concentrations were always below the detectable limit of the assay [42].

2.4. Discussion of VEGF-A plasma levels

“Larsson et al., have determined in 80 serum and EDTA plasma samples of healthy humans that the mean value \pm SD of VEGF in plasma was 32 ± 21 pg/ml [210]” [42]. They used the same array we did and no influence of age or sex was seen. Thus, we cannot exclude nor imply an effect of aflibercept or ranibizumab on VEGF serum levels as the actual concentration or any change in it was not measurable in our samples.

On one hand, *“the use of serum instead of plasma would be (conceptually) preferable since serum VEGF levels are several fold higher than plasma levels, because platelets express VEGF and secrete it during blood clotting [211]”* [42]. Webb et al. reported that serum VEGF levels were higher than plasma levels in adults (249.4 ± 46.4 versus 76.1 ± 10.7 pg/ml, $P < 0.0001$)[211]. On the other hand, though measuring of the levels would have been easier with serum,

plasma seems to be the preferred medium to measure true VEGF levels as VEGF secretion by platelets during clotting is significant and highly variable [211].

Following mathematical calculations, “*the systemic half-life of aflibercept is approximately 1.5 days and is greater than that of ranibizumab (6 hours) and less than that of bevacizumab (20 days)*” [206]. Maximum systemic concentrations of aflibercept are achieved approximately 2–3 days after intravitreal injection, and these maximal concentrations are estimated to be approximately 200-fold less than the concentration required for maximal VEGF binding [206, 212]. Therefore, it is unlikely that aflibercept will reduce systemic VEGF concentrations to a level that will disrupt key homeostatic mechanisms required for normal cardiovascular function [206]. Heier *et al.* did not detect aflibercept in the systemic circulation 2 weeks after intravitreal administration [115].

Data from oncology trials have shown that systemic clearance of aflibercept occurs by two major pathways [213]. The first pathway involves renal clearance following binding of VEGF, and this occurs when serum concentrations of aflibercept are relatively low. The second pathway occurs during states of relatively greater aflibercept concentration and involves pinocytic-mediated mechanisms and elimination by proteolysis [206]. After a single intravitreal injection, serum aflibercept concentrations can surely be assumed to have been very low in these studies. Thus, the renal pathway of elimination is most probable. This might partly explain why aflibercept was detected in the kidneys of all monkeys.

Preclinical pharmacokinetic analyses of ranibizumab after a single intravitreal injection performed by Gaudreault *et al.* [200] revealed that ranibizumab’s clearance from all ocular compartments had a terminal half-life or approximately 3 days after a single bilateral intravitreal injection with 500 or 2000 µg per eye. They also detected ranibizumab in the serum with concentrations they considered to be below the necessary threshold for a sufficient VEGF inhibition [202], [42]. Thus, comparably to the present study, in the study performed by Gaudreault *et al.* [200] both eyes were injected and the total dose reaching

systemic circulation might be about doubled. Also, the pharmacokinetics regarding a single eye as well as the chronological sequence of the maximum serum concentration is comparable. One group of the monkeys in Gaudreault's experiments was injected with the same amount of ranibizumab as in the present animal study (0,5mg = 500µg as also clinically practiced in humans). Even when more material (2000µg = 2mg) was intravitreally injected, serum concentration remained very low (150 and 616 ng/ml for 500 or 2000µg injected, respectively) and reached its maximum values after 6 hours [200]. In ocular compartments as in the serum, $t_{1/2}$ was approximately 3.5 days [200]. As a rule to compare the obtained results to the conditions in my study, "*the overall ranibizumab concentration after ITV administration was >1500-fold lower than the corresponding vitreous concentration*" [200]. Thus, in contrast to the mathematical calculated systemic half-life of six hours [206], the obtained half-life in the animal experiment was here 3.5 days for ranibizumab.

Avery *et al.* [141] stated that a lowering of systemic VEGF levels after intravitreal injection is much higher in the treatment with bevacizumab than with ranibizumab [141]. In comparison with aflibercept-injections, the systemic exposure after the third monthly intravitreal injection should be 13-fold greater for aflibercept than ranibizumab and 70-fold greater for bevacizumab than ranibizumab [141]. In summary, the systemic effect of ranibizumab appears to be the lowest, consistent with pharmacological differences between the agents [141], as already mentioned in the introduction part of this work. As systemic VEGF levels were not measurable, these assumptions could neither be proved nor refuted.

2.5. Quantification of the glomerular endothelial fenestrations and glomerular histology

The aim of quantifying the glomerular endothelial fenestrations and evaluating glomerular histology was to examine possible effects of the two intravitreally injected anti-VEGF agents on this strongly VEGF-dependent cellular phenotype.

For details concerning Material and Methods as well as Results, please see the

corresponding sections of this work.

No pathologic morphological changes were seen.

2.6. Discussion of the quantification of glomerular endothelial fenestrations

Statistical analyses

In the present study, examples of factors with an influence on the dispersion around the average value in a Gaussian distribution can be named: the observer, the picture quality/ the adjustment of the electron microscope, the fixation and preparation method, the individual monkey, the injected drug, the injection procedure, the concentration of the drug in the individual glomerulus, the randomly chosen excerpts of the glomeruli, the counting method and choice of images for evaluation. These factors and their possible influence on obtained results have to be discussed.

One would expect the control animal to have a more fenestrated glomerular endothelium as the anti-VEGF drugs used in the eye lead to a reduction of the number of VEGF-induced fenestrations in the retina. This was observed for bevacizumab in monkeys by Peters *et al* [86] and also in rats after bevacizumab-treatment by Shimomura *et al* [214]. After multiple injections of bevacizumab, Sugimoto *et al* saw a noticeable reduction in rabbit eyes [196]. Julien *et al* [148] also described a reduction of the number of fenestrations after the injection of ranibizumab but more prominent after aflibercept injection in the same monkeys as in this study. But in the statistical analyses for the kidneys performed –at least initially- this expected effect was not seen in the kidney but rather its contrary of an increase in fenestrations one day after intravitreal injection of the drugs. The not statistical significant trend of a reduction of the number of fenestrations can be seen in the course of time for the ranibizumab-treated animals comparing days one and seven after injection (samples of the untreated animal and the animal injected with aflibercept's vehicle pooled as control or only the untreated animal serving as control). For aflibercept, the increase in the number of fenestrations is statistically significant comparing days 1 and 7 and besides this, a statistically significant increase in the number

of fenestrations per μm compared to the control group/-s and all the other groups was observed.

Error of measurement

Evaluating the statistical analyses, errors of measurement also have to be considered. A gross error or random error would have occurred for example if the fixation method or detergents had been changed for this single experiment or samples. Due to good documentation of the fixation procedure, which was performed for all samples in the same way and within a short period of time by the same person, this can be excluded. Also, the adjustment of the electron microscope causing images which are hard to interpret or sharper compared images taken by other groups could modify the statistical analyses significantly. Indeed, images taken of samples of aflibercept day 1 are extremely sharp, but they absolutely do not differ from other samples in a way that would allow interpreting more or less fenestrae as comparable images show. This would in part explain the significantly higher amount in the number of fenestrae in the group Aflibercept day 1. On the other hand, the variation between Aflibercept day 1 and the other samples does not seem to be high enough to consider a gross error possible.

Another possibility is that a random error occurred due to the natural variability of biological objects- in this case the specific monkey or the interaction of this monkey's physiology with the drug. To be sure, the experiment would have to be repeated with another monkey or with a higher number of individuals per time point, which extends the possibilities of this study.

Another possibility of minimizing the random error of measurements would have been to carry out repeated measurements of different glomeruli, thus producing a high number of different images, or alternatively performing repeated measurements of the same images. Moreover, more than one blinded observer could have performed the analysis assuming either a different adjutancy of the electron microscope or differences in the counting results of fenestrae/ μm . Due to the already very high sample size, cost and effort, these procedures were not performed.

Here again, biological variability and the possible non-distinguishable interaction of the organism of the control animal with aflibercept's vehicle (a saline solution) have to be mentioned. This condition appears negligible due to the fact that there were no abnormalities detected in either the in-depth examinations of the eye tissues [148] or in my analyses of the kidneys of this control animal. It is known that the untreated monkey showed aplasia of the left kidney. This might have influenced the perfusion of the remaining organ and thus the concentration of the drug in the kidney. This modality would not have been integrated in statistical analysis. Uncertainty may remain as excessive blood and urine analyses aren't existent.

It should be noted that "*the heterogeneity of experimental animals regularly causes a considerable random sampling error as the dependent variable is often more influenced by deranging factors than by the examined factor*" [177] and is not only implied in this pilot study although the influence of one individual animal is comparably high due to the small number of animals. But again on the other hand, I could show that group means of the two control animals did not differ significantly which makes natural variability as a source of error improbable.

Another point worth being discussed is the theoretical possibility of taking kidney biopsies from each animal prior to treatments. These baseline values could be used to reduce the uncertainties about the influence of the individual's physiology on the experiments. However, the benefit of these procedures compared to the effort necessary as well as the additional deranging factors possibly caused (additional stress on animals, amount of sample material necessary for qualified analyses etc.) remains speculative.

In conclusion, the slightly better picture quality of the samples of aflibercept day 1 as well as the possible natural variability (especially concerning the monkeys injected with aflibercept and sacrificed one day after injection and the monkey injected with aflibercept's vehicle/ the two control animals) has to be considered, but also an actual effect of the drug aflibercept one day after injection is possible. Which effect aflibercept may cause in the kidney that might increase glomerular endothelial fenestrations is left to speculation. The

statistical significant reduction of fenestrations also observed in the course of time in aflibercept as well as a trend of reduction in ranibizumab samples also requires to be further studied.

Moreover, the general aspects of statistical analysis have to be considered. When no statistically significant difference could be detected, it does not mean that the means of the other samples are the same. In terms of statistics, you can only say that “*there wasn't enough evidence to show that they are different*” [176]. A significant difference could have possibly been shown by collecting more data.

Pooling of control samples

As sensitivity and power analysis comparing these two samples revealed, around 70 percent more observations would have been necessary to detect a significant difference at an alpha level of 0,05. Actually, more observations than the LSN (least significance number) are advisable [176] as the “*probability of finding a significant difference with LSN observations can be as low as 50%*” [176]. In conclusion, one can say that these two samples are congruent to a great extent.

Power

To increase the power of the statistical analysis, a couple of strategies can theoretically be considered. They include administering a large difference in doses [176], which would not have been reasonable as clinically the same doses are always applied and as this study was supposed to mimic clinical conditions in humans. A completely balanced instead of an unbalanced design [176] could have been realized with the same amount of measurements per group/ animal. On the other hand, this would not be in agreement with the study design to scan a whole glomerulus following the random SURS protocol as glomeruli do have different diameters. Also, the data can be considered to be roughly balanced due to high congruencies of sample sizes. The possibilities of increasing homogeneity of the subjects and thus reduce “noise” [176] was extended as far as practically realizable. The sample size was large with its total of observations compared to the number of variations (6 or 5 different groups

depending on the definition of the control group) due to the SURS protocol. Anyway, these points might be important to consider, but do not have any practical appliance here as the power is already maximized with the value of 1 and does not change even if the alpha level is decreased remarkably (to $>0,00001$).

Discussion of results of the quantification of glomerular endothelial cell fenestrations

The use of monkeys was absolutely necessary in this study as it also aimed to compare the effects of different drugs with different molecular structures. We carried out our research to examine possible side effects also probably caused by the existence or not of an Fc domain of the injected drugs. In contrast to rodents, the interaction between the Fc domain and the Fc receptors in monkeys mimic those present in humans [215]. In contrast to the fully human recombinant fusion protein aflibercept that contains the Fc region of human IgG1, ranibizumab is an Fc-domain- free antibody fragment. Members of our group had previously examined the effects of intravitreal bevacizumab on ocular tissues [86, 131, 134, 179] with local side-effects being among others reduction of the choriocapillaris lumina, number of fenestrations, photoreceptors' damage, formation of immune complexes and thrombotic microangiopathy. Different rationales especially for the thrombotic microangiopathy were offered. In brief, interactions of bevacizumab with thrombocytes [181] and activation of the complement cascade [180] were discussed and were mainly traced back to the Fc domain and complex formation with VEGF or heparin. It can thus be discussed if this set of problems might be reduced with the use of ranibizumab. Therefore, our group aimed to expand these studies to other drugs. In a previous study on the local effects of intravitreally injected ranibizumab and aflibercept performed in the same group of monkeys used in the present study, different interactions of the two drugs with ocular tissues were observed [148]. Julien *et al.* showed that besides different mechanisms of retina penetration, a reduction in the area of choriocapillaris was seen with both drugs. In aflibercept-treated samples, the reduction of the choriocapillaris endothelium thickness,

number of fenestrations and the areas with haemolysis were more pronounced than in controls or ranibizumab- treated samples. Whether this is linked to the Fc fragment of aflibercept remains suggestive.

We detected both drugs after both time points (one and seven days after injection) in the kidneys. The question was whether any effect on glomerular endothelial cell fenestrations could be measured. No significant reduction of the number of fenestrations per μm was found. In contrast and also surprisingly, aflibercept seemed to increase the number of fenestrations one day after injection compared to the controls or ranibizumab-treated monkeys. Simultaneously to VEGF-levels, the numbers of glomerular endothelial fenestrations per μm were not affected by ranibizumab to the same extent as by aflibercept.

The fact that VEGF expression in glomeruli has to be strictly regulated and the consequences of its dysregulation have already been described in the introduction section of this thesis. Other authors have already described a wide range of renal diseases occurring within weeks or months after intravitreal administration of VEGF inhibitors [216, 217], [42]. Also, there has been evidence that intravitreally injected drugs are absorbed systemically from the eye and can inhibit VEGF [216, 218-220], [42].

The differences in their molecular structures have also been suspected to influence on the elimination of the drugs. Not containing an Fc-fragment, ranibizumab is not protected from being eliminated from the serum. Thus, it might be rapidly cleared from circulation via renal elimination with a resulting serum concentration that is not sufficient for VEGF inhibition [200, 202] [42]. These assumptions seem to be in accordance with our data [42] as we could localize ranibizumab in the glomeruli of our samples one and seven days after intravitreal administration of the drugs but neither the VEGF levels nor the number of fenestrations was significantly influenced [42].

In contrast to ranibizumab, aflibercept does contain an Fc-fragment. Its binding stoichiometry to VEGF-A has been reported to be 1:1 [204]. Moreover, this complex remains stable in the circulation [204]. These two facts motivated the authors to speculate that the aflibercept-VEGF-A complex is inert and thus

aflibercept does not accumulate in renal glomeruli as does bevacizumab [204], [42]. The present study confirms these assumptions as for the first time aflibercept was detected in glomeruli after intravitreal injection [42]. Just as interesting: we detected a significant reduction of the glomerular VEGF level after aflibercept-treatment [42].

However, this study also reveals a rather unexpected result: As a consequence of the reduced VEGF level, not a reduction but an increase in the number of fenestrations was observed [42]. Peters *et al.* described a reduction of the number of fenestrations in the choriocapillaris after intravitreal anti-angiogenic therapy [86]- a phenomenon which would have appeared plausible for the kidneys in this study as well [42].

It is not yet completely clear to which extent regulation of fenestrations differs in the kidney and choriocapillaris. Ultrastructural analysis revealed and it is commonly accepted that the fenestrated endothelium of the choriocapillaris is covered by diaphragms [86]. In the kidney, the regulation of glomerular endothelial cell fenestrations seems to be very complex [42]. As an example, the development of endothelial fenestrations in the kidney is dependent on TGF- β 1 which it is not in the choriocapillaris [221], [42].

Another point that is controversy discussed is the existence or not of fenestral diaphragms in glomerular capillaries [46], [42]. A protein that is closely connected to this consideration is PV-1 (plasmalemmal vesicle-associated protein-1) [46], [42]. This protein is part of fenestral diaphragms and some authors suspect it to play a role in the formation of endothelial cell fenestrations [46]. If this protein is not found in endothelia, this fact is supposed to be equalized with a phenotype of fenestrations without diaphragms or with a matured endothelium as PV-1 is supposed to be necessary for the maturation of fenestrations and disappears in the course of time [46, 222] . Also, these two groups of scientists assume that this protein can be re-expressed in the case of damage and repair of endothelial cells and that diaphragms might re-appear under these circumstances [46, 222], [42].

We can thus speculate that the two proteins VEGF and PV-1 are expressed in the developing glomerular endothelium whereas only VEGF is vital to maintain

the fenestrated phenotype and PV-1 can be re-expressed in case of damage [46], [42]. Along with this speculation goes the variable presence of diaphragms [46], [42] as well as the observation of a “*reduction of fewer fenestrations by local or systemic VEGF- inhibition [68]*” [42].

However, there are groups of scientists who have made contradictory observations in the sense of a constant coverage of the glomerular endothelium with a diaphragm [47-49], [42]. Additionally to this discussion of a stable or variable existence of diaphragms, fixation procedures and their effect on the recognition of these structures have to be considered [42]. “*In our study, the fenestrations of the glomerular endothelial cells of adult monkeys were clearly not closed by diaphragms (Fig. 3A in [42]) which contrast to those observed in the choriocapillaris and reported in one of our previous monkey studies (Fig. 6 in [86])*” [42]. It should be noted that in this case we can exclude an influence of the techniques used but have to consider the fact that- in contrast to clinical practice- only a single administration of the anti-VEGF drugs was performed [42]. Moreover, in contrast to many patients requiring intravitreal anti-VEGF treatment, the monkeys in this study did not have a history of metabolic disease like diabetes which often manifests as diabetic retinopathy [42]. This microvascular disease might also affect the kidney and an intact VEGF-A secretion from podocytes has to be ensured for proper cellular functions [74], [42]. There has been a single report about a non-diabetic patient whose kidney functions had been unremarkable before the antiangiogenetic treatment of their wet AMD but who developed kidney toxicity after four intravitreal injections of bevacizumab [216], [42]. This might have been a rare event, but it advises caution. In diabetic patients, renal side effects are well-known after these procedures [218, 220, 223], [42].

“*Unfortunately we have no data concerning the urinary sediments. It would be of great interest to analyze them, especially as there are indications that anti VEGF therapies have influence on the kidneys, and can cause proteinuria and hypertension [224-226]. The analysis of the urinary sediments will also be an aim of our further studies.*” [42].

No morphological changes were seen in any of the kidney samples which

differs clearly from the results obtained from the retina of these monkeys. For example in contrast to the choriocapillaris, no microangiopathy or hemolysis was seen in any of the samples. If this is due to a lower drug concentration and if these observations would differ after repeated treatments or a longer timer period, cannot be concluded.

Is the increase of fenestrations one day after aflibercept injection a sign of a reaction of the glomerular endothelium to sheer stress or the potential damage? And why did the number of fenestrations tend to decrease again on day 7 after injection? Why was this phenomenon not seen to a comparable extent in ranibizumab treated examples? To answer these questions, PV-1 expression measurements are required. Moreover, in our studies, the tendencies can be seen of higher numbers of fenestrations on day 1 compared to day 7 in both aflibercept and ranibizumab samples (thus not statistically significant in ranibizumab groups). Due to the small number of study objects in this pilot study, it remains unclear if this is of clinical importance and if the possible decrease in number of fenestrations is due to the effect of VEGF- inhibition or due to a reaction of the endothelium on a possible impairment. The next question would be if this is a reaction to the specific injected drug or the VEGF inhibitory effect of the drug. *“What might happen if VEGFA is affected in a stimulated system is speculative and should be investigated. This might be a consequence of different antibody design. The immune complexes might be (an) inductor of thrombotic microangiopathy in the kidney [227]. Caution is needed when patients [...] (who) might also already [...] (have) renal disease are locally treated with these substances as they might definitively have systemic effects.” [42].*

2.7. Conclusion of analyses of kidney tissue samples

Already one day after a single intravitreal injection, both drugs could be detected within glomerular capillaries using immunohistochemical methods. A significant reduction of the anti-VEGF immune reactivity one day after injection of aflibercept compared to controls was seen in the podocytes. Moreover, a

significant decrease in VEGF levels was detected comparing days 1 and 7 after aflibercept-treatment. Comparing both drugs, VEGF-levels were lower in aflibercept samples whereas no effect on VEGF-levels was seen in ranibizumab-treated samples. It needs to be further investigated if these differences are based on aflibercept's higher affinity to VEGF or the higher stoichiometric concentration administered compared to ranibizumab [42].

The relevance of the statistically significant increase in the number of fenestrations one day after intravitreal injection of aflibercept compared to all other groups, which was not seen after ranibizumab-treatment, also needs to be further investigated. It remains unclear if this and the trend of a decrease in the number of fenestrations comparing samples one and seven days after injection of both drugs is a sign of a reaction of the glomerular endothelium on damage or stress or an effect of the anti-angiogenetic drugs. Moreover, studies on repeated intravitreal injections as clinically performed are necessary and possible effects on patients with renal history have to be monitored [42].

3. Conclusion of the work

In ocular as well as in kidney tissues, the two intravitreally injected drugs could be detected already one day after a single injection and also effects on the VEGF levels and the number of fenestrations of endothelia were seen this early. This shows that the drugs can escape from the blood-retinal barrier and reach distant organs like the kidney.

The first similarity concerning the observed effects was a reduction of the VEGF concentration in ciliary body and choriocapillaris and also in the kidney-however, here only after aflibercept injection. The second similarity comparing eye and kidney samples was a significant reduction of fenestrated endothelium in the ciliary body pigmented epithelium and in the choriocapillaris of the retina, which was also seen by trend comparing days 1 and 7 after injection of both drugs in the kidney. This can be interpreted to be the expected local impact of the anti-VEGF drugs in the eye and rises the question if already one day after intravitreal injection, an effect of the drug can also be present in the kidney.

Differences in the distribution patterns of the drugs were not very distinct in the

ciliary body and the kidney, but were more evident in the retina. Here, different physiological processes in the penetration of the retina were revealed which can probably be related to the different molecular structures of the drugs. Similar to the results obtained from kidney analyses of these monkeys, a higher effect in the reduction of the number of fenestrations was seen for aflibercept-treated samples in the ciliary body and the choriocapillaris. As a specialty- in contrast to eye tissue analyses- the quantification of the number of fenestrations in glomerular capillaries revealed a statistically significant increase one day after injection of aflibercept which remains unclear.

Concerning histology, no clinically observable changes in the kidneys of treated animals were seen. In eye analyses, vacuoles in the posterior pigmented epithelium of the iris of aflibercept-treated animals were observed. Their significance and content remains suggestive and needs to be further investigated. In retina and choroid, changes in the sense of reduction of the lumen of the choriocapillaris, haemolysis, microangiopathy, formation of protein complexes, RPE hypertrophy and cell death were seen. Most of these only occurred after aflibercept treatment or were here at least more distinct.

In future studies, all the named aspects should be further studied and also reevaluated after repeated intravitreal injections as patients in clinical routine usually demand several injections. The fact that the observed changes- especially concerning the number of fenestrations and the reduction of VEGF levels in the kidney- can not undoubtedly be related to an effect of the drugs but might also reflect a reaction of the endothelium on damage or stress should advise caution. In particular, the fact that all the described phenomena were more distinct or different after treatment with aflibercept should be kept in mind as this drug is comparably new. Also, often patients with a history of renal disease or diabetes require intravitreal anti-VEGF treatments and might carry a higher risk of systemic effects and should thus be monitored. This is of special interest as the number of anti-VEGF treatments in wet-AMD rises and as the fields of application in ophthalmology are being expanded to other indications such as diabetic retinopathy or neovascular glaucoma.

V) Summary

1. English summary

Fenestrated capillaries are found in tissues where filtration through a selective barrier is needed. This is for example the case in the eye where avascular tissues have to be nourished. Fenestrated capillaries of the choriocapillaries of the retina represent the blood-retina barrier and in the ciliary body aqueous humor has to be separated from the blood. In the kidney, the glomerular capillary wall realizes filtration through the blood-urinary barrier. This is realized by specialized fenestrated endothelium and this phenotype is strongly dependent on VEGF (vascular endothelial growth factor). One of the main functions of the VEGF family of signal molecules is its high neoangiogenic potential. As imbalances can cause severe complication, the application of systemic but also local anti-VEGF agents has to be well considered and monitored. Systemic application has been found to be effective in several types of neoplasms. Occurring side-effects are often unavoidable and dose-dependent. A local and very effective anti-VEGF therapy is the intravitreal application of anti-angiogenic agents mainly used to treat the wet form of age-related macular degeneration (wet AMD). In this approach, the abnormal growth of new blood vessels in the retina is inhibited, thus arresting or even reversing patients' vision loss. Presently, three different anti-VEGF agents (bevacizumab, ranibizumab and aflibercept) are successfully applied worldwide, but they might differ in their risks to cause side-effects due to their molecular design. As comparing the effects of the two molecularly different drugs on the kidney was one of the major aims of this study, only monkeys have been found to be suitable as study objects because the interactions between the Fc domain of antibodies and the Fc receptors are comparable to those in humans. The fully human, recombinant fusion protein aflibercept (which contains the Fc region of human IgG1) and ranibizumab (a Fc-domain-free antibody fragment) were compared especially regarding kidney tissues in comparison to ocular tissues like the retina/ choroid complex and ciliary body and iris. Also, previous studies had revealed that the interactions of these two anti-VEGF drugs with the retina and choroid clearly differ.

Ten cynomolgus monkeys were intravitreally injected either with ranibizumab or aflibercept and ophthalmological examinations were performed. Animals were sacrificed on days one or seven, respectively and eyes and kidneys were removed.

One untreated and one monkey treated with aflibercept's vehicle served as controls. Light and transmission electron microscopic as well as immunohistochemical and fluorescent microscopical studies were performed. Moreover, measurements of VEGF-plasma levels were performed but all doses were below the detectable limit of the assay. Using a systematic uniform random sampling protocol in TEM, the numbers of fenestrations per μm in glomerular capillaries were estimated and statistically analyzed.

Both the anti-VEGF drugs ranibizumab and aflibercept could be detected in kidney glomeruli by immunohistochemistry. No histological pathologies were found in any of the kidneys. Aflibercept significantly reduced VEGF levels in the kidney one and seven days after intravitreal injection- an effect that was not observed in ranibizumab samples. Also, an effect on the number of fenestrations of glomerular endothelial cells was found. Surprisingly, the number of fenestrations of the glomerular endothelium was significantly increased the first day after aflibercept-treatment compared to control and all other samples. Concerning the two time points (one and seven days after injection), a trend of a decrease in the number of fenestrations was seen after treatment with both drugs which was only significant for aflibercept. The significance and cause of the higher number of fenestrations one day after aflibercept injection remains unclear. Stress-related mechanisms as a reaction of the endothelium to possible damage or specific interactions between the drug and kidney tissues as well as the formation of immune complexes should be further examined.

Comparing the obtained results to the quantification of fenestrations of the ciliary body's vessels, a reduction of fenestrations was found in all samples with aflibercept reducing significantly more fenestrations than ranibizumab. Interestingly, in all eyes treated with aflibercept, vacuoles were found in the pigmented epithelium of the iris for which no rationale was found. It can only be speculated that these vacuoles are congruent with described microcysts of the pigmented iris epithelium or accumulations of glycogen in diabetic patients. Equally, further investigations are needed to estimate if an apparently higher effectiveness in eliminating fenestrations as seen with aflibercept is desirable for example in the treatment of neovascular glaucoma.

In conclusion, the possibility of side-effects occurring after a single intravitreal injection of anti-VEGF drugs not only locally in the eye but also in the kidney and other distant organs has to be considered as the drugs were detected in the kidneys

and as aflibercept reduced VEGF levels in glomeruli. The mechanisms and impacts of the detected increase of glomerular endothelial cell fenestrations by aflibercept one day after injection need to be further evaluated. Similarly, a possible effect in the sense of a reduction of VEGF-dependent fenestrations of glomerular capillaries in the course of time and after repeated injections requires further studies. Possible effects on the kidney might be more critical for patients with a prior history of nephrological disease and with repeated intravitreal injections as clinically practiced for the treatment of wet AMD. The observed effects in the kidney as well as in ocular tissues and potential differences between ranibizumab and the relatively new aflibercept as well as their possible impacts need to be further examined.

2. Deutsche Zusammenfassung

Fenestrierte Kapillaren finden sich in Geweben, in denen Filtration durch eine selektive Barriere realisiert werden muss. Dies ist beispielsweise im Auge der Fall, wo avaskuläre Gewebe ernährt werden müssen. Die fenestrierten Kapillaren der Choriocapillaris der Retina stellen die Blut-Retina-Schranke dar und im Ziliarkörper müssen Kammerwasser und Blut getrennt werden. In der Niere wird die Filtration von Primärharn durch die Blut-Harn-Schranke mit Hilfe der glomerulären Kapillarwand realisiert. Verschiedene Untersuchungen haben gezeigt, dass hierfür spezialisiertes fenestriertes Endothel notwendig ist und dass dieser Phänotyp stark von VEGF (englisch für vaskulärer endothelialer Wachstumsfaktor) abhängig ist. Eine der Hauptfunktionen der Familie der VEGF Signalmoleküle ist ihr hohes Potential, das Wachstum neuer Blutgefäße- die sogenannte (Neo-) Angiogenese- zu fördern. Da jegliche Dysregulation schwere Komplikationen nach sich ziehen kann, sollte die Anwendung systemischer aber auch lokaler Angiogenesehemmer wohl durchdacht und überwacht werden. In einer Vielzahl von Neoplasmen hat sich die systemische Anti-Angiogenesetherapie als effektiv gezeigt. Das Auftreten von Nebenwirkungen in Organen wie zum Beispiel Darm und Niere ist oft unvermeidbar und abhängig von der applizierten Dosis. Eine lokale und sehr effektive Therapie vor allem der feuchten altersbedingten Makuladegeneration stellt die intravitreale Applikation solcher Medikamente dar, bei der das überschießende Wachstum neuer Blutgefäße in der Retina gehemmt wird. Momentan werden weltweit drei verschiedene Medikamente in der Therapie dieser Erkrankung eingesetzt, zwischen denen Unterschiede bezüglich des Risikos der Auslösung von unerwünschten Wirkungen bestehen, die vermutlich

in deren unterschiedlichem molekularem Design und der Interaktion mit den betroffenen Geweben sowie dem Immunsystem des Patienten begründet sind. Hierbei scheint vor allem das Vorhandensein einer Fc Domäne von Bedeutung zu sein. Deshalb wurden in dieser Studie Affen als Studienobjekte gewählt, da nur so die spezifischen Interaktionen der Medikamente mit menschlichen Fc-Rezeptoren imitiert werden können.

Das erste Ziel der Untersuchungen war es, herauszufinden ob eine einzige intravitreale Injektion der beiden zu vergleichenden Medikamente möglicherweise systemische Nebenwirkungen hervorrufen kann. Des Weiteren interessierte der Vergleich der Wirkungen des vollständig humanen rekombinanten Fusionsprotein Aflibercept (das die Fc Domäne von humanem IgG1 enthält) und Ranibizumab (ein Antikörper-Fragment ohne Fc Domäne) vor allem in Bezug auf ihre Wirkung auf Nierenglomeruli und der Vergleich zu okularen Geweben wie dem Retina-Choroid-Komplex sowie Ziliarkörper und Iris nach einer einzigen intravitrealen Applikation. Hierzu wurden zehn Affen der Gattung *Macaca* entweder Ranibizumab oder Aflibercept injiziert. Ophthalmologische Untersuchungen wurden durchgeführt und die Tiere ein bzw. sieben Tage nach der Behandlung geopfert, wonach Augen und Nieren entnommen wurden. Ein unbehandelter Affe und ein Tier, dem die Trägersubstanz von Aflibercepts Injektionslösung injiziert wurden, dienten als Kontrollen. Licht- und transelektronenmikroskopische sowie fluoreszenzmikroskopische und immunhistologische Untersuchungen der Nieren ebenso wie eine Bestimmung der VEGF Level im Plasma wurden durchgeführt.

In der Tat konnten beide Medikamente durch immunhistochemische Methoden in den untersuchten Nierenglomeruli nachgewiesen werden. Im Gegensatz zu Ranibizumab reduzierte Aflibercept die VEGF Level in den Nieren einen sowie sieben Tage nach intravitrealer Injektion signifikant. Außerdem zeigte sich ein Effekt auf die Anzahl der Fenestrierungen des glomerulären Endothels. Überraschenderweise nahm die Anzahl der Fenestrierungen des glomerulären Endothels am ersten Tag nach der Injektion von Aflibercept im Vergleich zu Kontrollen und Proben aller anderen Affen stark signifikant zu. Die Unterschiede zwischen den anderen Proben waren weniger deutlich. Bezüglich der beiden Zeitpunkte (ein und sieben Tage nach Injektion) zeigte sich vor allem für die mit Aflibercept behandelten Affen eine Abnahme der Fenestrierungen, die als Tendenz auch in der Ranibizumab-Gruppe zu sehen war. Histologisch zeigten keine der

Nieren pathologische Auffälligkeiten.

Gemäß früheren Untersuchungen der Retina, wäre eine Verringerung der Anzahl der Fenestrierungen durch antiangiogenetische Behandlung auch in der Niere mit ihrem vergleichbaren Phänotyp erwartet worden. Bedeutung und Ursache der Zunahme an Fenestrierungen einen Tag nach der Injektion von Aflibercept bleibt unklar. Stressbedingte Mechanismen wie zum Beispiel eine Reaktion des Endothels auf mögliche Schädigungen oder spezifische Interaktionen des Medikaments mit Nierengewebe sowie die Bildung von Immunkomplexen sollten untersucht werden.

Die fenestrierten Kapillaren des Ziliarkörpers tragen auch zur Aufrechterhaltung des intraokularen Drucks bei. Auch bei der Quantifizierung dieser Fenestrierungen wurde eine Reduzierung der Anzahl in allen Proben gefunden, wobei der Effekt von Aflibercept sowohl einen als auch sieben Tage nach Injektion im Vergleich zu Ranibizumab signifikant höher war. Interessanterweise wurden in der Iris aller mit Aflibercept behandelte Tiere Vakuolen gefunden. Es wurde bisher noch keine abschließende Erklärung für deren Auftreten gefunden und die scheinbar höhere Effektivität von Aflibercept muss hier noch weiter untersucht und bewertet werden.

Zusammenfassend sollte beachtet werden, dass Nebenwirkungen nach intravitrealer Injektion von antiangiogenetischen Medikamenten nicht nur lokal im Auge, sondern auch in der Niere und anderen entfernten Organen auftreten können. Hinweise hierfür liefert diese Studie, da die Medikamente in allen untersuchten Nieren nachgewiesen wurden und da Aflibercept das VEGF Level in den untersuchten Glomeruli schon nach einer einzigen Injektion reduzierte. Mechanismen und Auswirkungen der erhöhten Anzahl an Fenestrierungen im Endothel der glomerulären Kapillaren einen Tag nach Aflibercept-Injektion sollten weiter untersucht werden. Ebenso muss ein möglicher Effekt im Sinne einer Reduktion der VEGF-abhängigen Fenestrierung der Nierenkapillaren im Laufe der Zeit und nach wiederholten Injektionen näher untersucht werden. Mögliche die Niere betreffende Effekte wären wahrscheinlich für Patienten mit nephrologischen Vorerkrankungen sowie bei wiederholter intravitrealer Injektion, wie es klinisch in der Behandlung der feuchten altersbedingten Makuladegeneration die Regel ist, kritischer.

VI) References

1. Ferrara, N., *VEGF and the quest for tumour angiogenesis factors*. Nat Rev Cancer, 2002. **2**(10): p. 795-803.
2. Ferrara, N., *Vascular endothelial growth factor*. Arterioscler Thromb Vasc Biol, 2009. **29**(6): p. 789-91.
3. Ferrara, N., Carver-Moore, K., et al., *Heterozygous embryonic lethality induced by targeted inactivation of the VEGF gene*. Nature, 1996. **380**(6573): p. 439-42.
4. Carmeliet, P., Ferreira, V., et al., *Abnormal blood vessel development and lethality in embryos lacking a single VEGF allele*. Nature, 1996. **380**(6573): p. 435-9.
5. Yla-Herttuala, S., Rissanen, T.T., et al., *Vascular endothelial growth factors: biology and current status of clinical applications in cardiovascular medicine*. J Am Coll Cardiol, 2007. **49**(10): p. 1015-26.
6. Senger, D.R., Galli, S.J., et al., *Tumor cells secrete a vascular permeability factor that promotes accumulation of ascites fluid*. Science, 1983. **219**(4587): p. 983-5.
7. Ferrara, N. and Henzel, W.J., *Pituitary follicular cells secrete a novel heparin-binding growth factor specific for vascular endothelial cells*. Biochem Biophys Res Commun, 1989. **161**(2): p. 851-8.
8. Plouet, J., Schilling, J., et al., *Isolation and characterization of a newly identified endothelial cell mitogen produced by AtT-20 cells*. EMBO J, 1989. **8**(12): p. 3801-6.
9. Stuttfeld, E. and Ballmer-Hofer, K., *Structure and function of VEGF receptors*. IUBMB Life, 2009. **61**(9): p. 915-22.
10. Robinson, C.J. and Stringer, S.E., *The splice variants of vascular endothelial growth factor (VEGF) and their receptors*. J Cell Sci, 2001. **114**(Pt 5): p. 853-65.
11. Clauss, M., Gerlach, M., et al., *Vascular permeability factor: a tumor-derived polypeptide that induces endothelial cell and monocyte procoagulant activity, and promotes monocyte migration*. J Exp Med, 1990. **172**(6): p. 1535-45.
12. Pepper, M.S., Ferrara, N., et al., *Vascular endothelial growth factor (VEGF) induces plasminogen activators and plasminogen activator inhibitor-1 in microvascular endothelial cells*. Biochem Biophys Res Commun, 1991. **181**(2): p. 902-6.
13. Unemori, E.N., Ferrara, N., et al., *Vascular endothelial growth factor induces interstitial collagenase expression in human endothelial cells*. J Cell Physiol, 1992. **153**(3): p. 557-62.
14. Pekala, P., Marlow, M., et al., *Regulation of hexose transport in aortic endothelial cells by vascular permeability factor and tumor necrosis factor-alpha, but not by insulin*. J Biol Chem, 1990. **265**(30): p. 18051-4.
15. Alon, T., Hemo, I., et al., *Vascular endothelial growth factor acts as a survival factor for newly formed retinal vessels and has implications for retinopathy of prematurity*. Nat Med, 1995. **1**(10): p. 1024-8.
16. Vincenti, V., Cassano, C., et al., *Assignment of the vascular endothelial growth factor gene to human chromosome 6p21.3*. Circulation, 1996. **93**(8): p. 1493-5.
17. Houck, K.A., Ferrara, N., et al., *The vascular endothelial growth factor family: identification of a fourth molecular species and characterization of alternative splicing of RNA*. Mol Endocrinol, 1991. **5**(12): p. 1806-14.
18. Tischer, E., Mitchell, R., et al., *The human gene for vascular endothelial growth factor. Multiple protein forms are encoded through alternative exon splicing*. J Biol Chem, 1991. **266**(18): p. 11947-54.
19. Leung, D.W., Cachianes, G., et al., *Vascular endothelial growth factor is a secreted*

-
- angiogenic mitogen*. Science, 1989. **246**(4935): p. 1306-9.
20. Houck, K.A., Leung, D.W., et al., *Dual regulation of vascular endothelial growth factor bioavailability by genetic and proteolytic mechanisms*. J Biol Chem, 1992. **267**(36): p. 26031-7.
 21. Poltorak, Z., Cohen, T., et al., *VEGF145, a secreted vascular endothelial growth factor isoform that binds to extracellular matrix*. J Biol Chem, 1997. **272**(11): p. 7151-8.
 22. Lei, J., Jiang, A., et al., *Identification and characterization of a new splicing variant of vascular endothelial growth factor: VEGF183*. Biochim Biophys Acta, 1998. **1443**(3): p. 400-6.
 23. Gospodarowicz, D., Abraham, J.A., et al., *Isolation and characterization of a vascular endothelial cell mitogen produced by pituitary-derived folliculo stellate cells*. Proc Natl Acad Sci U S A, 1989. **86**(19): p. 7311-5.
 24. Hashimoto, E., Ogita, T., et al., *Rapid induction of vascular endothelial growth factor expression by transient ischemia in rat heart*. Am J Physiol, 1994. **267**(5 Pt 2): p. H1948-54.
 25. Plate, K.H., Breier, G., et al., *Vascular endothelial growth factor is a potential tumour angiogenesis factor in human gliomas in vivo*. Nature, 1992. **359**(6398): p. 845-8.
 26. Minchenko, A., Salceda, S., et al., *Hypoxia regulatory elements of the human vascular endothelial growth factor gene*. Cell Mol Biol Res, 1994. **40**(1): p. 35-9.
 27. Shweiki, D., Itin, A., et al., *Vascular endothelial growth factor induced by hypoxia may mediate hypoxia-initiated angiogenesis*. Nature, 1992. **359**(6398): p. 843-5.
 28. Eremina, V., Baelde, H.J., et al., *Role of the VEGF--a signaling pathway in the glomerulus: evidence for crosstalk between components of the glomerular filtration barrier*. Nephron Physiol, 2007. **106**(2): p. p32-7.
 29. Jakeman, L.B., Winer, J., et al., *Binding sites for vascular endothelial growth factor are localized on endothelial cells in adult rat tissues*. J Clin Invest, 1992. **89**(1): p. 244-53.
 30. Shibuya, M., Yamaguchi, S., et al., *Nucleotide sequence and expression of a novel human receptor-type tyrosine kinase gene (flt) closely related to the fms family*. Oncogene, 1990. **5**(4): p. 519-24.
 31. Soker, S., Takashima, S., et al., *Neuropilin-1 is expressed by endothelial and tumor cells as an isoform-specific receptor for vascular endothelial growth factor*. Cell, 1998. **92**(6): p. 735-45.
 32. de Vries, C., Escobedo, J.A., et al., *The fms-like tyrosine kinase, a receptor for vascular endothelial growth factor*. Science, 1992. **255**(5047): p. 989-91.
 33. Terman, B.I., Dougher-Vermazen, M., et al., *Identification of the KDR tyrosine kinase as a receptor for vascular endothelial cell growth factor*. Biochem Biophys Res Commun, 1992. **187**(3): p. 1579-86.
 34. Pajusola, K., Aprelikova, O., et al., *FLT4 receptor tyrosine kinase contains seven immunoglobulin-like loops and is expressed in multiple human tissues and cell lines*. Cancer Res, 1992. **52**(20): p. 5738-43.
 35. Finnerty, H., Kelleher, K., et al., *Molecular cloning of murine FLT and FLT4*. Oncogene, 1993. **8**(8): p. 2293-8.
 36. Kaipainen, A., Korhonen, J., et al., *Expression of the fms-like tyrosine kinase 4 gene becomes restricted to lymphatic endothelium during development*. Proc Natl Acad Sci U S A, 1995. **92**(8): p. 3566-70.
 37. IvyRoseLtd. Human Body Study Section [cited 2016 26.03.]; Available from: http://www.ivyroses.com/HumanBody/Urinary/Urinary_System_Nephron_Diag

- [ram.php](#).
38. Lang, F., *Niere*, in *Basiswissen Physiologie*. 2000, Springer-Verlag Berlin Heidelberg New York. p. 235-259.
 39. Schulte, E., *Niere und ableitende Harnwege*, in *MLP Duale Reihe Anatomie*. 2007, Georg Thieme Verlag. p. 756-770.
 40. Jarad, G. and Miner, J.H., *Update on the glomerular filtration barrier*. *Curr Opin Nephrol Hypertens*, 2009. **18**(3): p. 226-32.
 41. Tesarova, P. and Tesar, V., *Proteinuria and hypertension in patients treated with inhibitors of the VEGF signalling pathway--incidence, mechanisms and management*. *Folia Biol (Praha)*, 2013. **59**(1): p. 15-25.
 42. Tschulakow, A., Christner, S., et al., *Effects of a single intravitreal injection of aflibercept and ranibizumab on glomeruli of monkeys*. *PLoS One*, 2014. **9**(11): p. e113701.
 43. Deen, W.M., *What determines glomerular capillary permeability?* *J Clin Invest*, 2004. **114**(10): p. 1412-4.
 44. Obeidat, M., Obeidat, M., et al., *Glomerular endothelium: a porous sieve and formidable barrier*. *Exp Cell Res*, 2012. **318**(9): p. 964-72.
 45. Muller-Deile, J., Worthmann, K., et al., *The balance of autocrine VEGF-A and VEGF-C determines podocyte survival*. *Am J Physiol Renal Physiol*, 2009. **297**(6): p. F1656-67.
 46. Satchell, S.C. and Braet, F., *Glomerular endothelial cell fenestrations: an integral component of the glomerular filtration barrier*. *Am J Physiol Renal Physiol*, 2009. **296**(5): p. F947-56.
 47. Hjalmarsen, C., Johansson, B.R., et al., *Electron microscopic evaluation of the endothelial surface layer of glomerular capillaries*. *Microvasc Res*, 2004. **67**(1): p. 9-17.
 48. Rostgaard, J. and Qvortrup, K., *Electron microscopic demonstrations of filamentous molecular sieve plugs in capillary fenestrae*. *Microvasc Res*, 1997. **53**(1): p. 1-13.
 49. Rostgaard, J. and Qvortrup, K., *Sieve plugs in fenestrae of glomerular capillaries--site of the filtration barrier?* *Cells Tissues Organs*, 2002. **170**(2-3): p. 132-8.
 50. Huber, T.B. and Benzing, T., *The slit diaphragm: a signaling platform to regulate podocyte function*. *Curr Opin Nephrol Hypertens*, 2005. **14**(3): p. 211-6.
 51. Ulfig, N., *Die Niere*, in *Kurzlehrbuch Histologie*. 2005, Georg Thieme Verlag. p. 177-185.
 52. Gnudi, L., Benedetti, S., et al., *Vascular growth factors play critical roles in kidney glomeruli*. *Clin Sci (Lond)*, 2015. **129**(12): p. 1225-36.
 53. Breier, G., Albrecht, U., et al., *Expression of vascular endothelial growth factor during embryonic angiogenesis and endothelial cell differentiation*. *Development*, 1992. **114**(2): p. 521-32.
 54. Marti, H.H. and Risau, W., *Systemic hypoxia changes the organ-specific distribution of vascular endothelial growth factor and its receptors*. *Proc Natl Acad Sci U S A*, 1998. **95**(26): p. 15809-14.
 55. Izzedine, H., Rixe, O., et al., *Angiogenesis inhibitor therapies: focus on kidney toxicity and hypertension*. *Am J Kidney Dis*, 2007. **50**(2): p. 203-18.
 56. Datta, K., Li, J., et al., *Regulation of vascular permeability factor/vascular endothelial growth factor (VPF/VEGF-A) expression in podocytes*. *Kidney Int*, 2004. **66**(4): p. 1471-8.
 57. Amaral, S.L., Roman, R.J., et al., *Renin gene transfer restores angiogenesis and vascular endothelial growth factor expression in Dahl S rats*. *Hypertension*, 2001. **37**(2 Pt 2): p. 386-90.

58. Gruden, G., Thomas, S., et al., *Interaction of angiotensin II and mechanical stretch on vascular endothelial growth factor production by human mesangial cells*. J Am Soc Nephrol, 1999. **10**(4): p. 730-7.
59. Saijonmaa, O., Nyman, T., et al., *Upregulation of angiotensin-converting enzyme by vascular endothelial growth factor*. Am J Physiol Heart Circ Physiol, 2001. **280**(2): p. H885-91.
60. Hayashi, K., Miyamoto, A., et al., *Regulation of angiotensin II production and angiotensin receptors in microvascular endothelial cells from bovine corpus luteum*. Biol Reprod, 2000. **62**(1): p. 162-7.
61. Schrijvers, B.F., Flyvbjerg, A., et al., *The role of vascular endothelial growth factor (VEGF) in renal pathophysiology*. Kidney Int, 2004. **65**(6): p. 2003-17.
62. Brown, L.F., Berse, B., et al., *Vascular permeability factor mRNA and protein expression in human kidney*. Kidney Int, 1992. **42**(6): p. 1457-61.
63. Uchida, K., Uchida, S., et al., *Glomerular endothelial cells in culture express and secrete vascular endothelial growth factor*. Am J Physiol, 1994. **266**(1 Pt 2): p. F81-8.
64. Iijima, K., Yoshikawa, N., et al., *Human mesangial cells and peripheral blood mononuclear cells produce vascular permeability factor*. Kidney Int, 1993. **44**(5): p. 959-66.
65. Simon, M., Grone, H.J., et al., *Expression of vascular endothelial growth factor and its receptors in human renal ontogenesis and in adult kidney*. Am J Physiol, 1995. **268**(2 Pt 2): p. F240-50.
66. Kim, B.S. and Goligorsky, M.S., *Role of VEGF in kidney development, microvascular maintenance and pathophysiology of renal disease*. Korean J Intern Med, 2003. **18**(2): p. 65-75.
67. Eremina, V., Jefferson, J.A., et al., *VEGF inhibition and renal thrombotic microangiopathy*. N Engl J Med, 2008. **358**(11): p. 1129-36.
68. Izzedine, H., Escudier, B., et al., *Kidney diseases associated with anti-vascular endothelial growth factor (VEGF): an 8-year observational study at a single center*. Medicine (Baltimore), 2014. **93**(24): p. 333-9.
69. Eremina, V., Sood, M., et al., *Glomerular-specific alterations of VEGF-A expression lead to distinct congenital and acquired renal diseases*. J Clin Invest, 2003. **111**(5): p. 707-16.
70. Noguchi, K., Yoshikawa, N., et al., *Activated mesangial cells produce vascular permeability factor in early-stage mesangial proliferative glomerulonephritis*. J Am Soc Nephrol, 1998. **9**(10): p. 1815-25.
71. Thomas, S., Vanuystel, J., et al., *Vascular endothelial growth factor receptors in human mesangium in vitro and in glomerular disease*. J Am Soc Nephrol, 2000. **11**(7): p. 1236-43.
72. Shahbazi, M., Fryer, A.A., et al., *Vascular endothelial growth factor gene polymorphisms are associated with acute renal allograft rejection*. J Am Soc Nephrol, 2002. **13**(1): p. 260-4.
73. Bello-Reuss, E., Holubec, K., et al., *Angiogenesis in autosomal-dominant polycystic kidney disease*. Kidney Int, 2001. **60**(1): p. 37-45.
74. Tufro, A. and Veron, D., *VEGF and podocytes in diabetic nephropathy*. Semin Nephrol, 2012. **32**(4): p. 385-93.
75. Nicol, D., Hii, S.I., et al., *Vascular endothelial growth factor expression is increased in renal cell carcinoma*. J Urol, 1997. **157**(4): p. 1482-6.
76. Tomisawa, M., Tokunaga, T., et al., *Expression pattern of vascular endothelial growth factor isoform is closely correlated with tumour stage and vascularisation*

- in renal cell carcinoma*. Eur J Cancer, 1999. **35**(1): p. 133-7.
77. Shulman, K., Rosen, S., et al., *Expression of vascular permeability factor (VPF/VEGF) is altered in many glomerular diseases*. J Am Soc Nephrol, 1996. **7**(5): p. 661-6.
 78. Iruela-Arispe, L., Gordon, K., et al., *Participation of glomerular endothelial cells in the capillary repair of glomerulonephritis*. Am J Pathol, 1995. **147**(6): p. 1715-27.
 79. Kim, Y.G., Suga, S.I., et al., *Vascular endothelial growth factor accelerates renal recovery in experimental thrombotic microangiopathy*. Kidney Int, 2000. **58**(6): p. 2390-9.
 80. Ostendorf, T., Kunter, U., et al., *VEGF(165) mediates glomerular endothelial repair*. J Clin Invest, 1999. **104**(7): p. 913-23.
 81. Nowak, J.Z., *AMD--the retinal disease with an unprecised etiopathogenesis: in search of effective therapeutics*. Acta Pol Pharm, 2014. **71**(6): p. 900-16.
 82. Kolb, H., Nelson, R., et al. *Webvision The Organization of the Retina and Visual System*. 2012 [cited 2016 10.02.]; Available from: <http://webvision.med.utah.edu>.
 83. Jager, R.D., Mieler, W.F., et al., *Age-related macular degeneration*. N Engl J Med, 2008. **358**(24): p. 2606-17.
 84. Adamis, A.P., Shima, D.T., et al., *Synthesis and secretion of vascular permeability factor/vascular endothelial growth factor by human retinal pigment epithelial cells*. Biochem Biophys Res Commun, 1993. **193**(2): p. 631-8.
 85. Guerrin, M., Moukadi, H., et al., *Vasculotropin/vascular endothelial growth factor is an autocrine growth factor for human retinal pigment epithelial cells cultured in vitro*. J Cell Physiol, 1995. **164**(2): p. 385-94.
 86. Peters, S., Heiduschka, P., et al., *Ultrastructural findings in the primate eye after intravitreal injection of bevacizumab*. Am J Ophthalmol, 2007. **143**(6): p. 995-1002.
 87. Spitalnik, P. and Witkin, J. *The Eye: Microscopic Examination, #119. Eye, sagittal section*. SBPMD Histology Laboratory Manual [cited 2016 27.02.]; Available from: http://www.columbia.edu/itc/hs/medical/sbpm_histology_old/lab/lab15_eyemicroscope.html.
 88. Freddo, T.F., Gong, Haiyan, *Anatomy of the Ciliary Body and Outflow Pathways*, in *Duane's Clinical Ophthalmology* 2011, Lippincott Williams & Wilkins.
 89. Ford, K.M., Saint-Geniez, M., et al., *Expression and role of VEGF--a in the ciliary body*. Invest Ophthalmol Vis Sci, 2012. **53**(12): p. 7520-7.
 90. Salvi, S.M., Akhtar, S., et al., *Ageing changes in the eye*. Postgrad Med J, 2006. **82**(971): p. 581-7.
 91. Ferris, F.L., 3rd, Wilkinson, C.P., et al., *Clinical classification of age-related macular degeneration*. Ophthalmology, 2013. **120**(4): p. 844-51.
 92. Fine, S.L., Berger, J.W., et al., *Age-related macular degeneration*. N Engl J Med, 2000. **342**(7): p. 483-92.
 93. Ardeljan, D. and Chan, C.C., *Aging is not a disease: distinguishing age-related macular degeneration from aging*. Prog Retin Eye Res, 2013. **37**: p. 68-89.
 94. Organisciak, D.T. and Vaughan, D.K., *Retinal light damage: mechanisms and protection*. Prog Retin Eye Res, 2010. **29**(2): p. 113-34.
 95. Nguyen, D.H., Luo, J., et al., *Current therapeutic approaches in neovascular age-related macular degeneration*. Discov Med, 2013. **15**(85): p. 343-8.
 96. Dong, A., Xie, B., et al., *Oxidative stress promotes ocular neovascularization*. J Cell Physiol, 2009. **219**(3): p. 544-52.
 97. Cong, R., Zhou, B., et al., *Smoking and the risk of age-related macular degeneration:*

-
- a meta-analysis*. Ann Epidemiol, 2008. **18**(8): p. 647-56.
98. Evans, J.R. and Lawrenson, J.G., *Antioxidant vitamin and mineral supplements for slowing the progression of age-related macular degeneration*. Cochrane Database Syst Rev, 2012. **11**: p. CD000254.
 99. Folkman, J., Merler, E., et al., *Isolation of a tumor factor responsible for angiogenesis*. J Exp Med, 1971. **133**(2): p. 275-88.
 100. Folkman, J., *Tumor angiogenesis: therapeutic implications*. N Engl J Med, 1971. **285**(21): p. 1182-6.
 101. Cao, Y. and Langer, R., *A review of Judah Folkman's remarkable achievements in biomedicine*. Proc Natl Acad Sci U S A, 2008. **105**(36): p. 13203-5.
 102. Cao, Y., O'Reilly, M.S., et al., *Expression of angiostatin cDNA in a murine fibrosarcoma suppresses primary tumor growth and produces long-term dormancy of metastases*. J Clin Invest, 1998. **101**(5): p. 1055-63.
 103. Browder, T., Butterfield, C.E., et al., *Antiangiogenic scheduling of chemotherapy improves efficacy against experimental drug-resistant cancer*. Cancer Res, 2000. **60**(7): p. 1878-86.
 104. Kieran, M.W., Turner, C.D., et al., *A feasibility trial of antiangiogenic (metronomic) chemotherapy in pediatric patients with recurrent or progressive cancer*. J Pediatr Hematol Oncol, 2005. **27**(11): p. 573-81.
 105. Ezekowitz, A., Mulliken, J., et al., *Interferon alpha therapy of haemangiomas in newborns and infants*. Br J Haematol, 1991. **79** Suppl 1: p. 67-8.
 106. Folkman, J., *Angiogenesis in psoriasis: therapeutic implications*. J Invest Dermatol, 1972. **59**(1): p. 40-3.
 107. Folkman, J., *Angiogenesis--retrospect and outlook*. EXS, 1992. **61**: p. 4-13.
 108. Adamis, A.P., Shima, D.T., et al., *Inhibition of vascular endothelial growth factor prevents retinal ischemia-associated iris neovascularization in a nonhuman primate*. Arch Ophthalmol, 1996. **114**(1): p. 66-71.
 109. Schmidt-Erfurth, U.M., Richard, G., et al., *Guidance for the treatment of neovascular age-related macular degeneration*. Acta Ophthalmol Scand, 2007. **85**(5): p. 486-94.
 110. Presta, L.G., Chen, H., et al., *Humanization of an anti-vascular endothelial growth factor monoclonal antibody for the therapy of solid tumors and other disorders*. Cancer Res, 1997. **57**(20): p. 4593-9.
 111. Hurwitz, H., Fehrenbacher, L., et al., *Bevacizumab plus irinotecan, fluorouracil, and leucovorin for metastatic colorectal cancer*. N Engl J Med, 2004. **350**(23): p. 2335-42.
 112. Rosenfeld, P.J., *Intravitreal avastin: the low cost alternative to lucentis?* Am J Ophthalmol, 2006. **142**(1): p. 141-3.
 113. Rosenfeld, P.J., Brown, D.M., et al., *Ranibizumab for neovascular age-related macular degeneration*. N Engl J Med, 2006. **355**(14): p. 1419-31.
 114. Brown, D.M., Kaiser, P.K., et al., *Ranibizumab versus verteporfin for neovascular age-related macular degeneration*. N Engl J Med, 2006. **355**(14): p. 1432-44.
 115. Heier, J.S., Brown, D.M., et al., *Intravitreal aflibercept (VEGF trap-eye) in wet age-related macular degeneration*. Ophthalmology, 2012. **119**(12): p. 2537-48.
 116. Sigford, D.K., Reddy, S., et al., *Global reported endophthalmitis risk following intravitreal injections of anti-VEGF: a literature review and analysis*. Clin Ophthalmol, 2015. **9**: p. 773-81.
 117. Tah, V., Orland, H.O., et al., *Anti-VEGF Therapy and the Retina: An Update*. J Ophthalmol, 2015: p. 627674.
 118. Bikbov, M.M., Babushkin, A.E., et al., *[Anti-VEGF-agents in treatment of*

-
- neovascular glaucoma*]. *Vestn Oftalmol*, 2012. **128**(5): p. 50-3.
119. Grisanti, S., Biester, S., et al., *Intracameral bevacizumab for iris rubeosis*. *Am J Ophthalmol*, 2006. **142**(1): p. 158-60.
 120. Tolentino, M., *Systemic and ocular safety of intravitreal anti-VEGF therapies for ocular neovascular disease*. *Surv Ophthalmol*, 2011. **56**(2): p. 95-113.
 121. Barkmeier, A.J. and Akduman, L., *Bevacizumab (avastin) in ocular processes other than choroidal neovascularization*. *Ocul Immunol Inflamm*, 2009. **17**(2): p. 109-17.
 122. Kiss, I., Bortliceck, Z., et al., *Efficacy and toxicity of bevacizumab on combination with chemotherapy in different lines of treatment for metastatic colorectal carcinoma*. *Anticancer Res*, 2014. **34**(2): p. 949-54.
 123. Izzedine, H., Massard, C., et al., *VEGF signalling inhibition-induced proteinuria: Mechanisms, significance and management*. *Eur J Cancer*, 2010. **46**(2): p. 439-48.
 124. Frangie, C., Lefaucheur, C., et al., *Renal thrombotic microangiopathy caused by anti-VEGF-antibody treatment for metastatic renal-cell carcinoma*. *Lancet Oncol*, 2007. **8**(2): p. 177-8.
 125. Izzedine, H., Brocheriou, I., et al., *Thrombotic microangiopathy and anti-VEGF agents*. *Nephrol Dial Transplant*, 2007. **22**(5): p. 1481-2.
 126. Vigneau, C., Lorcy, N., et al., *All anti-vascular endothelial growth factor drugs can induce 'pre-eclampsia-like syndrome': a RARE study*. *Nephrol Dial Transplant*, 2014. **29**(2): p. 325-32.
 127. Eremina, V. and Quaggin, S.E., *Biology of anti-angiogenic therapy-induced thrombotic microangiopathy*. *Semin Nephrol*, 2010. **30**(6): p. 582-90.
 128. Foster, R.R., Saleem, M.A., et al., *Vascular endothelial growth factor and nephrin interact and reduce apoptosis in human podocytes*. *Am J Physiol Renal Physiol*, 2005. **288**(1): p. F48-57.
 129. Maynard, S., Epstein, F.H., et al., *Preeclampsia and angiogenic imbalance*. *Annu Rev Med*, 2008. **59**: p. 61-78.
 130. Izzedine, H., Isnard-Bagnis, C., et al., *Gemcitabine-induced thrombotic microangiopathy: a systematic review*. *Nephrol Dial Transplant*, 2006. **21**(11): p. 3038-45.
 131. Schraermeyer, U. and Julien, S., *Effects of bevacizumab in retina and choroid after intravitreal injection into monkey eyes*. *Expert Opin Biol Ther*, 2013. **13**(2): p. 157-67.
 132. Fontaine, O., Olivier, S., et al., *The effect of intravitreal injection of bevacizumab on retinal circulation in patients with neovascular macular degeneration*. *Invest Ophthalmol Vis Sci*, 2011. **52**(10): p. 7400-5.
 133. Rofagha, S., Bhisitkul, R.B., et al., *Seven-year outcomes in ranibizumab-treated patients in ANCHOR, MARINA, and HORIZON: a multicenter cohort study (SEVEN-UP)*. *Ophthalmology*, 2013. **120**(11): p. 2292-9.
 134. Schraermeyer, U. and Julien, S., *Formation of immune complexes and thrombotic microangiopathy after intravitreal injection of bevacizumab in the primate eye*. *Graefes Arch Clin Exp Ophthalmol*, 2012. **250**(9): p. 1303-13.
 135. von Hanno, T., Kinge, B., et al., *Retinal artery occlusion following intravitreal anti-VEGF therapy*. *Acta Ophthalmol*, 2010. **88**(2): p. 263-6.
 136. Hosseini, H., Lotfi, M., et al., *Effect of intravitreal bevacizumab on retrobulbar blood flow in injected and uninjected fellow eyes of patients with neovascular age-related macular degeneration*. *Retina*, 2012. **32**(5): p. 967-71.
 137. Singer, M., *Advances in the management of macular degeneration*. *F1000Prime Rep*, 2014. **6**: p. 29.

138. Solomon, S.D., Lindsley, K., et al., *Anti-vascular endothelial growth factor for neovascular age-related macular degeneration*. Cochrane Database Syst Rev, 2014. **8**: p. CD005139.
139. Shahar, J., Avery, R.L., et al., *Electrophysiologic and retinal penetration studies following intravitreal injection of bevacizumab (Avastin)*. Retina, 2006. **26**(3): p. 262-9.
140. Kim, H., Robinson, S.B., et al., *FcRn receptor-mediated pharmacokinetics of therapeutic IgG in the eye*. Mol Vis, 2009. **15**: p. 2803-12.
141. Avery, R.L., *What is the evidence for systemic effects of intravitreal anti-VEGF agents, and should we be concerned?* Br J Ophthalmol, 2014. **98 Suppl 1**: p. i7-10.
142. Matsuyama, K., Ogata, N., et al., *Plasma levels of vascular endothelial growth factor and pigment epithelium-derived factor before and after intravitreal injection of bevacizumab*. Br J Ophthalmol, 2010. **94**(9): p. 1215-8.
143. Carneiro, A.M., Costa, R., et al., *Vascular endothelial growth factor plasma levels before and after treatment of neovascular age-related macular degeneration with bevacizumab or ranibizumab*. Acta Ophthalmol, 2012. **90**(1): p. e25-30.
144. Investigators, I.S., Chakravarthy, U., et al., *Ranibizumab versus bevacizumab to treat neovascular age-related macular degeneration: one-year findings from the IVAN randomized trial*. Ophthalmology, 2012. **119**(7): p. 1399-411.
145. Najafian, B. and Mauer, M., *Quantitating glomerular endothelial fenestration: an unbiased stereological approach*. Am J Nephrol, 2011. **33 Suppl 1**: p. 34-9.
146. Ferrara, N., Damico, L., et al., *Development of ranibizumab, an anti-vascular endothelial growth factor antigen binding fragment, as therapy for neovascular age-related macular degeneration*. Retina, 2006. **26**(8): p. 859-70.
147. Julien, S., Biesemeier, A., et al., *In vitro induction of protein complexes between bevacizumab, VEGF-A(1)(6)(5) and heparin: explanation for deposits observed on endothelial veins in monkey eyes*. Br J Ophthalmol, 2013. **97**(4): p. 511-7.
148. Julien, S., Biesemeier, A., et al., *Different effects of intravitreally injected ranibizumab and aflibercept on retinal and choroidal tissues of monkey eyes*. Br J Ophthalmol, 2014.
149. Julien, S., Heiduschka, P., et al., *Immunohistochemical localisation of intravitreally injected bevacizumab at the posterior pole of the primate eye: implication for the treatment of retinal vein occlusion*. Br J Ophthalmol, 2008. **92**(10): p. 1424-8.
150. Ludinsky, M., Christner, S., et al., *The effects of VEGF-A-inhibitors aflibercept and ranibizumab on the ciliary body and iris of monkeys*. Graefes Arch Clin Exp Ophthalmol, 2016. **254**(6): p. 1117-25.
151. Peters, S., Heiduschka, P., et al., *Immunohistochemical localisation of intravitreally injected bevacizumab in the anterior chamber angle, iris and ciliary body of the primate eye*. Br J Ophthalmol, 2008. **92**(4): p. 541-4.
152. Julien, S., Tschulakow, A.V., et al., *Effects of a single intravitreal injection of aflibercept and ranibizumab on glomeruli of monkeys*. Investigative Ophthalmology & Visual Science, 2014. **55**(13): p. 1946-1946.
153. Inc., G. *HIGHLIGHTS OF PRESCRIBING INFORMATION*. [cited 2016 24.06.]; Available from: http://www.gene.com/download/pdf/lucentis_prescribing.pdf.
154. Inc., R.P. *HIGHLIGHTS OF PRESCRIBING INFORMATION*. [cited 2017 17.03.]; Available from: <http://www.regeneron.com/Eylea/eylea-fpi.pdf>.
155. Inc., R.D.S. *Quantikine® ELISA Human VEGF Immunoassay*. [cited 2016 13.04.]; Available from: <https://resources.rndsystems.com/pdfs/datasheets/dve00.pdf>.
156. Ruifrok, A.C. and Johnston, D.A., *Quantification of histochemical staining by color deconvolution*. Anal Quant Cytol Histol, 2001. **23**(4): p. 291-9.

157. Drury, J.A., Nik, H., et al., *Endometrial cell counts in recurrent miscarriage: a comparison of counting methods*. *Histopathology*, 2011. **59**(6): p. 1156-62.
158. Kachouie, N., Kang, L., et al., *Arraycount, an algorithm for automatic cell counting in microwell arrays*. *Biotechniques*, 2009. **47**(3): p. x-xvi.
159. Eibl, O. and Schraermeyer, U., *Anleitung zum Praktikum Analytische Elektronenmikroskopie für Naturwissenschaftler und Mediziner*, 2014.
160. Busch, H., "Berechnung der Bahn von Kathodenstrahlen im axialsymmetrischen elektromagnetischen Felder, ". *Annalen der Physik*, 1926. **386**(25): p. 974-993.
161. Busch, H., *Über die Wirkungsweise der Konzentrierungsspule bei der Braunschen Röhre*. *Archiv für Elektrotechnik*, 1927. **18**(6): p. 583-594.
162. M. Knoll, E.R., *Das Elektronenmikroskop*. *Zeitschrift für Physik*, 1932. **78**(5-6): p. 318-339.
163. Ruska, E., *Das Elektronenmikroskop als Übermikroskop*. *Forschungen und Fortschritte*, 1934. **10**: p. 8.
164. Ruska, E., *Beiträge zur Elektronenoptik*. 1937.
165. Reimer, L., *Transmission Electron Microscopy*. 1989: Springer-Verlag.
166. Duerrschnabel, M., *Advanced methods for structural characterization and structure-property correlation for functional materials of layered compounds*, 2013, Eberhard Karls Universität Tübingen.
167. Eibl, O., *Grundlagen und Verfahren der angewandten Elektronenmikroskopie*, 2004.
168. Riedel, E., *Allgemeine und Anorganische Chemie*. 2010: Walter de Gruyter GmbH & Co.
169. McIntosh, J.R., *Cellular Electron Microscopy*. 2007: Academic Press.
170. H. Plattner, J.H., *Zellbiologie*. 2002: Thieme Verlag.
171. D. Williams, C.C., , *Transmission Electron Microscopy*. *Plenum Press*, 1996. 1996: Plenum Press.
172. Eroms, M. [cited 2016 30.06.]; Available from: <http://www.physik.uni-regensburg.de/forschung/schwarz/Mikroskopie/06-TEM.pdf>.
173. Reimer, L. and Kohl, H., *Transmission Electron Microscopy: Physics of Image Formation and Microanalysis*. 5 ed. Springer Series in Optical Sciences. Vol. 36. 1984, New York: Springer-Verlag New York.
174. Kondo, H. and Ushiki, T., *Stratified laminae fenestratae (alveolus fenestratus endothelialis) in the glomerular capillaries of the mouse kidney*. *Arch Histol Jpn*, 1985. **48**(1): p. 117-22.
175. Gibson, I.W., Downie, I., et al., *The parietal podocyte: a study of the vascular pole of the human glomerulus*. *Kidney Int*, 1992. **41**(1): p. 211-4.
176. Sall, J., Lehman, A., et al., *JMP Start Statistics*. Second Edition ed, ed. C. Hinrichs. 2001, Pacific Grove, CA, USA: DUXBURY Thomson Learning.
177. Harms, V., *Biomathematik, Statistik und Dokumentation*. 1998, Kiel-Mönkeberg: HARMS VERLAG.
178. Mojica, G., Hariprasad, S.M., et al., *Short-term intraocular pressure trends following intravitreal injections of ranibizumab (Lucentis) for the treatment of wet age-related macular degeneration*. *Br J Ophthalmol*, 2008. **92**(4): p. 584.
179. Heiduschka, P., Fietz, H., et al., *Penetration of bevacizumab through the retina after intravitreal injection in the monkey*. *Invest Ophthalmol Vis Sci*, 2007. **48**(6): p. 2814-23.
180. Meyer, C.H. and Holz, F.G., *Preclinical aspects of anti-VEGF agents for the treatment of wet AMD: ranibizumab and bevacizumab*. *Eye (Lond)*, 2011. **25**(6): p. 661-72.

181. Meyer, T., Robles-Carrillo, L., et al., *Bevacizumab immune complexes activate platelets and induce thrombosis in FCGR2A transgenic mice*. J Thromb Haemost, 2009. **7**(1): p. 171-81.
182. Stewart, M.W., *Clinical and differential utility of VEGF inhibitors in wet age-related macular degeneration: focus on aflibercept*. Clin Ophthalmol, 2012. **6**: p. 1175-86.
183. Lang, F. and Qadri, S.M., *Mechanisms and significance of eryptosis, the suicidal death of erythrocytes*. Blood Purif, 2012. **33**(1-3): p. 125-30.
184. Schaer, D.J., Buehler, P.W., et al., *Hemolysis and free hemoglobin revisited: exploring hemoglobin and hemin scavengers as a novel class of therapeutic proteins*. Blood, 2013. **121**(8): p. 1276-84.
185. Carreon, T., van der Merwe, E., et al., *Aqueous outflow - A continuum from trabecular meshwork to episcleral veins*. Prog Retin Eye Res, 2017. **57**: p. 108-133.
186. Fan, N., Wang, P., et al., *Ocular Blood Flow and Normal Tension Glaucoma*. Biomed Res Int, 2015. **2015**: p. 308505.
187. Rodrigues, G.B., Abe, R.Y., et al., *Neovascular glaucoma: a review*. Int J Retina Vitreous, 2016. **2**: p. 26.
188. Yazdani, S., Hendi, K., et al., *Intravitreal bevacizumab (Avastin) injection for neovascular glaucoma*. J Glaucoma, 2007. **16**(5): p. 437-9.
189. Wolf, A., von Jagow, B., et al., *Intracameral injection of bevacizumab for the treatment of neovascular glaucoma*. Ophthalmologica, 2011. **226**(2): p. 51-6.
190. Ghanem, A.A., El-Kannishy, A.M., et al., *Intravitreal bevacizumab (avastin) as an adjuvant treatment in cases of neovascular glaucoma*. Middle East Afr J Ophthalmol, 2009. **16**(2): p. 75-9.
191. Luke, J., Nassar, K., et al., *Ranibizumab as adjuvant in the treatment of rubeosis iridis and neovascular glaucoma--results from a prospective interventional case series*. Graefes Arch Clin Exp Ophthalmol, 2013. **251**(10): p. 2403-13.
192. Tu, Y., Fay, C., et al., *Ranibizumab in patients with dense cataract and proliferative diabetic retinopathy with rubeosis*. Oman J Ophthalmol, 2012. **5**(3): p. 161-5.
193. Liu, L., Xu, Y., et al., *Intravitreal ranibizumab injection combined trabeculectomy versus Ahmed valve surgery in the treatment of neovascular glaucoma: assessment of efficacy and complications*. BMC Ophthalmol, 2016. **16**: p. 65.
194. Olmos, L.C., Sayed, M.S., et al., *Long-term outcomes of neovascular glaucoma treated with and without intravitreal bevacizumab*. Eye (Lond), 2016. **30**(3): p. 463-72.
195. SooHoo, J.R., Seibold, L.K., et al., *Aflibercept for the treatment of neovascular glaucoma*. Clin Exp Ophthalmol, 2015. **43**(9): p. 803-7.
196. Sugimoto, Y., Mochizuki, H., et al., *Histological findings of uveal capillaries in rabbit eyes after multiple intravitreal injections of bevacizumab*. Curr Eye Res, 2013. **38**(4): p. 487-96.
197. Jovanovik-Pandova, L., Watson, P.G., et al., *Ciliary tissue transplantation in the rabbit*. Exp Eye Res, 2006. **82**(2): p. 247-57.
198. Yanoff, M., Fine, B.S., et al., *Diabetic lacy vacuolation of iris pigment epithelium; a histopathologic report*. Am J Ophthalmol, 1970. **69**(2): p. 201-10.
199. Fischer, R., Henkind, P., et al., *Microcysts of the human iris pigment epithelium*. Br J Ophthalmol, 1979. **63**(11): p. 750-3.
200. Gaudreault, J., Fei, D., et al., *Preclinical pharmacokinetics of Ranibizumab (rhuFabV2) after a single intravitreal administration*. Invest Ophthalmol Vis Sci, 2005. **46**(2): p. 726-33.
201. Frampton, J.E., *Ranibizumab: a review of its use in the treatment of neovascular age-related macular degeneration*. Drugs Aging, 2013. **30**(5): p. 331-58.

202. Barbazetto, I.A., Saroj, N., et al., *Incidence of new choroidal neovascularization in fellow eyes of patients treated in the MARINA and ANCHOR trials*. Am J Ophthalmol, 2010. **149**(6): p. 939-946 e1.
203. Holash, J., Davis, S., et al., *VEGF-Trap: a VEGF blocker with potent antitumor effects*. Proc Natl Acad Sci U S A, 2002. **99**(17): p. 11393-8.
204. Rudge, J.S., Holash, J., et al., *VEGF Trap complex formation measures production rates of VEGF, providing a biomarker for predicting efficacious angiogenic blockade*. Proc Natl Acad Sci U S A, 2007. **104**(47): p. 18363-70.
205. Al-Halafi, A.M., *Vascular endothelial growth factor trap-eye and trap technology: Aflibercept from bench to bedside*. Oman J Ophthalmol, 2014. **7**(3): p. 112-5.
206. Balaratnasingam, C., Dhrami-Gavazi, E., et al., *Aflibercept: a review of its use in the treatment of choroidal neovascularization due to age-related macular degeneration*. Clin Ophthalmol, 2015. **9**: p. 2355-71.
207. Pieramici, D.J. and Rabena, M.D., *Anti-VEGF therapy: comparison of current and future agents*. Eye (Lond), 2008. **22**(10): p. 1330-6.
208. Stewart, M.W. and Rosenfeld, P.J., *Predicted biological activity of intravitreal VEGF Trap*. Br J Ophthalmol, 2008. **92**(5): p. 667-8.
209. CADTH, *Common Drug Review, Clinical Review Report*. Aflibercept (Eylea): Treatment of Neovascular (Wet) Age-Related Macular Degeneration (wAMD). 2015, Ottawa (ON).
210. Larsson, A., Skoldenberg, E., et al., *Serum and plasma levels of FGF-2 and VEGF in healthy blood donors*. Angiogenesis, 2002. **5**(1-2): p. 107-10.
211. Webb, N.J., Bottomley, M.J., et al., *Vascular endothelial growth factor (VEGF) is released from platelets during blood clotting: implications for measurement of circulating VEGF levels in clinical disease*. Clin Sci (Lond), 1998. **94**(4): p. 395-404.
212. Avery, R.L., Castellarin, A.A., et al., *Systemic pharmacokinetics following intravitreal injections of ranibizumab, bevacizumab or aflibercept in patients with neovascular AMD*. Br J Ophthalmol, 2014. **98**(12): p. 1636-41.
213. Dixon, J.A., Oliver, S.C., et al., *VEGF Trap-Eye for the treatment of neovascular age-related macular degeneration*. Expert Opin Investig Drugs, 2009. **18**(10): p. 1573-80.
214. Shimomura, Y., Hirata, A., et al., *Changes in choriocapillaris fenestration of rat eyes after intravitreal bevacizumab injection*. Graefes Arch Clin Exp Ophthalmol, 2009. **247**(8): p. 1089-94.
215. Nguyen, D.C., Scinicariello, F., et al., *Characterization and allelic polymorphisms of rhesus macaque (Macaca mulatta) IgG Fc receptor genes*. Immunogenetics, 2011. **63**(6): p. 351-62.
216. Pelle, G., Shweke, N., et al., *Systemic and kidney toxicity of intraocular administration of vascular endothelial growth factor inhibitors*. Am J Kidney Dis, 2011. **57**(5): p. 756-9.
217. Anto, H.R., Hyman, G.F., et al., *Membranous nephropathy following intravitreal injection of bevacizumab*. Can J Ophthalmol, 2012. **47**(1): p. 84-6.
218. Georgalas, I., Papaconstantinou, D., et al., *Renal injury following intravitreal anti-VEGF administration in diabetic patients with proliferative diabetic retinopathy and chronic kidney disease--a possible side effect?* Curr Drug Saf, 2014. **9**(2): p. 156-8.
219. Davidovic, S.P., Nikolic, S.V., et al., *Changes of serum VEGF concentration after intravitreal injection of Avastin in treatment of diabetic retinopathy*. Eur J Ophthalmol, 2012. **22**(5): p. 792-8.
220. Diabetic Retinopathy Clinical Research, N., Scott, I.U., et al., *A phase II randomized*

-
- clinical trial of intravitreal bevacizumab for diabetic macular edema.* Ophthalmology, 2007. **114**(10): p. 1860-7.
221. Liu, A., Dardik, A., et al., *Neutralizing TGF-beta1 antibody infusion in neonatal rat delays in vivo glomerular capillary formation 1.* Kidney Int, 1999. **56**(4): p. 1334-48.
222. Ichimura, K., Stan, R.V., et al., *Glomerular endothelial cells form diaphragms during development and pathologic conditions.* J Am Soc Nephrol, 2008. **19**(8): p. 1463-71.
223. Jamrozy-Witkowska, A., Kowalska, K., et al., *[Complications of intravitreal injections--own experience].* Klin Oczna, 2011. **113**(4-6): p. 127-31.
224. Zhu, X., Wu, S., et al., *Risks of proteinuria and hypertension with bevacizumab, an antibody against vascular endothelial growth factor: systematic review and meta-analysis.* Am J Kidney Dis, 2007. **49**(2): p. 186-93.
225. Lafayette, R.A., McCall, B., et al., *Incidence and relevance of proteinuria in bevacizumab-treated patients: pooled analysis from randomized controlled trials.* Am J Nephrol, 2014. **40**(1): p. 75-83.
226. Roncone, D., Satoskar, A., et al., *Proteinuria in a patient receiving anti-VEGF therapy for metastatic renal cell carcinoma.* Nat Clin Pract Nephrol, 2007. **3**(5): p. 287-93.
227. Stokes, M.B., Erazo, M.C., et al., *Glomerular disease related to anti-VEGF therapy.* Kidney Int, 2008. **74**(11): p. 1487-91.

VII) Personnel contribution

Erklärung zum Eigenanteil der Dissertationsschrift

Die Arbeit wurde in der Universitätsklinik für Augenheilkunde der Universität Tübingen, Forschungsinstitut für Augenheilkunde, Sektion für experimentelle vitreoretinale Chirurgie unter Betreuung von Prof. Dr. Ulrich Schraermeyer durchgeführt.

Die Konzeption der Studie erfolgte durch Prof. Dr. Ulrich Schraermeyer (Leiter der Sektion) in Zusammenarbeit mit PD Dr. Sylvie Julien- Schraermeyer (stellvertretende Leiterin der Sektion).

Die licht- und elektronenmikroskopischen Untersuchungen der Nieren sowie deren Auswertungen wurden nach Einarbeitung durch Prof. Dr. Ulrich Schraermeyer und Sigrid Schultheiss von mir eigenständig durchgeführt. Die Einbettung und Fixierung der Proben wurden von Tatjana Taubitz und Sigrid Schultheiss durchgeführt. Die immunhistochemischen Analysen wurden von Nan Su (Ziliarkörper und Iris) und Alexander Tschulakow (Niere) durchgeführt. Die Bestimmung der VEGF Serumlevel erfolgte durch PD Dr. Sylvie Julien-Schraermeyer. Maximilian Ludinsky führte die licht- und elektronenmikroskopischen Untersuchungen von Ziliarkörper und Iris durch.

Die statistische Auswertung erfolgte eigenständig durch mich und wurde durch den Statistiker Jakob Smigierski überprüft.

Ich versichere, das Manuskript selbständig verfasst zu haben und keine weiteren als die von mir angegebenen Quellen verwendet zu haben.

Für weitere Details betreffend der Beteiligung einzelner Personen an den genannten Publikationen und die Genehmigung zur Verwendung der Veröffentlichungen siehe Anlagen.

Die Genehmigung zur Verwendung von Textauszügen und Abbildungen aus den aus dieser Arbeit entstandenen Publikationen ist in den Geschäftsbedingungen der beiden Verlage (Springer/ Graefes Archive und PLoS One) verankert und wurde mir gesondert per Email bestätigt. Die Erlaubnis zur Verwendung von Abbildungen aus Publikationen wurde mir von den genannten Autoren ebenfalls schriftlich erteilt.

Stuttgart, den 19.03.2017

Sarah Christner

VIII) Publications

Parts of the present dissertation have already been published in the following publications:

1. „Effects of a Single Intravitreal Injection of Aflibercept and Ranibizumab on Glomeruli of Monkeys“

- Authors of the publication: Sarah Christner[#], Alexander Tschulakow[#], Sylvie Julien, Maximilian Ludinsky, Markus van der Giet, Ulrich Schraermeyer
- Published in journal: PLoS one, volume 9, issue 11, pages e113701
- Publication date: November 21, 2014

[#]both authors contributed equally to this work

- Cited as: Tschulakow, A., Christner, S., Julien, S., Ludinsky, M., van der Giet M., Schraermeyer, U., *Effects of a single intravitreal injection of aflibercept and ranibizumab on glomeruli of monkeys*. PloS one, 2014. **9**(11):p.e113701.

2. „The Effects of VEGF-A-inhibitors aflibercept and ranibizumab on the ciliary body and iris of monkeys“

- Authors of the publication: Maximilian Ludinsky[#], Sarah Christner[#], Su Nan, Tatjana Taubitz, Alexander Tschulakow, Antje Biesemeier, Sylvie Julien-Schraermeyer, Ulrich Schraermeyer
- Published in journal: Graefes Arch Clin Exp Ophthalmol
- Publication date: April 22, 2016

[#] Both authors are first authors

- Cited as: Ludinsky, M., Christner, S., Su, N., Taubitz, T., Tschulakow, A., Biesemeier, A., Julien-Schraermeyer, S., Schraermeyer, U., *The effects of VEGF-A-inhibitors aflibercept and ranibizumab on the ciliary body and iris of monkeys*. Graefes Arch Clin Exp Ophthalmol, 2016. **254**(6): p. 1117-25.

3. Poster presented at the annual ARVO meeting

My findings were presented as a poster at the biggest annual meeting (ARVO) for Research in Vision and Ophthalmology in Orlando in USA in 2014.

- Authors of the publication: Sylvie Julien, Alexander Tschulakow, Sarah Christner, Ulrich Schraermeyer
- Published in Journal:. Investigative Ophthalmology & Visual Science
- Publication date: April 30, 2014
- Cited as: Julien, S., Tschulakow, A., Christner,S., Schraermeyer, U., *Effects of a single intravitreal injection of aflibercept and ranibizumab on glomeruli of monkeys*. Investigative Ophthalmology & Visual Science, 2014. **55**(13): p. 1946-1946.

IX) Appendix

Declaration of personnel contribution concerning the publications

Erklärung zum Eigenanteil

1) „Effects of a single intravitreal injection of aflibercept and ranibizumab on glomeruli of monkeys“

Konzipiert und entworfen wurde die Studie von	Sylvie Julien-Schraermeyer ^{1,2} , Ulrich Schraermeyer ^{1,2*}
Experimente wurden durchgeführt von	Sarah Christner ^{1,#} , Alexander Tschulakow ^{1,#}
Die Daten wurden analysiert von	Sarah Christner ^{1,#} , Alexander Tschulakow ^{1,#} , Sylvie Julien-Schraermeyer ^{1,2} , Maximilian Ludinsky ¹ , Markus van der Giet ³ , Ulrich Schraermeyer ^{1,2}
Die Reagenzien, Materialien und Mittel zur Analyse wurden bereitgestellt von	Ulrich Schraermeyer ^{1,2*}
Das Manuskript wurde geschrieben von	Sarah Christner ^{1,#} , Alexander Tschulakow ^{1,#} , Sylvie Julien-Schraermeyer ^{1,2}
Die Revision des Manuskripts zur Veröffentlichung wurde durchgeführt von	Sarah Christner ^{1,#} , Alexander Tschulakow ^{1,#} , Antje Biesemeier ¹
Die Arbeit wurde betreut von	Ulrich Schraermeyer ^{1,2*}

#Diese Autoren trugen in gleichem Umfang zur Arbeit bei

¹Section of Experimental Vitreoretinal Surgery, Centre for Ophthalmology, Tuebingen, Germany

²STZ OcuTox Preclinical Drug Assessment, Hechingen, Germany

³Division of Nephrology, Charité University Medicine, Charité Campus Benjamin Franklin, Berlin, Germany

*Korrespondenz: Prof. Dr. Ulrich Schraermeyer, Section of Experimental Vitreoretinal Surgery, Centre for Ophthalmology, Schleichstrasse 12/1, 72076 Tuebingen, Germany.

Email: Ulrich.Schraermeyer@med.uni-tuebingen.de

Tel.: +49 7071 29 80715, Fax: +49 7071 29 4554

2) „ The Effects of VEGF-A-inhibitors aflibercept and ranibizumab on the ciliary body and iris of monkeys”

Konzipiert und entworfen wurde die Studie von	Ulrich Schraermeyer ^{1,2*}
Experimente wurden durchgeführt von	Maximilian Ludinsky ^{1,#} , Nan Su ^{1,3} , Tatjana Taubitz ¹
Die Daten wurden analysiert von	Maximilian Ludinsky ^{1,#} Nan Su ^{1,3} , Sarah Christner ^{1,#} , Alexander Tschulakow ¹ , Ulrich Schraermeyer ^{1,2*}
Die Reagenzien, Materialien und Mittel zur Analyse wurden bereitgestellt von	Ulrich Schraermeyer ^{1,2*}
Das Manuskript wurde geschrieben von	Maximilian Ludinsky ^{1,#} , Sarah Christner ^{1,#} , Nan Su ^{1,3}
Die Revision des Manuskripts zur Veröffentlichung wurde durchgeführt von	Sarah Christner ^{1,#} , Antje Biesemeier ¹ , Sylvie Julien-Schraermeyer ^{1,2} , Maximilian Ludinsky ^{1,#} , Tatjana Taubitz ¹
Die Arbeit wurde betreut von	Ulrich Schraermeyer ^{1,2*}

die Autoren sind beide Hauptautoren dieser Arbeit

¹Section of Experimental Vitreoretinal Surgery, Centre for Ophthalmology, Tuebingen, Germany

²STZ OcuTox Preclinical Drug Assessment, Hechingen, Germany

³trug zur Arbeit betreffend der Untersuchungen und Auswertungen des pigmentierten Epithels bei.

*Korrespondenz: Prof. Dr. Ulrich Schraermeyer, Section of Experimental Vitreoretinal Surgery, Centre for Ophthalmology, Schleichstrasse 12/1, 72076 Tuebingen, Germany.

Email: Ulrich.Schraermeyer@med.uni-tuebingen.de

Tel.: +49 7071 29 80715, Fax: +49 7071 29 4554

Dr. Sylvie Julien-Schraermeyer war an der Konzeption der Studien beteiligt und hat Hilfestellung bei der Auswertung der Daten sowie der Verfassung der Manuskripte geleistet: Hilfe bei Textbausteinen zu Materials and Methods in (1), Teile der Discussion in (1), Korrektur und Überarbeitung beider Manuskripte (1)+(2) bezüglich formeller und inhaltlicher Fehler.

Alexander Tschulakow hat die Versuche zur immunhistochemischen Quantifizierung von VEGF in den Glomeruli durchgeführt und ausgewertet und entsprechende Textbausteine im Manuskript (1) beigetragen: Materials and Methods: Punkte 3. und 4., Results Punkt 1., Figures and legends: 1.,4.,5.,6. Er war außerdem an der Vorbereitung und Überarbeitung der Revision des Manuskripts (1) zur Veröffentlichung beteiligt. Außerdem trug er zur Auswertung und Interpretation der Daten betreffend Manuskript (2) bei und beteiligte sich an fachlichen Diskussion der Arbeitsgruppe.

Frau Nan Su hat die immunhistochemische Quantifizierung von VEGF im Iris- und Ciliarkörperepithel durchgeführt sowie entsprechende Textbausteine im Manuskript (2) beigetragen: Material and Methods: Punkt 5.+ 8., Results: 2 Abschnitte über immunhistochemistry, Figures and legends: 3.

Dr. Antje Biesemeier hat Hilfestellung bei der Auswertung der Daten sowie der Verfassung des Manuskripts (2) geleistet und trug zur Korrektur und Überarbeitung beider Manuskripte bezüglich formeller und inhaltlicher Fehler im Zuge der Vorbereitung (der Revision bei 2) zur Veröffentlichung (1+2) bei.

Tatjana Taubitz hat Gewebe präpariert und eingebettet, trug zur Interpretation der Daten betreffend Manuskript (2) bei, beteiligte sich an der fachlichen Diskussion und trug zur Korrektur und Überarbeitung des Manuskripts 2 bezüglich formeller und inhaltlicher Fehler im Zuge der Vorbereitung zur Veröffentlichung bei.

Markus van der Giet trug zur Beurteilung der Morphologie des Nierengewebes im Zuge der Verfassung von Manuskript (1) sowie der wissenschaftlichen Einordnung unserer Ergebnisse bei.

„Ich stimme dieser Erklärung zum Eigenanteil zu und bestätige die Richtigkeit der Angaben. Des Weiteren bin ich mit der Verwendung der Veröffentlichungen bzw. Daten im Rahmen der Dissertationsschriften von Sarah Christner und Maximilian Ludinsky einverstanden.“

Autor	Datum	Unterschrift
Ulrich Schraermeyer	13.4.2016	Schraermeyer
Sarah Christner	13.4.2016	Christner
Maximilian Ludinsky	18.4.2016	Ludinsky
Sylvie Julien-Schraermeyer	13.4.2016	Sylvie
Alexander Tschulakow	13.04.2016	Tschulakow
Su Nan	18.04.2016	Su Nan
Antje Biesemeier	15.04.2016	Biesemeier
Tatjana Taubitz	19.04.2016	Taubitz
Markus van der Giet	13.04.2016	van der Giet

X) Acknowledgement

First of all, I would like to express my great gratitude to Prof. Dr. Ulrich Schraermeyer who gave me the opportunity to work on this thesis and his support and guidance during the whole process.

Furthermore, I would like to thank PD Dr. Sylvie Julien-Schraermeyer who was also an important contact person for me. Thanks for your guidance, repeated proof-reading and the numerous valuable suggestions as well as practical support during the publications and this thesis.

This study was financially supported by Novartis Pharma GmbH.

Thanks to Sigrid Schultheiss for technical assistance and demonstrations as well as for the supervision of my electron microscopic work. I am also thankful for the good cooperation with Maximilian Ludinsky and the professional discussion. For the support concerning data analysis and writing and proof-reading of the publications I thank Dr. Antje Bieseimer, Alexander Tschulakow, Tatjana Taubitz, Prof. Dr. Markus van der Giet and Nan Su. Special thanks to Alexander Tschulakow and Tatjana Taubitz for the performance of several procedures and Dr. Antje Bieseimer for the good personal contact. Thanks to Judith Birch for the proof-reading and linguistic remarks and the great help with formality around publication and graduation. Jakob Smigierski was a professional help in the interpretation and selection of my performed statistical analyses.

A great thanks to my family and friends for the tireless support during my academic studies and my graduation. Thanks to my partner, Matthias Guschke, for the mental and active support und the endless tolerance. Thank you for your unshakable belief in me. Thanks to all my friends and colleagues for listening, motivating and encouraging.

All the credit is due to my parents, Rainer and Andrea Christner, I want to dedicate this work to. Without them, nothing would have been possible of all this.

XI) Curriculum vitae

Sarah Christner

■ Personal Data

Name: Sarah Christner
Date and place of birth: September 25, 1986, Kirchheim/Teck
Nationality: German

■ School Career

1993-1997 Elementary School Erkenbrechtsweiler

1997- 2006 High school Hölderlin Gymnasium Nürtingen
- 21.06.2006 General qualification for university
entrance (Abitur)

■ Academic Career

2006- 2012 Studies of dentistry at Eberhard Karls Universität
Tübingen
24.09.2007 Natural scientific intermediate
examination (Naturwissenschaftliche
Vorprüfung)
02.10.2009 First state examination
(Zahnärztliche Vorprüfung)
29.11.2012 Second state examination
(Staatsexamen Zahnmedizin)
11.12.2012 license to practice dentistry
(Approbation als Zahnärztin)

- 2012- today Graduation at University Eye Hospital Tübingen
in the Section for experimental vitreoretinal surgery
- November 2014 Publication in the Journal PloS One
- April 2016 Publication in the Journal Graefes Archive for Clinical
and Experimental Ophthalmology